RADIOMETRIC DETECTION OF OIL SLICKS

A. T. Edgerton, et al

Aerojet-General Corporation
El Monte, California

January 1970

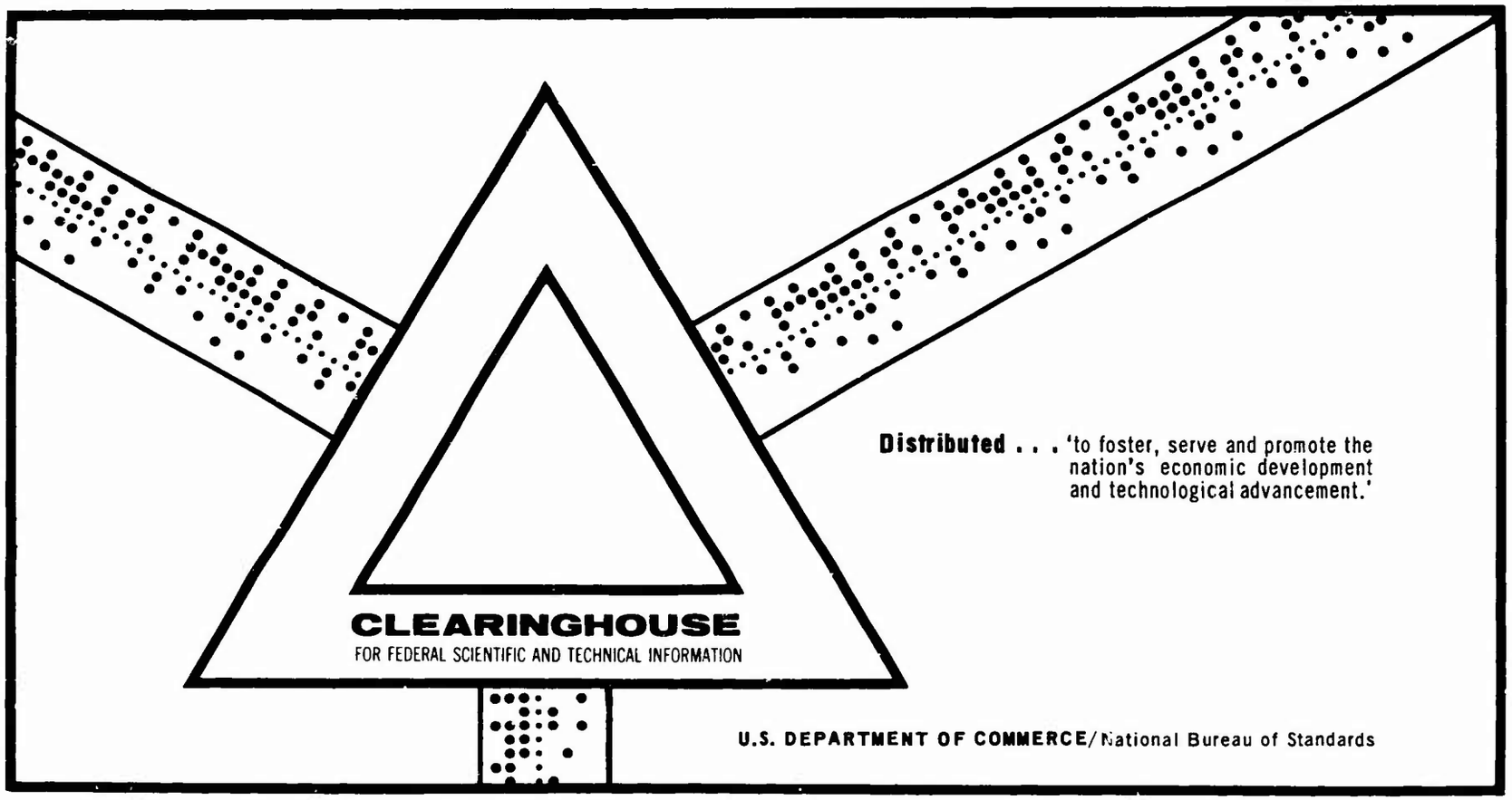

Report No. SD 1335-1

RADIOMETRIC DETECTION OF OIL SLICKS

A.T. Edgerton and D.T. Trexler

AEROJET- GENERAL CORPORATION
9200 East Flair Drive
El Monte, California

JANUARY 1970

FINAL REPORT

Prepared for

UNITED STATES COAST GUARD
Applied Technology Division
Washington, D.C. 20590

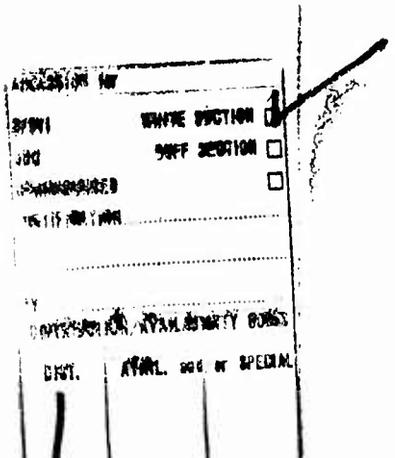

The contents of this report reflect the views of the Aerojet-General Corporation which is responsible for the facts and the accuracy of the data presented herein. The contents do not necessarily reflect the official views or policy of the Department of Transportation. This report does not constitute a standard, specification or regulation.

Report No. SD 1335-1

RADIOMETRIC DETECTION OF OIL SLICKS

A. T. Edgerton & D. T. Trexler

AEROJET-GENERAL CORPORATION
9200 East Flair Drive
El Monte, California

January 1970

Final Report

Contract No. DOT-CG-93, 288A

Prepared for

UNITED STATES COAST GUARD
APPLIED TECHNOLOGY DIVISION
WASHINGTON, D.C. 20590

FOREWORD

This report covers research conducted by Geosciences Group, Microwave Systems Division of Aerojet-General Corporation, El Monte, California for the Applied Technology Division of the U. S. Coast Guard, Washington, D. C. This work was performed under contract number DOT-CG-93, 228A, "Radiometric Detection of Oil Slicks," between 14 March 1969 and 26 October 1969. This document represents the final technical report.

Several persons and agencies furnished cooperative support and assistance during the performance of this program. Cmdr. J. M. O'Connell, Lt. Cmdr. Lehr and C. Catoe of the U. S. Coast Guard, Applied Tech. Div., provided invaluable administrative and technical guidance which facilitated the research. Capt. Pearce, Capt. Busche and Cmdr. Hamilton of the Operations Office of the Eleventh Coast Guard District, Long Beach, California were instrumental in selecting a desirable area for the at-sea test phase of the program.

The assistance provided by Dr. Floyd F. Sabins and A. Beyer of Chevron Oil Field Research Company, in providing crude oil samples for the laboratory and field test phases of the program is greatly appreciated.

Recognition must be given to specific members of the Geosciences Group for their individual contributions to the program. Mr. G. Poe performed the measurements of the dielectric properties and assisted in interpretation of the laboratory data. Mr. J. Jenkins operated the airborne radiometer system. Mr. D. Meeks acted as observer aboard the AGC-owned vessel during the at-sea tests.

ABSTRACT

A study has been performed to assess the feasibility of using microwave radiometry for detection of oil pollution. The investigation stems from the U. S. Coast Guard's requirement for an airborne surveillance system which can detect oil pollution during inclement weather and during the hours of darkness. Laboratory and airborne measurements were made of a variety of oil base pollutants. Laboratory investigations evaluated microwave response as a function of oil film thickness, physical temperature of the oil-water system, pollutant type, sensor wavelength, antenna polarization, and observation angle. These studies consisted of dual-polarization radiometric measurements (observational wavelengths of 0.8 cm and 2.2 cm) of Bunker "C" fuel oil, gasoline, and 20, 30, and 40 API gravity crude oil. The dielectric properties of these pollutants were also measured by means of a 0.81-cm ellipsometer. The results of the laboratory measurements were used to select the most suitable microwave radiometer for the airborne measurements. The airborne experiments consisted of measurements of small oil slicks on the open ocean off the Southern California Coast. Measurements were made from a Cessna 210 aircraft instrumented with a dual-polarized 0.81 cm radiometer oriented with a forward antenna viewing angle of 45° from nadir. Pollutants examined during the tests include marine diesel fuel; 20, 30, and 42 API gravity crude oils; and a mixture of diesel fuel and 20-gravity crude oil. Measurements were made under various atmospheric and low sea state conditions, including several at night.

TABLE OF CONTENTS

TABLE OF CONTENTS (Cont)

TABLE OF CONTENTS (Cont)

ILLUSTRATIONS

TABLE OF CONTENTS (Cont)

TABLES

LIST OF ABBREVIATIONS AND SYMBOLS

API GRAVITY	The Standard American Petroleum Institute method for specifying the density of crude petroleum. The density in degrees API is equal to $\frac{141.5}{P} - 131.5$, where P is the specific gravity measured at 60° F.
GHZ	Gigahertz 10^9 cycles per second
h	Horizontal Polarization
$^{\circ}K$	Degrees Kelvin
K	Complex Dielectric Constant
K'	Real part of the Complex Dielectric Constant
K''	Imaginary part of the Complex Dielectric Constant
MHz	Megahertz 10^6 cycles per second
R	Reflectivity
T_B	Radiometric Brightness Temperature
TDS	Total Dissolved Solids
v	Vertical Polarization
α	Absorptivity
ρ	Fresnel Reflection Coefficient
θ	Antenna Viewing Angle
ΔT	T_B (Oil Slick) - T_B (Adjacent Unpolluted Ocean Surface)

Section 1

INTRODUCTION AND SUMMARY

This document summarizes a U. S. Coast Guard sponsored study of the feasibility of using microwave radiometry for detection of oil pollution. The study was stimulated by the need for an airborne surveillance system which can detect oil pollution during inclement weather and during the night-time. These conditions preclude reliance on optical or infrared detection systems.

The work, performed under Contract No. DOT-CG-93, 228A, consisted of laboratory and airborne measurements of a variety of oil base pollutants. Measurements were performed as a function of oil film thickness, physical temperature of the oil-water system, pollutant type, sensor wavelength, antenna polarization and angle of observation. Airborne data were collected over a variety of sea state and weather conditions. Experimental data combined with operational requirements of the USCG, were utilized to define sensor system requirements and possible configurations for a pollution surveillance system.

Laboratory investigations, Section 2, consisted of dual wavelength, dual polarization radiometric measurements of various oil base pollutants as a function of oil film thickness, thermometric temperature of the oil-water system, antenna polarization and angle of observation. Pollutants used for these measurements included both refined and crude petroleum. Pollutants examined in the laboratory include Bunker "C" fuel oil, gasoline, 20, 30 and 40 API Gravity Crude Oil. Radiometric measurements were performed with observational wavelengths of 0.8 cm (37 GHz) and 2.2 cm (13.4 GHz). The dielectric properties of the pollutants were also determined by means of an 0.81 cm ellipsometer or precision reflectometer. The real and imaginary parts of the dielectric constant were subsequently used to calculate absorptivities of the pollutants on sea water for film thicknesses of 0.1 mm, 0.5 mm and 1.0 mm. Laboratory data

were used in determining the most suitable microwave radiometer configuration for the airborne phase of the program.

The airborne phase, Section 3, consisted of at-sea tests using a Cessna 210 aircraft instrumented with a dual polarized 0.81-cm radiometer oriented with a forward antenna viewing angle of 45°. Small oil slicks were formed on the open ocean off the Southern California Coast and utilized for these tests. The spills, ranging in volume from 165 to 350 gallons, were conducted in an area designated by the Operations Officer of the Eleventh Coast Guard District. Pollutants examined during at-sea tests include Marine Diesel Fuel, 20, 30, 42 API Gravity Crude Oils, and a mixture of Diesel Fuel and 20-Gravity Crude. Overflights of the slicks were made under various atmospheric and low sea state conditions, including several overflights at night.

Data derived from the laboratory and airborne radiometric measurements have led to a better understanding of the mechanisms of oil-water systems that affect the microwave response. Results of radiometric measurements performed during the laboratory phase of the program showed that: 1) the microwave signature of an oil film is inversely proportional to sensor wavelength, 2) horizontally polarized signatures were twice the vertically polarized signatures for oil films of a flat water surface, and 3) all signatures were positive; i.e., greater than calm water without oil. The airborne measurements using an 8.1 mm dual-polarized radiometer on small oil slicks showed that: 1) thinner oil-films than anticipated from laboratory findings could be detected, 2) ocean surface roughness affects the microwave signature of an oil slick since the radiometric brightness temperature of the sea increases with increased sea state, and 3) oil-films modify sea state conditions by reducing the surface roughness.

A more detailed discussion of the results of the study is presented in Section 4, along with conclusions and recommendations for further research. A discussion of system requirements and configurations of pollution surveillance systems is provided in Appendix C.

Section 2

LABORATORY INVESTIGATIONS

2.1 PURPOSE

Laboratory studies were conducted to establish the dependence of microwave emission on such parameters as 1) oil thickness, 2) oil type, 3) physical temperature of the oil-water system, 4) observation wavelength, 5) antenna polarization (vertical or horizontal), and 6) antenna viewing angle, θ. Laboratory data were also used to define the most useful radiometer configuration for at-sea tests.

Radiometric data were taken for gasoline, Bunker "C" fuel oil, 20, 30 and 40 API Gravity Crude Oil using observational wavelengths of 0.81 cm and 2.2 cm. The dielectric properties of these petroleum products were also measured to facilitate interpretation of the radiometric data. The real and imaginary parts of the dielectric constants were measured and absorptivities were computed as a function of oil film thickness and angle of observation.

Details of the laboratory investigations are presented in the following sections. Section 2.2 provides a summary of instrumentation and the experimental apparatus used for the study. Dielectric constant and radiometric measurements are outlined in Sections 2.3 and 2.4 respectively.

2.2 INSTRUMENTATION

The Aerojet-General Microwave Field Laboratory and ellipsometer were used for the laboratory phase of this program.

The field laboratory includes 0.81 and 2.2 cm dual polarized radiometers with an automatic data recording and control system. Instrumentation is housed in a 16-foot mobile laboratory and a 1-1/2 ton flat bed truck. Figure 2-1 is an external view of the mobile laboratory. The trailer houses monitoring, recording and control equipment associated with the radiometric sensors as well as meteorological instruments. The

Figure 2-1. MOBILE FIELD LABORATORY

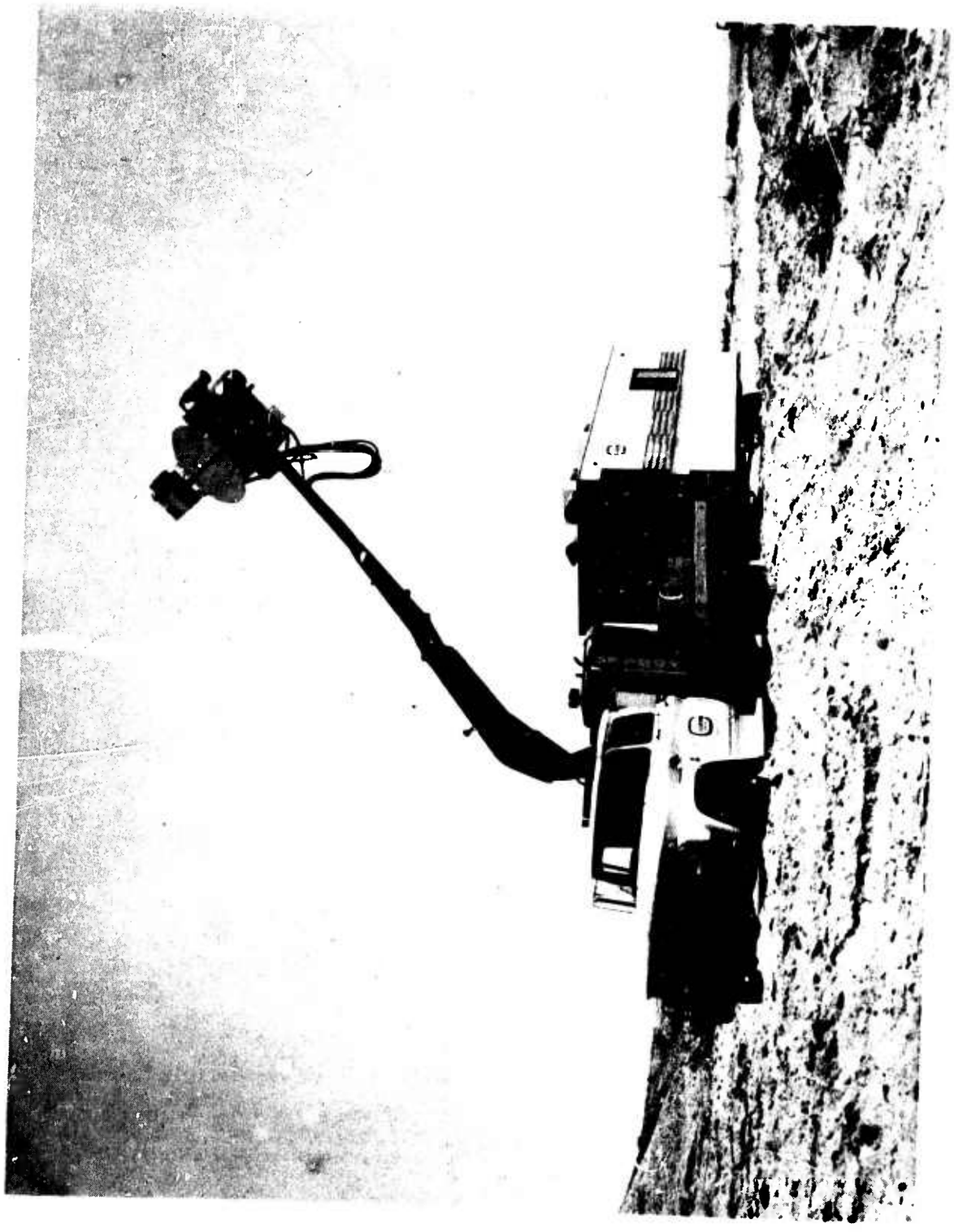

truck serves as the mounting platform for the diesel power generator and the radiometer mounting boom. The boom is a hydraulically operated crane, 16 feet in length, controlled from a position near the cab of the truck. A remote control head is mounted on the end of the boom to allow the radiometer to be scanned in the elevation plane through an angle of 180°. The programming of this head is controlled by a digital data acquisition system in the trailer. The end points of terrain scans are adjusted to coincide with the local gravity vector, scanning from nadir to zenith. Scan steps have been set at 5°, but other values, including non-equal steps, can be obtained as desired.

The microwave radiometers and accessory equipment are mounted on a common plate, attached to the movable boom head, as shown in Figure 2-2. They contain the switch which selects the three input configurations, horizontal polarization, vertical polarization, and a calibration load. The basic specifications of the radiometers are presented in Table 2-1.

Table 2-1

Specifications of 2.2 and 0.81-cm Radiometers

Parameters	Radiometers	
Center Frequency wavelength	13.4 GHz	37 GHz
Wavelength	2.2 cm	0.81 cm
Bandwidth	300 MHz	300 MHz
Sensitivity	0.5°K/sec	0.5°K/sec
Antenna Beamwidth	5°	5°
Antenna Types	Lens-Horn	Lens-Horn

Integration period 0.4 to 10.0 seconds (all radiometers)

Accessory equipment in the field laboratory includes meteorological instrumentation, thermistors and geophysical instruments. The meteorological instruments include the following: thermistors for monitoring air

Figure 2-2. CLOSE-UP VIEW OF RADIOMETER

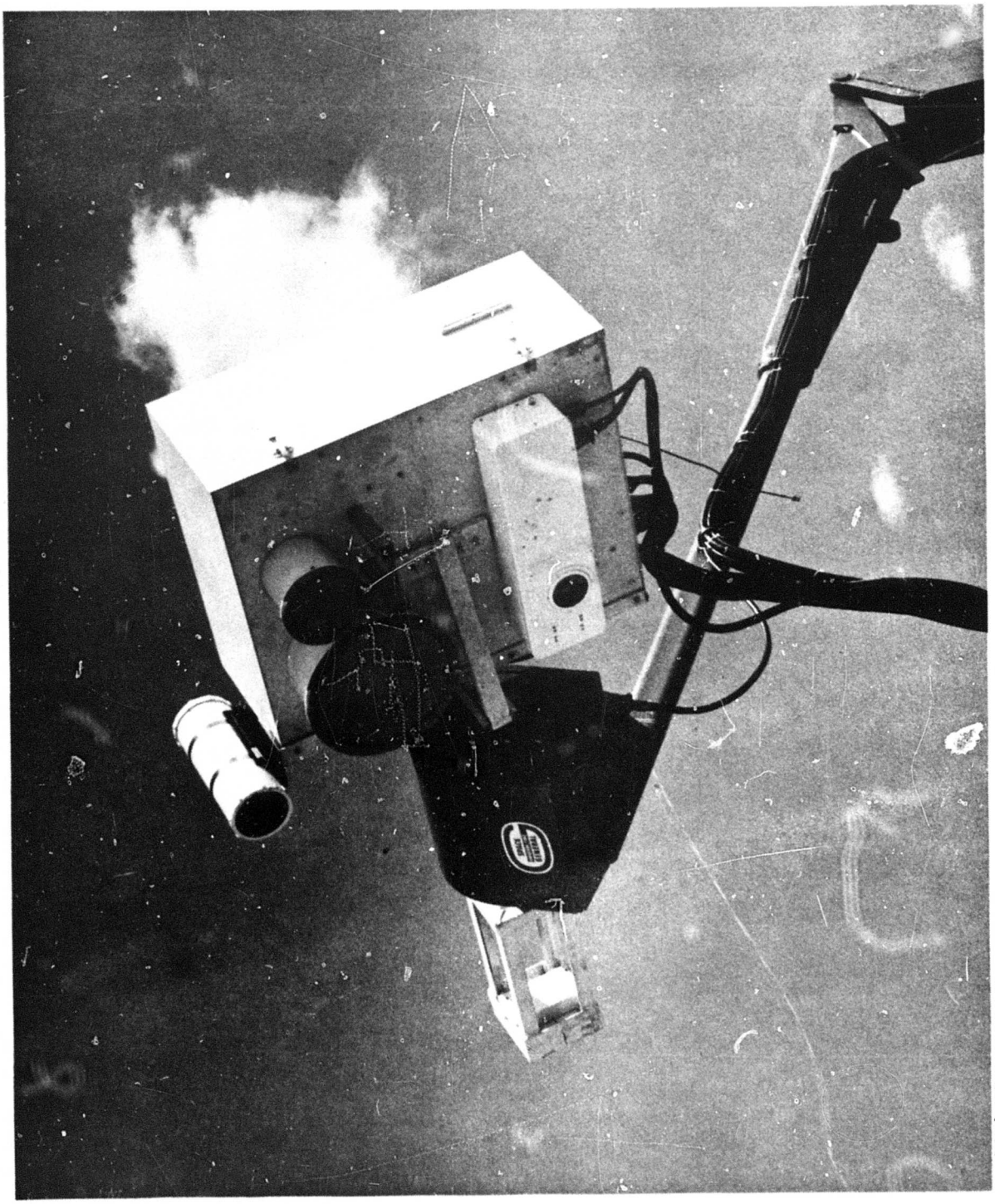

829/191

temperature, barometer, relative humidity meter, and wind speed and direction apparatus. All instrument outputs are recorded directly on digital tape.

Radiometric measurements of oil pollutants were conducted using the microwave laboratory and an environmental chamber, Figure 2-3. The chamber dimensions are 20x10x6 feet and the chamber houses a 16x6x1-1/2 foot tank. Temperature in the chamber can be controlled between -40°C and ambient. Sea water was placed in the tank for each experiment by adding 4000 pounds (water depth of six inches) of industrial grade water (TDS 240 ppm) and sodium chloride equivalent to 3.6%. Pollutants were subsequently placed on the sea water in volumes equivalent to film thicknesses of 0.1, 0.5 and 1.0 mm, and microwave radiometric measurements were conducted. It should be noted, however, that the more viscous oils did not produce even, uniformly distributed films on the water surface, but tended to collect in more or less random globules and patches of irregular thickness.

Dielectric properties of pollutants were measured by means of an ellipsometer or precision reflectometer tuned to 0.81 cm, Figure 2-4.

This instrument was built primarily for use in making dielectric constant measurements; however, it has other applications.

The effects of surface roughness on reflection coefficients can be determined with the ellipsometer. The reflection coefficient of a sample can be measured as a function of both incidence and reflection angles. If this type of measurement is performed on samples with different degrees of roughness, the proportions of power going into non-specular reflection and increased absorption can be evaluated. This is not only useful in radiometry, but also can be correlated with radar bistatic cross-sections.

The equipment consists of the following assemblies:

1) Transmitting Arm
2) Receiving Arm
3) Electronics Package
4) Frame for Transmitting and Receiving Assemblies
5) The X-Y Recorder

Figure 2-3. ENVIRONMENTAL CHAMBER

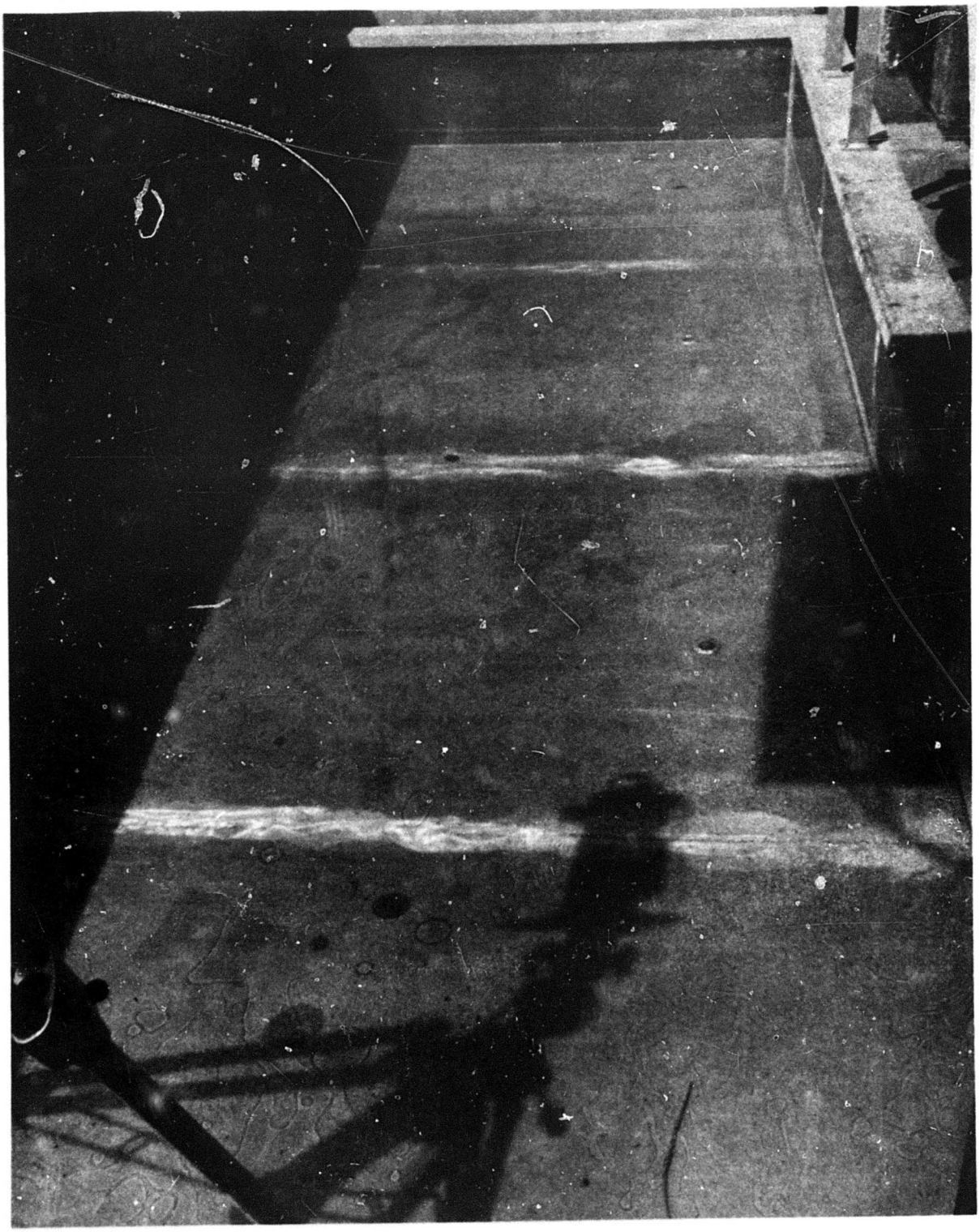

Figure 2-4. PHOTO OF ELLIPSOMETER

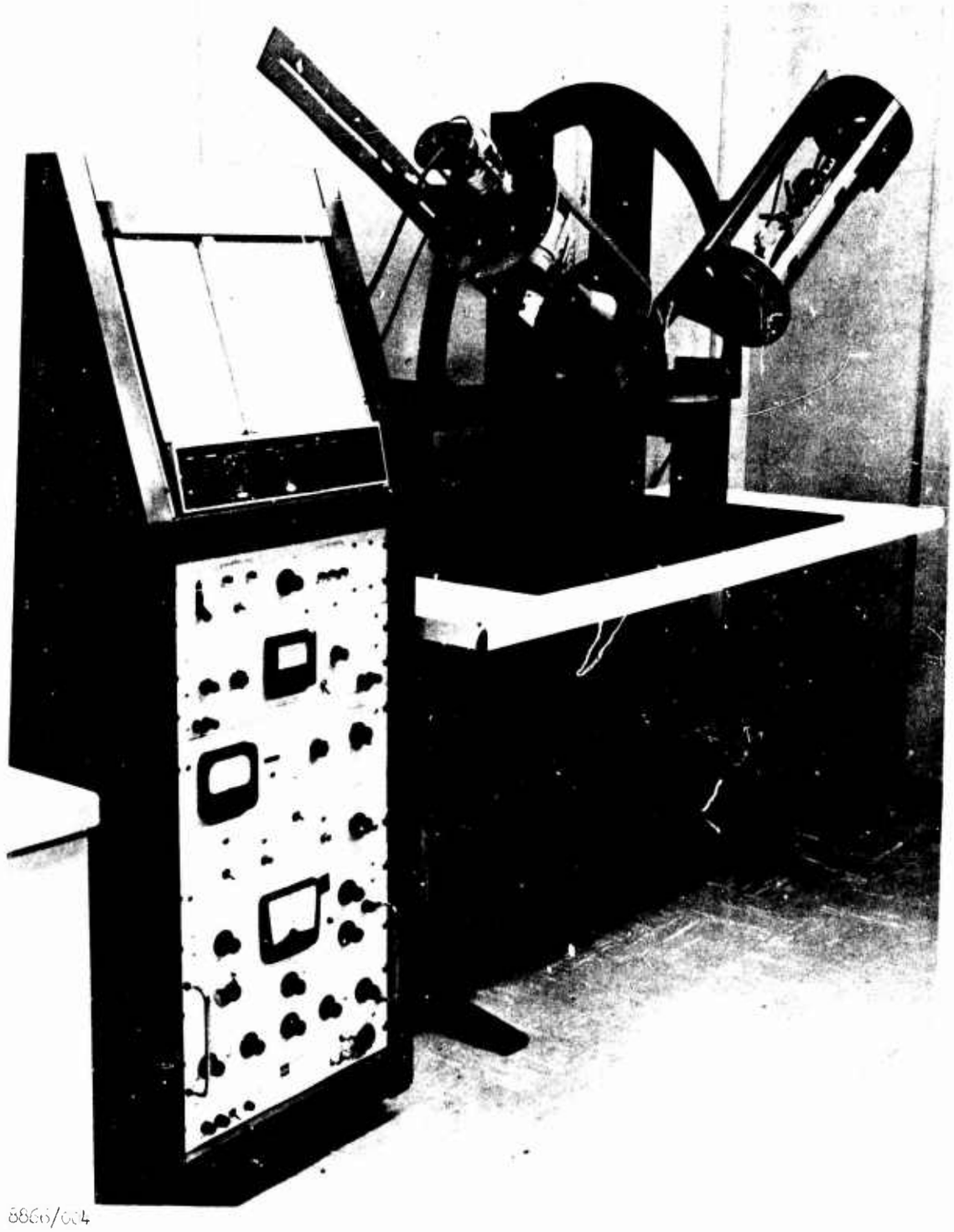

8866/004

The transmitting and receiving assemblies mounted on the frame, are capable of adjustment so the angles of incidence and reflection can be varied. The receiving arm is rotated around its axis by an electric motor drive, monitored by an electric pick-off which indicates the degree of rotation. This signal is the drive for the x-axis of the recorder.

The electronics assembly includes klystron power supplies, ratio meter, a control and power supply for the rotation motor and the rotation pick-off signal. The electronics assembly, plotter and frame contain no microwave equipment and, therefore, can be used for any frequency of operation within the range of interest.

2.3 ELLIPSOMETRIC MEASUREMENTS (DIELECTRIC CONSTANT)

2.3.1 INTRODUCTION

The complex dielectric constant of a non-magnetic, homogeneous, isotropic, semi-infinitely extended material having a smooth planar surface, as well as zero temperature gradient, completely characterizes the electromagnetic absorptivity of the material if conservation of energy is assumed. The absorptivity, α, at observation angle θ, (see Figure 2-5) is related to the reflectivity, R, by

$$\alpha^{(h,v)}(\theta) = 1 - R^{(h,v)}(\theta) \qquad (1)$$

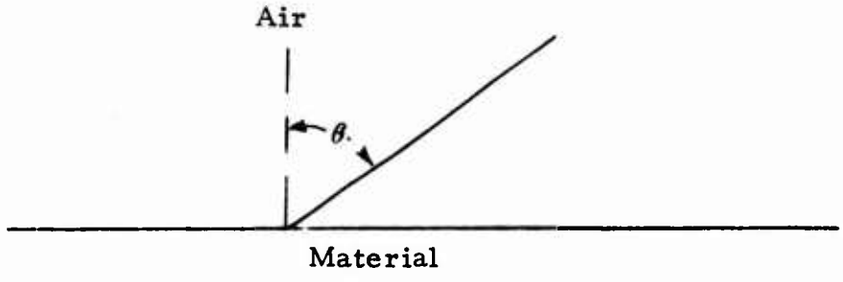

Figure 2-5. Semi-infinitely Extended material with Dielectric Constant K

where (h, v) denotes the polarization state under consideration. The reflectivity, R, is given by the Fresnel reflection coefficients:

$$R^{(h,v)}(\theta) = \left|\rho(h,v)(\theta)\right|^2 \tag{2}$$

and

$$\rho^h(\theta) = \frac{\cos\theta - \sqrt{K - \sin^2}}{\cos\theta + \sqrt{K - \sin^2\theta}} \tag{3}$$

$$\rho^v(\theta) = \frac{K\cos\theta - \sqrt{K - \sin^2\theta}}{K\cos\theta + \sqrt{K - \sin^2\theta}} \tag{4}$$

and K is the complex dielectric constant.

The absorptivity of a material possessing smooth planar layers of different materials such as seen in Figure 2-6 is again given by (1) under the conditions stated above.

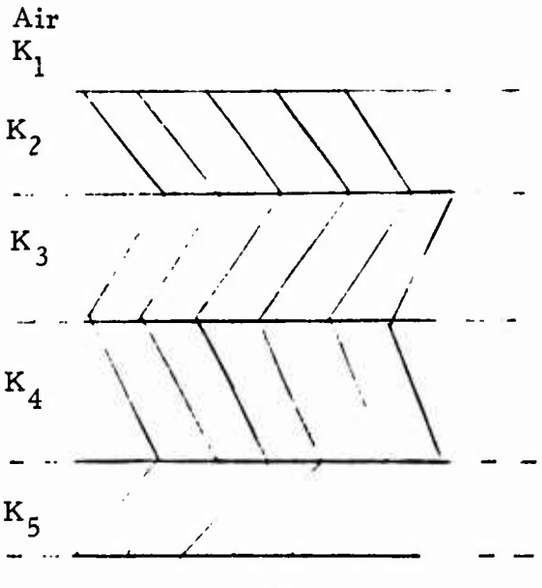

A. Layered Structures with Dielectric Constants K_1, K_2, ...

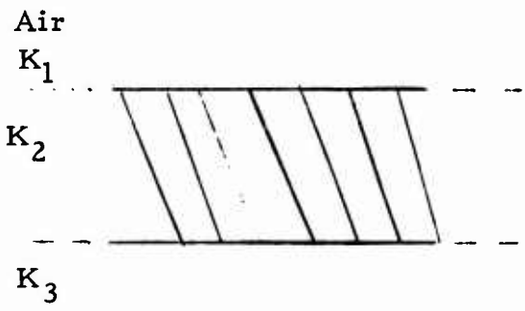

B. Two-Layered Structure with Dielectric Constants K_1, K_2, and K_3

Figure 2-6. Layered Structures with Varying Dielectric Constants

However, the reflectivity is no longer given by (2). For the case of a layered structure, as shown in Figure 2-6A, the reflectivity can be shown to be

$$R^{(h,v)} = \left| \frac{\rho_{12}^{(h,v)} e^{2i\psi t} + \rho_{23}^{(h,v)}}{e^{2i\psi t} + \rho_{12}^{(h,v)} \rho_{23}^{(h,v)}} \right|^2 \tag{5}$$

where ρ_{12} and ρ_{23} are the Fresnel reflection coefficients for interfaces between layers 1 and 2; and 2 and 3, respectively. The thickness of the intermediate layer is t.

The quantity ψ is

$$\psi = -2\pi \lambda^{-1} \sqrt{K_2 - \sin^2\theta} \tag{6}$$

where is the wavelength in air under consideration and K_2 is the dielectric constant of the intermediate layer. The reflection coefficients are

$$\rho_{\ell n}^{h} = \frac{\sqrt{K_\ell - \sin^2\theta} - \sqrt{K_n - \sin^2\theta}}{\sqrt{K_\ell - \sin^2\theta} + \sqrt{K_n - \sin^2\theta}} \quad \ell, n = 1, 2, 3 \tag{7}$$

$$\rho_{\ell n}^{(v)} = \frac{K_n \sqrt{K_\ell - \sin^2\theta} - K \sqrt{K_n - \sin^2\theta}}{K_n \sqrt{K_\ell - \sin^2\theta} + K \sqrt{K_n - \sin^2\theta}} \quad \ell, n = 1, 2, 3 \tag{8}$$

Here we are concerned with presenting the absorptivities of a few materials at a frequency of 37 GHz ($\lambda = 0.81$ cm). Layered structures are also considered. In particular, the absorptivities of ocean water and a few oils are given. The values of the dielectric constants were obtained

from measurements with Aerojet's 37-GHz ellipsometer[4]. In each case, the absorptivities were calculated using (equation 5) from a knowledge of the dielectric constants.

2.3.2 RESULTS

The dielectric constants of ocean water, 40 gravity crude oil, 30 gravity crude oil, 20 gravity crude oil, Bunker "C" fuel oil and gasoline were measured at 0.8-cm wavelength. The values obtained are given in Table 2-2. The maximum absolute error in the real and imaginary parts are given when their measurement was possible.

Table 2-2

DIELECTRIC CONSTANTS AT 37 GHz

Material	Dielectric Constant
Ocean Water at 23°C 35 ppt	K' = 20.94 ± 1.40 K" = 26.84 ± 1.50
40 Gravity Crude Oil 23°C	K' = 1.85 ±0.03 K" < 0.0148
30 Gravity Crude Oil 23°C	K' = 2.06 ±0.05 K" < 0.0150
20 Gravity Crude Oil 23°C	K' = 2.29 ±0.05 K" < 0.0198
Bunker "C" Fuel Oil 23°C	K' = 2.41 ±0.05 K" < 0.0213
Gasoline	K' = 2.08 ±0.05 K" < 0.0017
40 Gravity Crude Oil 20°C Aged 3 days in Open Air	K' = 2.10 ±0.05 K" = 0.229 ±0.02
Bunker "C" Fuel Oil 20°C Aged 3 days in Open Air	K' = 2.94 ±0.07 K" = 0.298 ±0.02

For some of the oils only an upper bound could be placed on the imaginary part of the dielectric constant. This lack of knowledge of the imaginary part for very low loss materials is primarily due to the present experimental limitation of measuring power ratios below 50 db. In any case, since the real part is much larger than the imaginary part, the absorptivities of the low loss oils can be determined with negligible error introduced despite the unknown value of the imaginary part. For example, with 1 mm of 30 gravity crude oil over ocean water, the vertical polarization absorptivities at viewing angles of 30, 45 and 60 degrees for maximum value of imaginary part and a value of zero are respectively:

	30°	45°	60°
With K" = 0.015	0.67761	0.67225	0.65272
With K" = 0.0	0.67591	0.67042	0.65073

Appendix A contains the absorptivity data calculated from the measured dielectric constants of Bunker "C" fuel oil, gasoline, and the three crude oils. Absorptivities are given for the following thicknesses of petroleum over sea water:

- An infinite thickness
- 1 mm
- 0.5 mm
- 0.1 mm
- 0.10 microns

The data were calculated assuming a constant thermometric temperature of 23°C. Absorptivity data are also given for 40 gravity crude and Bunker "C" oil which were "aged" for three days in the open air.

The absorptivity data given in Appendix A show that no appreciable change occurs in the absorptivity of water until the thickness of the oil is greater than 0.1 mm. An interesting point occurs in each case for the vertical polarization absorptivity of oils over water. The absorptivities of the oil have approximately the same value as that of water at angles near the Brewster angle of the oil. This fact can perhaps be used as a means of calibration for passive microwave measurement systems.

2.3.3 CONCLUSIONS REGARDING DIELECTRIC PROPERTIES OF PETROLEUM SAMPLES

The imaginary part of the dielectric constant of "fresh" oils was found to be extremely small at 0.8-cm wavelength - less than 0.02 at 23°C. For "fresh" oil, the real part decreases almost linearly with increasing API gravity, and for oil "aged" three days in open air, the real part was found to increase slightly (see Figure 2-7). The major difference in dielectric properties of "aged" and "fresh" oils appears to occur in the imaginary part. For example, an increase of over two orders of magnitude was observed for Bunker "C" fuel oil. The absorptivity of all oils over ocean water was found to be the same as that of water for oil thicknesses less than 0.1 micron. An increase of less than 0.01 occurred for thicknesses around 0.01 mm.

The calculations presented herein and the experimental evidence obtained thus far supports the feasibility of detecting oil slicks of thickness of greater than 0.1 mm with the 0.8-cm (37 GHz) radiometer. For thicknesses less than 0.1 mm, a higher frequency (shorter wavelength) appears necessary. Higher frequency radiometers such as a 94 GHz have been developed but were not available at the time of this study. An improved 94-GHz (λ= 0.3 cm) radiometer is now under development and will be available for oil pollution research in early to mid-1970.

2.4 RADIOMETRIC MEASUREMENTS

2.4.1 GASOLINE

Gasoline was added to sea water in the environmental tank in quantities of 0.89 ml, 892 ml and 8,920 ml to form gasoline films on the water surface of 1 micron, 0.1-mm and 1-mm thickness. Three microwave scans (measurements of radiometric temperature vs. antenna viewing angle, θ) were performed of each thickness. The 0.89 ml of gasoline did not spread uniformly over the water surface, but remained in small droplets floating on the water. Both the 892 ml and 8,920 ml volumes of gas spread more-or-less uniformly over the surface covering at thicknesses of 0.2 mm and 1 mm, respectively. The reason for the 0.2 mm thickness for 892 ml of pollutant is that the gasoline covered only 50% of the surface

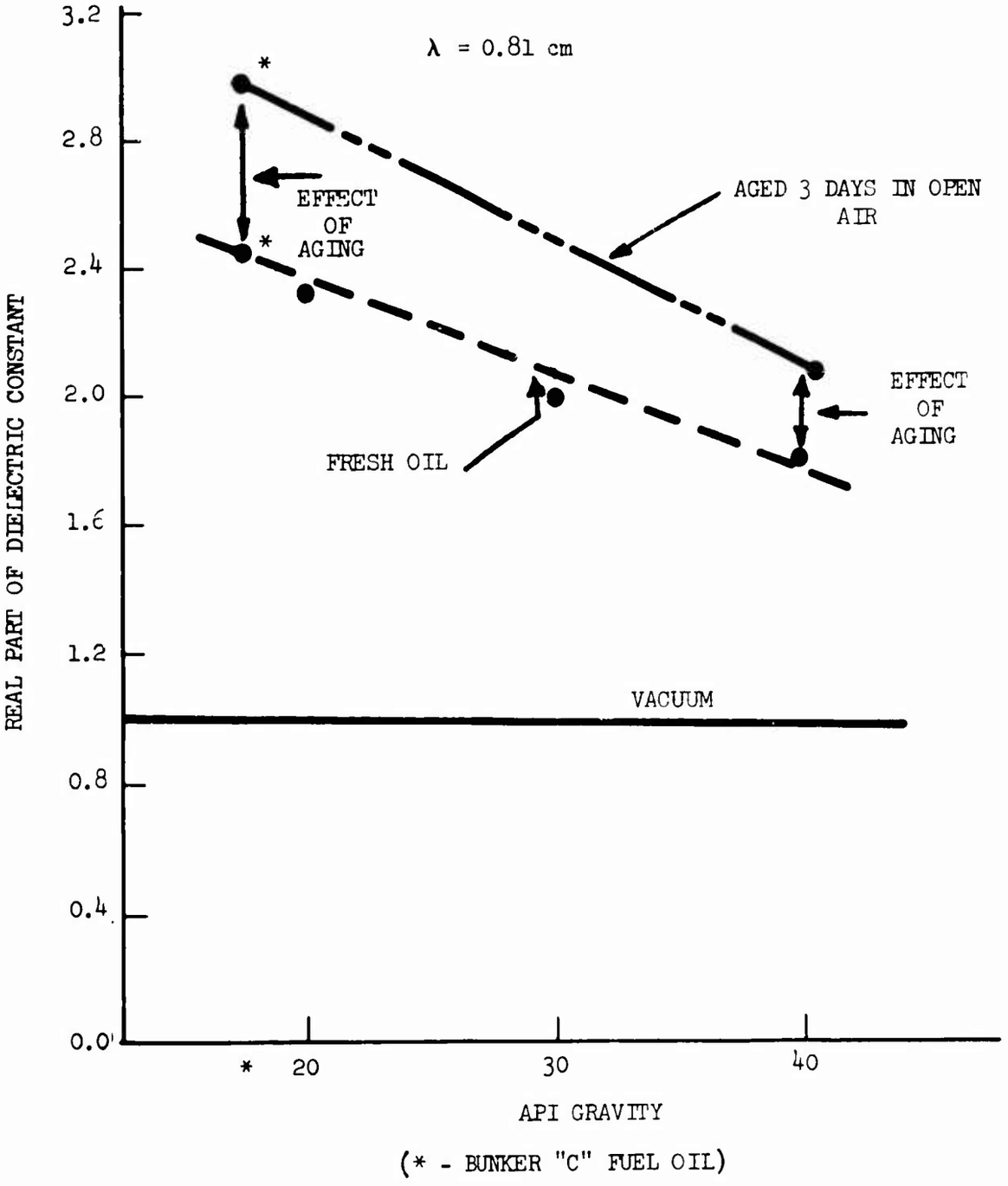

Figure 2-7. DIELECTRIC CONSTANT OF CRUDE OILS VERSUS API GRAVITY

and was concentrated within the sensor field of view.

Data from 1 micron and 0.2-mm thicknesses indicated that the gasoline was not detectable by either radiometer. The 1-mm film of gasoline caused the 0.81 cm brightness temperature to shift upward by as much as $40^{\circ}K$ for the vertical polarization and $43^{\circ}K$ for the horizontal polarization ($\theta = 20^{\circ}$). During two successive scans (10 minutes apart) the 0.81 cm brightness temperatures decreased $2^{\circ}K$, probably due to decreasing thickness of the gasoline film associated with evaporation. Air temperature during the 1-mm thickness experiment ranged from $20.3^{\circ}C$ to $23.2^{\circ}C$. Decrease in thickness during the measurements was only slight but was sufficient to affect the radiometric temperature.

In the microwave frequency region the dissipative losses of gasoline are quite low and the radiation emitted from the top surface of the gasoline film on water (for thicknesses less than one wavelength) originates solely from the underlying water body. The amount of this radiation is determined by the effective emissivity (or reflectance) at the upper gasoline surface. The effective reflectance is a function of the individual reflections occurring at the two interfaces and the distance between them. The reflection coefficients at the interfaces are functions of both the dielectric constants of the materials and the angle of incidence. Since the attenuation in gasoline is very small it is expected that for narrow-band radiation the radiometric temperature will execute an oscillatory pattern as a function of the gasoline thickness. As the gasoline film thickness increases, attenuation in the gasoline also increases, and the oscillations become damped. These oscillations occur as the microwave or optical path length through the gasoline increases through critical lengths which cause interference phenomena. Gasoline thickness was not monitored during the experiment.

The emission characteristics of layered media are considered in Section 2.4 of this report. Work of a similar nature, involving a layer of ice on water is discussed in a technical report for the Office of Naval Research.[1] As a matter of comparison, at 10 GHz ($\lambda = 3$ cm) the real part of the dielectric constant for ice is 3.17[2] and that for aviation gasoline

(100 octane) is 1.92. Water, on the other hand, has a dielectric constant (real part) that approaches 23.0 (standard temperature).

Since significant variations in observed brightness temperatures occur for the three scans, the measurements were repeated using fixed viewing angles of 15°, 30° and 45°. Table 2-3 summarizes results of these measurements.

Table 2-3

2.2-cm and 0.81-cm Antenna Temperatures, °K

View Angle	λ = 2.2 cm V	λ = 2.2 cm H	λ = 0.81 cm V	λ = 0.81 cm H
		Saline Water		
15°	134	127	165	159
30°	141	118	175	150
45°	160	113	193	143
		0.1 mm Gasoline		
15°	134	126	164	156
30°	141	118	176	154
45°	162	115	199	152
		0.5 mm Gasoline		
15°	136	129	174	168
30°	142	120	179	158
45°	160	114	196	150
		1.0 mm Gasoline		
15°	139	132	185	176
30°	143	122	183	162
45°	159	111	194	140

The 0.81-cm radiometer was responsive to 0.1 mm of gasoline at the highest viewing angle and was very responsive to gasoline at thicknesses greater than 0.5 mm at all three angles of view. The 2.2-cm radiometer is only slightly affected by gasoline as thick as 1.0 mm. Data collected for $\theta = 45^{\circ}$ are of questionable value because at this viewing angle the radiometers may have been viewing part of the tank wall.

An additional experiment was performed to determine the effect of increased gasoline thickness and to further examine an apparent oscillation in brightness temperatures noted during the first experiments. Gasoline was added to increase the thickness to 2.0 mm and the radiometers recorded vertical and horizontal brightness temperatures at a viewing angle of 30° for a period of 1.36 hours, as evaporation occurred. Figure 2-8 shows the 0.81 cm temperature variations observed during part of this time interval. These data exhibit a definite, although irregular, oscillatory pattern resulting from decreasing gasoline film thickness. The horizontally polarized component exhibited the largest oscillations and therefore a greater sensitivity to changing film thickness. Irregularities in the oscillatory pattern are attributed to disturbances of the gasoline surface by wind currents. The 2.2 cm temperatures remained substantially constant during the 1.36 hours.

2.4.2 BUNKER "C" FUEL OIL

Initial measurements of Bunker "C" fuel oil were performed on 9 April 1969. Bunker "C" fuel oil was added to the water to produce equivalent film thicknesses of 0.1 and 1.0 millimeters, and radiometric temperatures were measured for antenna viewing angles of 15, 30 and 45 degrees from nadir. Due to its high viscosity, the Bunker "C" fuel oil did not disperse evenly over the saline water surface, but coalesced into globules on the water surface, Figure 2-9. When enough oil was added to produce the equivalent of an 0.1-mm film, only about 20 percent of the water surface was covered with oil. Even the addition of 8,920 milliliters of oil, equivalent to a one millimeter film, did not completely cover the surface.

Water temperature at start of measurements was 18°C. At the completion of measurements the thermometric water temperature increased 2°C.

The 0.1 mm film of Bunker "C" fuel oil gave rise to 0.81 cm brightness temperature increase of 3°K for the horizontal polarization at a viewing angle of 30°. This small increase in radiometric temperature

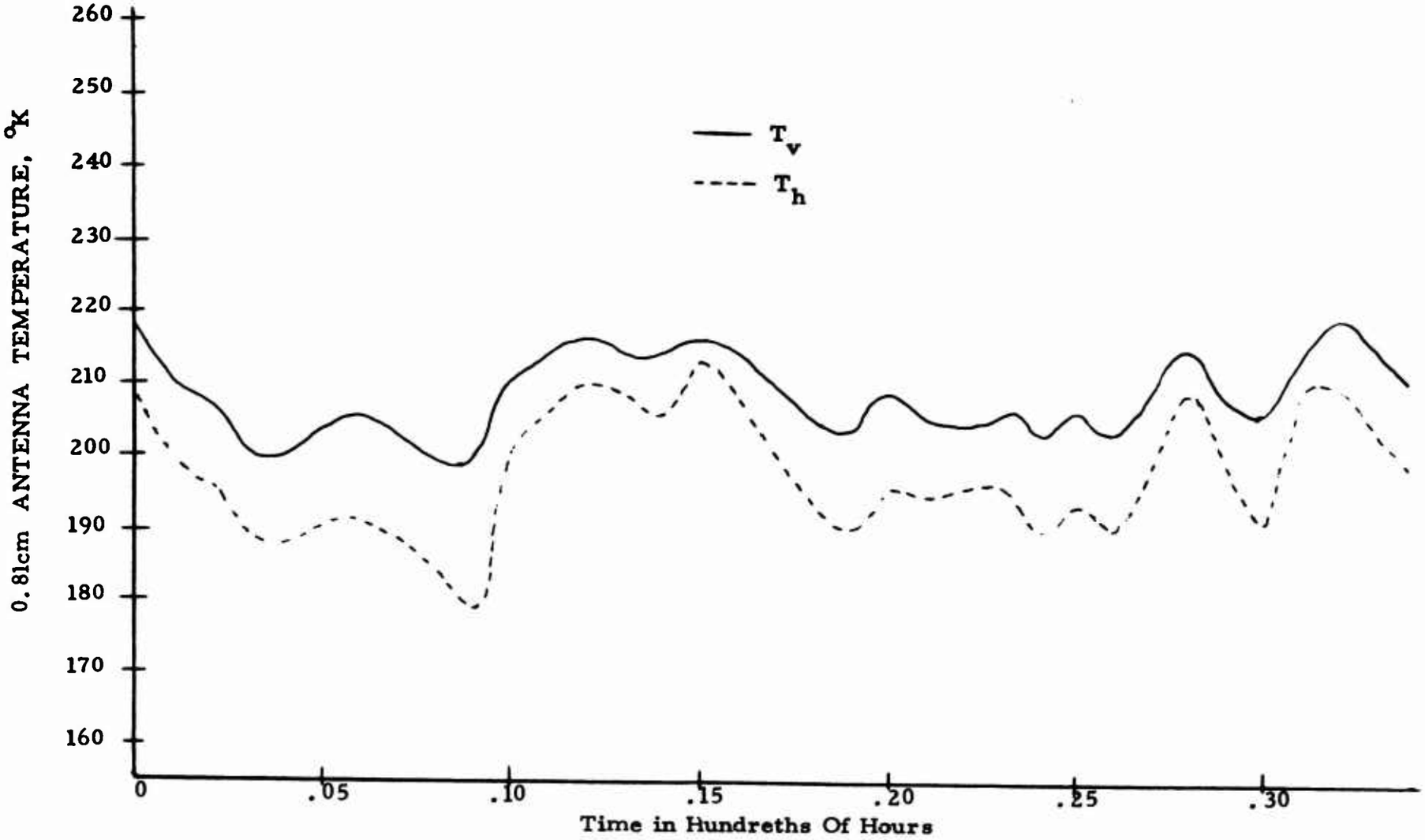

Figure 2-8. 0.81cm VERTICAL AND HORIZONTAL POLARIZATION RESPONSE TO 2.0 mm OF GASOLINE ON SEA WATER, $\theta = 30^{\circ}$

Figure 2-9. SALINE WATER SURFACE WITH SUFFICIENT BUNKER "C" TO FORM A CONTINUOUS 1-mm THICK FILM

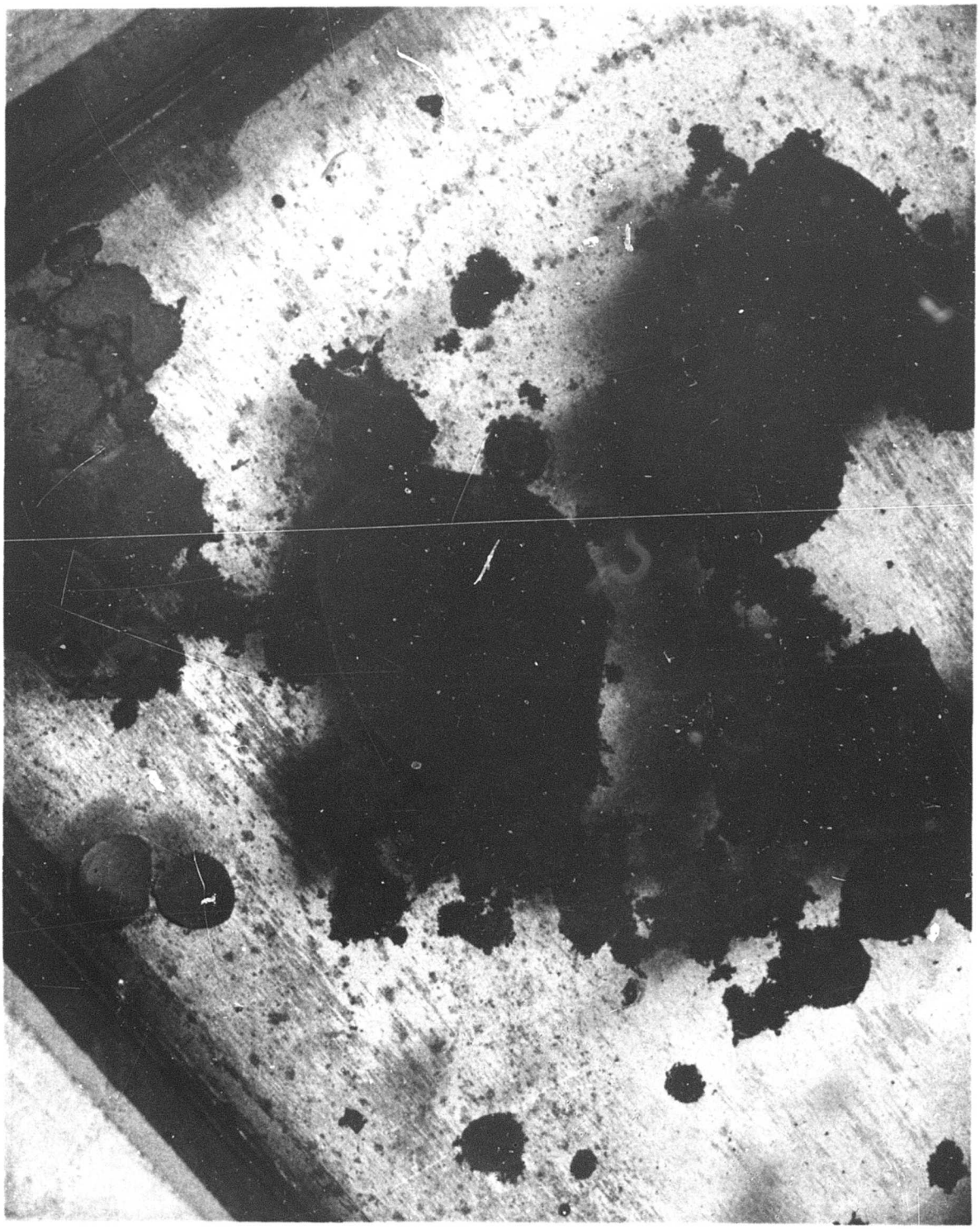

is undoubtedly due to the small percent of the surface covered by oil. With a greater oil thickness, 1-mm, the horizontal polarization temperature increased 24°K, and the vertical polarization increased 19°K for $\theta = 30°$. Radiometric temperatures observed by the 2.2-cm radiometer increased less than 5°K for all viewing angles for the 0.1-mm thickness. After a volume of oil sufficient to cover the surface had been added, the horizontal polarization temperature increased on the order of 30°K, while the vertical polarization temperature increased 25°K.

The 1-mm thickness of Bunker "C" fuel oil was aged in the environmental chamber for three days to determine the effects of aging on the microwave emission characteristics. On 12 April, radiometric measurements were made of the aged Bunker "C" fuel oil. The radiometric temperatures observed were lower than those recorded for fresh Bunker "C" fuel oil of the same thickness. All angles of view had higher radiometric temperatures than saline water without oil on the surface. The horizontal polarization temperatures for the 0.81-cm radiometer were 22°K greater than water at a viewing angle of 15 degrees. The 2.2-cm radiometer did not show an increase in radiometric temperature for the aged oil compared to the fresh oil. This response may be due in part to the dry nature of the aged oil. The surface of the oil had a consistency of tar and was very dry.

2.4.3 30-GRAVITY CRUDE OIL

On 12 April, radiometric measurements were performed on fresh 30-gravity crude oil. The experiment began at 13.32 hours and was completed at 14.51 hours. The thermometric temperature of the water was 292°K at the start of the experiment, and had increased 2°K at the end. Enough 30-gravity crude oil was added to form surface thicknesses of 0.1-mm, 0.5-mm, and 1.0-mm. The radiometric response of the 0.81-cm radiometer was less than 5°K in the horizontal polarization for thicknesses of 0.1-mm. At a thickness of 0.5-mm, the radiometric temperature increased 17°K for all viewing angles, and when 1.0-mm of oil covered the

surface, the radiometric temperature increased 50°K. The 2.2-cm response was low for all thicknesses of oil and only approached 10°K in the horizontal polarization after 1.0-mm had been added to the surface.

After three days of aging in the environmental chamber, radiometric measurements of the 30-gravity crude oil were repeated. The thermometric temperature of the water at the start and end of the measurements was 305°K. The 0.81-cm radiometer response in the horizontal polarization was higher by 35°K for $\theta = 15°$ and 60°K warmer for $\theta = 30°$. The 2.2-cm radiometer showed little or no response to the aged 30-gravity crude oil.

2.4.4 40-GRAVITY CRUDE OIL

Radiometric measurements of 40-gravity crude oil were performed on 16 April at 11.65 hours. The thermometric temperature of the water was 298°K at the start and temperature had increased by 3°K at the completion.

The response of both polarizations of the 0.81-cm radiometer was negligible for a thickness of 0.1-mm. With an increase in thickness to 0.5-mm, the response ranged from 13°K to 54°K higher at 15- and 30-degree viewing angles, respectively. After the oil thickness was increased to 1.0-mm, horizontal polarization temperatures for all viewing angles were greater than 50°K higher than water without oil on the surface. Vertical polarization temperatures were on the order of 40°K higher at 15- and 30-degree viewing angles.

From these measurements, the 2.2-cm radiometer appears unresponsive to light-weight, thin, low-viscosity oils. The maximum 2.2-cm response was 11°K in the horizontal polarization after 1-mm of oil was added to the surface. Only slight increases in radiometric temperature (on the order of 5°K for both vertical and horizontal polarization), were recorded for the 0.1-mm and 0.5-mm films.

2.4.5 20-GRAVITY CRUDE OIL

Radiometric measurements of 20-gravity crude oil were performed on 17 April. The measurements were initiated at 13.56 hours and completed at 14.86 hours. The water temperature remained a constant 300°K throughout this period.

The 0.81-cm radiometer showed negligible radiometric temperature increase at 0.1-mm thickness. A thickness of 0.5-mm produced an 8°K increase in radiometric temperature, in the horizontal polarization, and a 9°K increase in the vertical polarization. After the addition of 8920 mls of oil (equivalent to a 1.0 mm film), the radiometric temperatures increased on the order of 20°K in both the vertical and horizontal polarizations and at all viewing angles.

The 2.2-cm radiometer responded to oil thicknesses greater than 0.5-mm. With 0.5-mm of oil on the surface, the horizontal and vertical polarizations increased 15°K; with 1-mm of oil on the surface, the horizontal and vertical polarizations increased 20°K. The higher temperatures recorded for the 2.2-cm radiometer are not fully understood at present, but is probably due to unequal dispersion of the viscous oil and slightly different positions of the radiometer view spots. In all other instances, the 0.8-cm radiometer had higher temperature at both polarizations regardless of oil thickness, but in this experiment, only at a thickness of 1-mm did the 0.81-cm radiometer produce higher radiometric temperatures.

On 28 April 1969, radiometric measurements were performed on 20-gravity crude oil which had aged eleven days in the environmental chamber. Measurements were made during daytime hours between 15.05 and 16.00, and in the early morning hours of 29 April between 0.5 and 0.84 hours. The thermometric temperature of the water was 301°K during the daytime measurements, and 290°K in the early morning measurements of 29 April.

These measurements were undertaken at the discretion of Aerojet because of ambiguities noted in infrared radiometric temperatures of the Santa Barbara oil slick measured during an aircraft overflight.
Along with microwave radiometric temperatures, a Barnes PRT-5 (Precision Radiation Thermometer) was used by Aerojet to measure the infrared radiometric temperature. During the daylight measurements the infrared radiometric temperature of the oil was 297.5°K while the infrared radiometric

water temperature was 299.5°K. During the early morning measurements, the infrared radiometric temperature of the oil was 288°K, while the water was again 2°K warmer at 290°. In all cases, both during the daytime and early morning measurements, the microwave brightness temperature of oil on the surface was warmer by a factor of 20°K at 0.81-cm. Figure 2-10 shows the response of the 0.81-cm radiometer (horizontal polarization) to 20-gravity crude oil at 1-mm thickness. For all viewing angles, the radiometric temperature for oil on the surface is greater by 10 to 15 degrees except for the aged oil at a 15° viewing angle. At a viewing angle of 30 degrees, the radiometric temperature in all cases was 20°K to 30°K warmer than that of water at a comparable viewing angle.

2.5 COMPARISON OF RADIOMETRIC TEMPERATURES FOR VARIOUS POLLUTANTS

As evidenced by the foregoing discussion, petroleum contamination of the sea surface can be detected by microwave radiometry. In general, higher radiometric temperatures were recorded for pollutants than for water at all viewing angles. Figure 2-11 shows the horizontal brightness temperature for the 0.81-cm radiometer as a function of viewing angle. The 0.81-cm radiometric temperatures for all pollutants are higher than water by 10°K to 60°K at all viewing angles. The most pronounced difference occurs with 30- and 40-gravity crude oils, undoubtedly due to their dispersive nature. These pollutants do not react as the other more viscous oils such as 20-gravity crude oil and Bunker "C" fuel oil. The lowest radiometric temperature differential was observed for gasoline, due to its relative transparency in the microwave region. Figure 2-12 shows increased brightness temperatures observed for various thicknesses of gasoline films for $\theta = 30°$. Note that the shorter wavelength 0.81 cm signatures are approximately 3 times greater at both polarizations than that of the 2.2 cm sensor. This result is particularly meaningful because

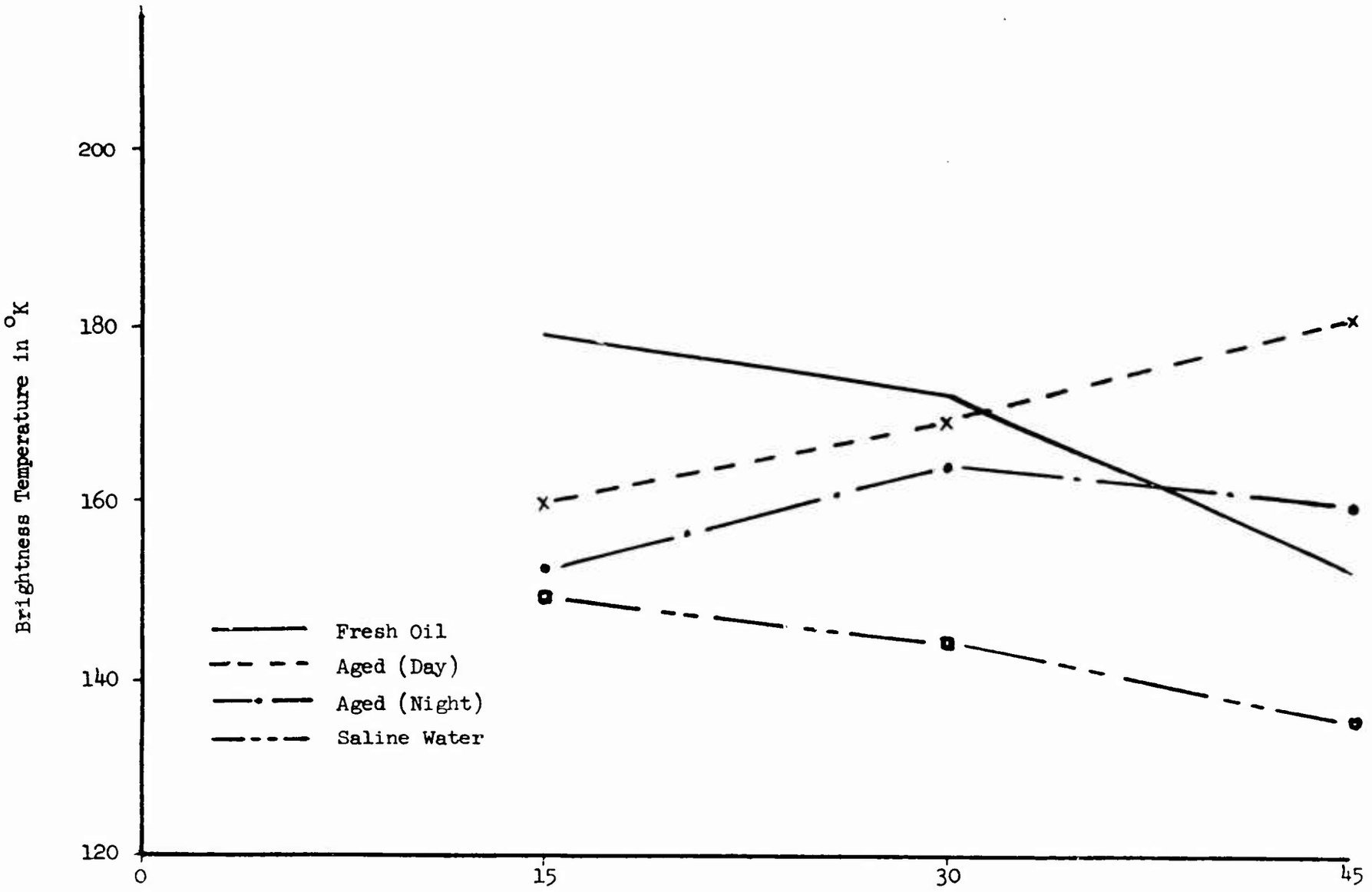

Figure 2-10. 0.8-cm HORIZONTAL POLARIZATION BRIGHTNESS TEMPERATURE FOR FRESH 20 API GRAVITY CRUDE OIL, AGED 20 API GRAVITY (DAY & NIGHT) AND SALINE WATER

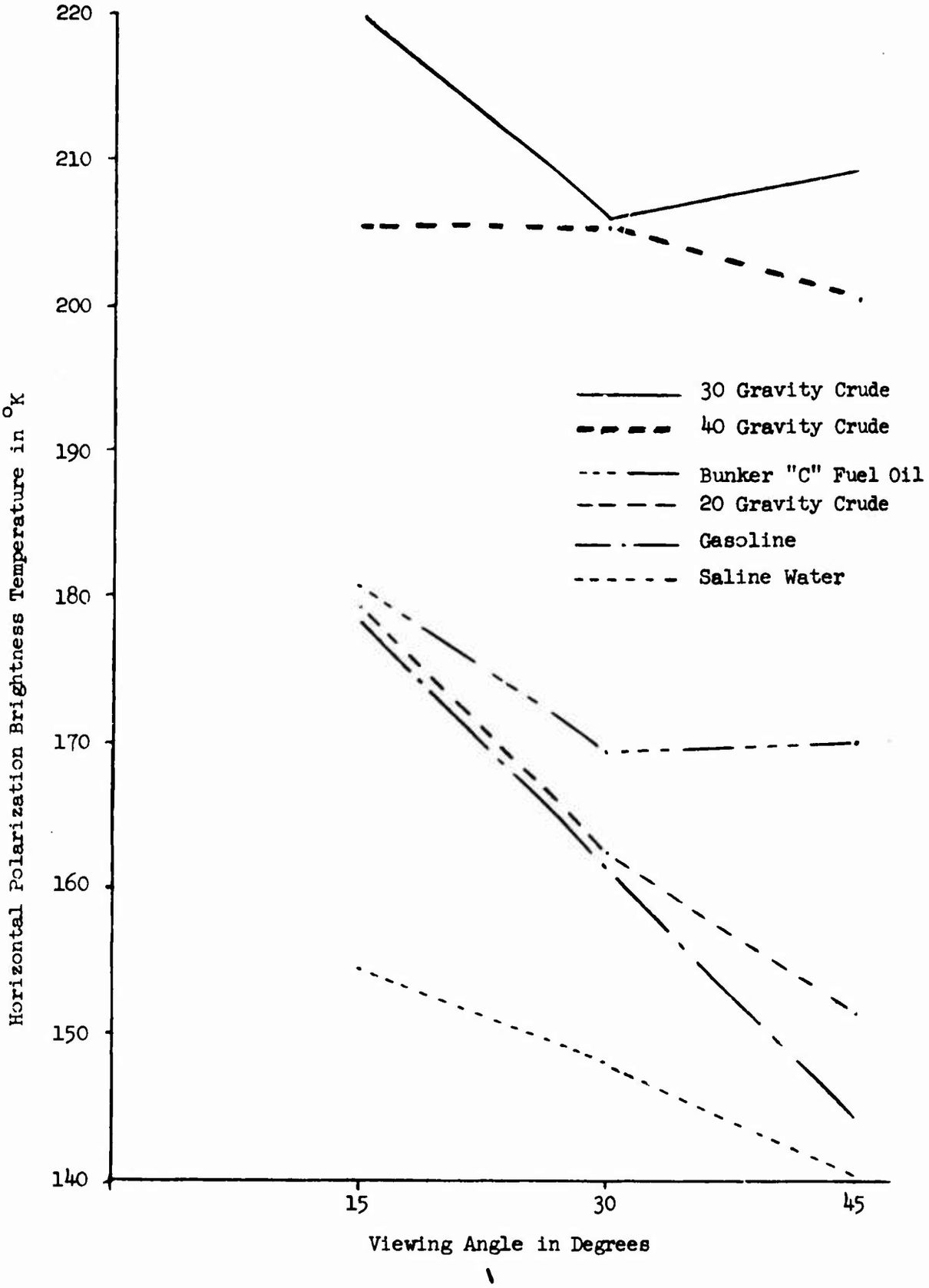

Figure 2-11. 0.8 cm HORIZONTAL POLARIZATION BRIGHTNESS TEMPERATURE FOR POLLUTANTS USED IN LABORATORY MEASUREMENT PHASE

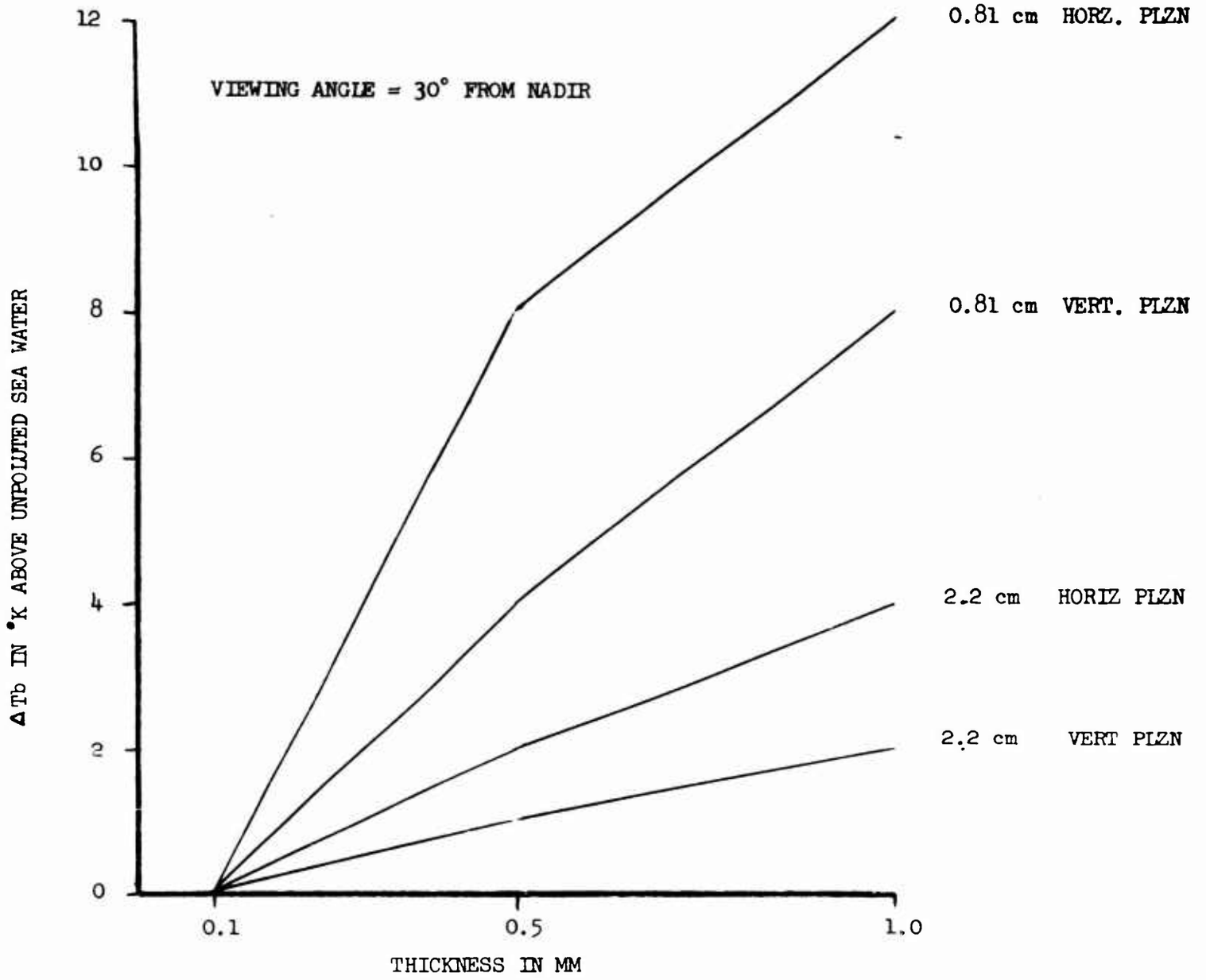

Figure 2-12 RELATIVE RESPONSE OF 0.81 cm and 2.2 cm BRIGHTNESS TEMPERATURE TO GASOLINE FILM THICKNESS

the gasoline films examined during laboratory studies were more uniform than those of other pollutants, and comparisons of data collected with the 2 microwave radiometers are most meaningful under these conditions. The two instruments were not focused on exactly the same portion of the water surface and, consequently, data taken of discontinuous or non-uniform oil films are more difficult to compare. The gasoline data indicate that the microwave sensor response is inversely proportional to sensor wavelength.

Figure 2-13 and Table 2-4 illustrate the microwave brightness temperature response of all oil products examined in the laboratory phase of this study. Conclusions drawn from this phase of the study are that the shorter wavelength radiometer (λ = 0.81 cm) is more responsive to oil films on the water surface and that the horizontally polarized configuration is more sensitive than vertical polarization at either wavelength. On this basis, the 0.81 cm dual polarized sensor was selected for at-sea tests.

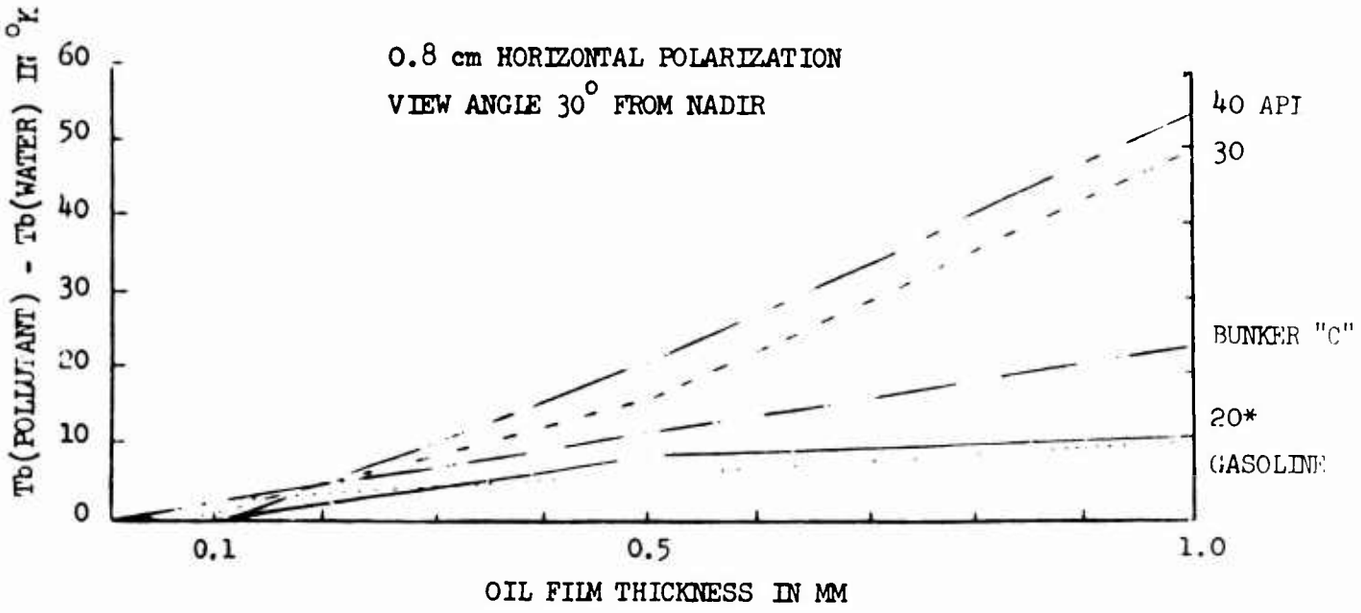

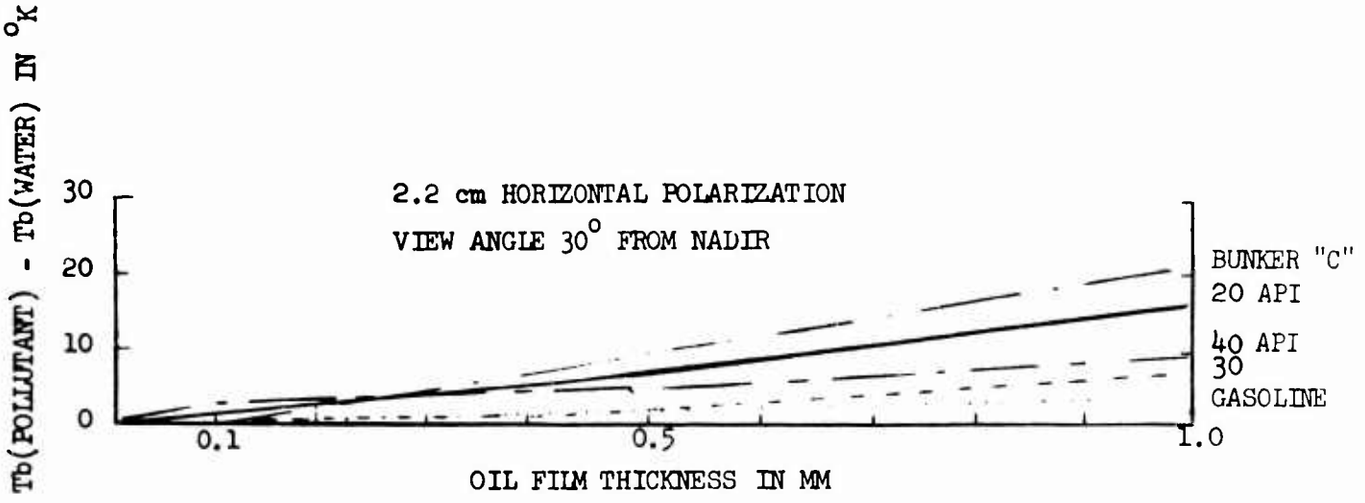

* Low values may be due to non-uniform distribution of oil

Figure 2-13. SUMMARY OF MICROWAVE RESPONSE TO PETROLEUM SAMPLES EXAMINED DURING LABORATORY EXPERIMENTS

Table 2-4

SUMMARY OF 0.81-CM RADIOMETRIC BRIGHTNESS TEMPERATURES FOR POLLUTANTS USED IN LABORATORY MEASUREMENTS (30^{o} VIEWING ANGLE)

Thickness	0.1 mm		0.5 mm		1.0 mm		1.0 mm Aged	
Polarization / Pollutant	T_v	T_h	T_v	T_h	T_v	T_h	T_v	T_h
Gasoline	176	154	179	158	183	162	-	-
Bunker "C"	175	152	-	-	190	173	178	156
20 Gravity	171	143	180	152	188	161	-	-
30 Gravity	180	157	190	173	215	207	222	216
40 Gravity	172	145	209	199	212	206	-	-

REFERENCES

1. A. T. Edgerton, et al, Passive Microwave Measurements of Snow, Soils, and Snow-Ice-Water Systems, Technical Report No. 4 (SGD 829-4), Office of Naval Research Contract NOnr 4767(00)NR 387-033, 15 February 1968.

2. A. Von Hippel, Editor, Dielectric Materials and Applications, Technology Press of MIT, 1954.

3. Private Communication with A. Stogryn, June 1969, Aerojet-General Corporation, El Monte, California.

4. Technical Report No. 3, Space-General Corporation, SGC-829R-5, February 1967.

Section 3

AIRBORNE MEASUREMENTS OF CONTROLLED SPILLS

3.1 INTRODUCTION

Sea tests consisting of airborne measurements of controlled oil spills were performed off the Southern California Coast during the period of 15 August through 12 September 1969.

Flights were performed with a Cessna 210 aircraft instrumented with a dual polarized 0.81 cm radiometer oriented with a forward antenna viewing angle of 45° above nadir. Small slicks of known volume were formed on the open ocean in the vicinity of longitude 119° 08' west and latitude 33° 45' north. The spills, ranging in volume from 165 to 350 gallons, were conducted in an area designated by the Operations Officer of the Eleventh Coast Guard District. Pollutants used for the study included both refined and crude petroleum, including marine diesel fuel, 20, 30 and 42 API gravity crude, and a mixture of diesel fuel and 20 gravity crude. The crude oils were provided free of charge by Chevron Research Laboratory (Standard Oil Co. of California). Flights were conducted under a variety of atmospheric and low sea state conditions, including flights at night. Measurements were also taken of the Santa Barbara oil slick.

3.2 INSTRUMENTATION AND EXPERIMENTAL METHODS

A 25-foot boat owned and operated by Aerojet-General Corporation was used to transport oil to the spill area and as a platform for collecting correlative information. Near the end of the flight program a chartered 65 foot vessel was also employed. Oil was transported to the spill area in 55 gallon drums and discharged with a 10 GPM capacity electric pump, Figures 3-1 and 3-2.

Aerojet's dual polarized 0.81 cm microwave radiometer was mounted in the rear of a chartered Cessna 210 aircraft. The radiometer antenna and 35 mm boresight camera were mounted external to the aircraft as a modified baggage door, Figures 3-3 and 3-4. The antenna and camera were mounted looking forward of the aircraft at an angle of 45° above nadir.

Figure 3-1. PHOTO OF PUMP TO DISCHARGE OIL

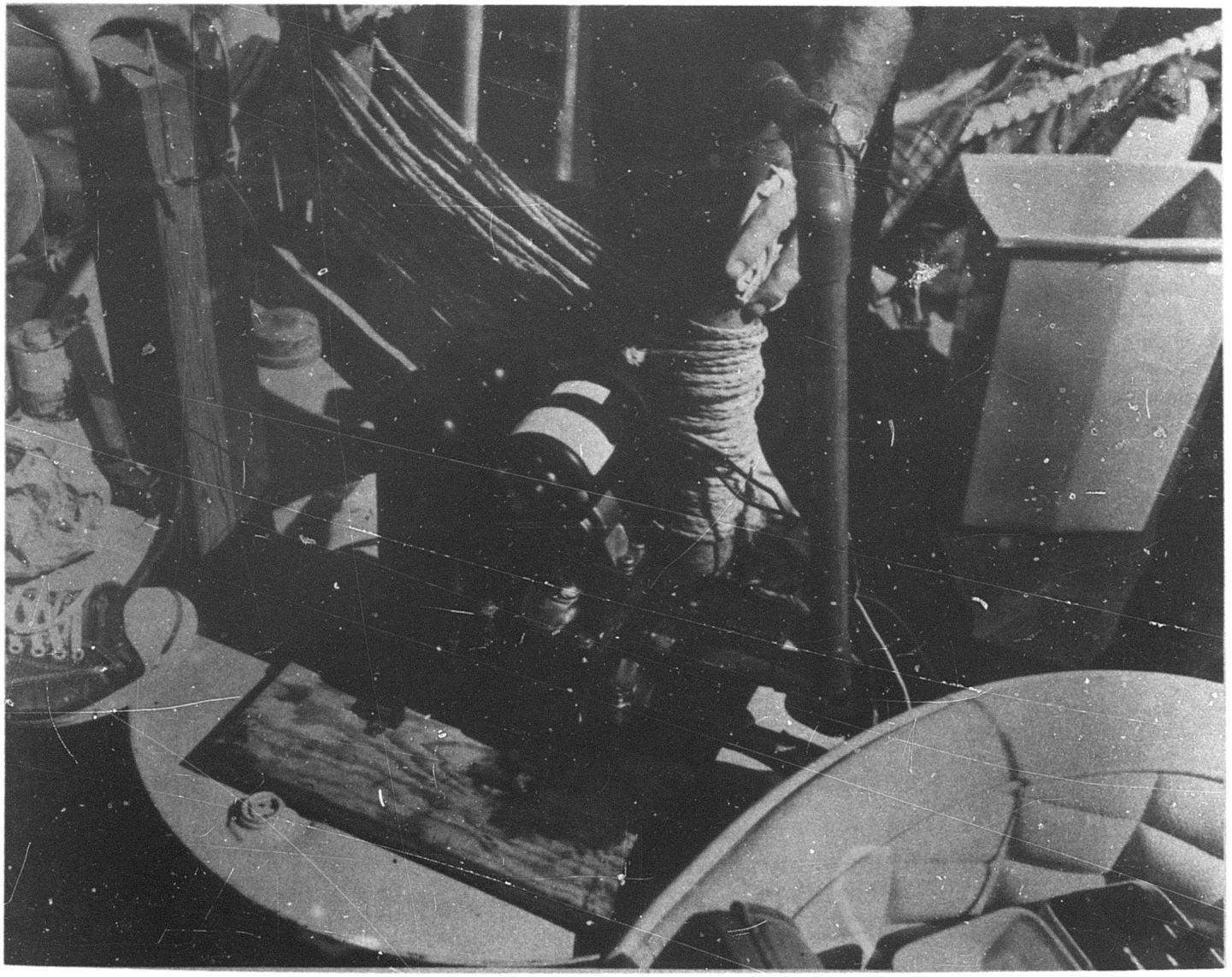

Figure 3-2. FORMATION OF SLICK

Figure 3-3. EXTERNAL MOUNTING FOR 0.81-cm ANTENNA AND 35mm BORESIGHT CAMERA

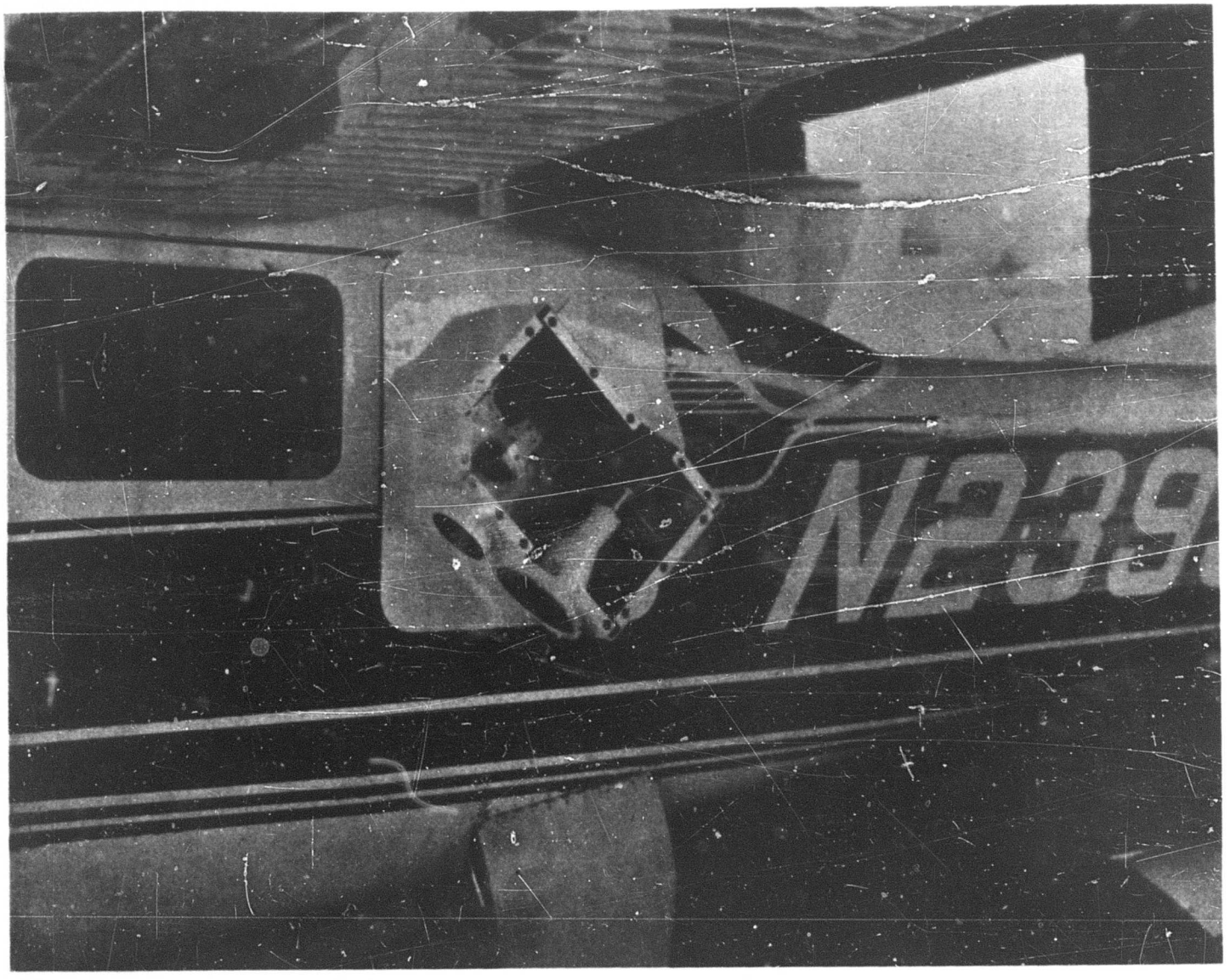

Figure 3-4. CLOSE-UP OF 0.81-cm ANTENNA MOUNTING

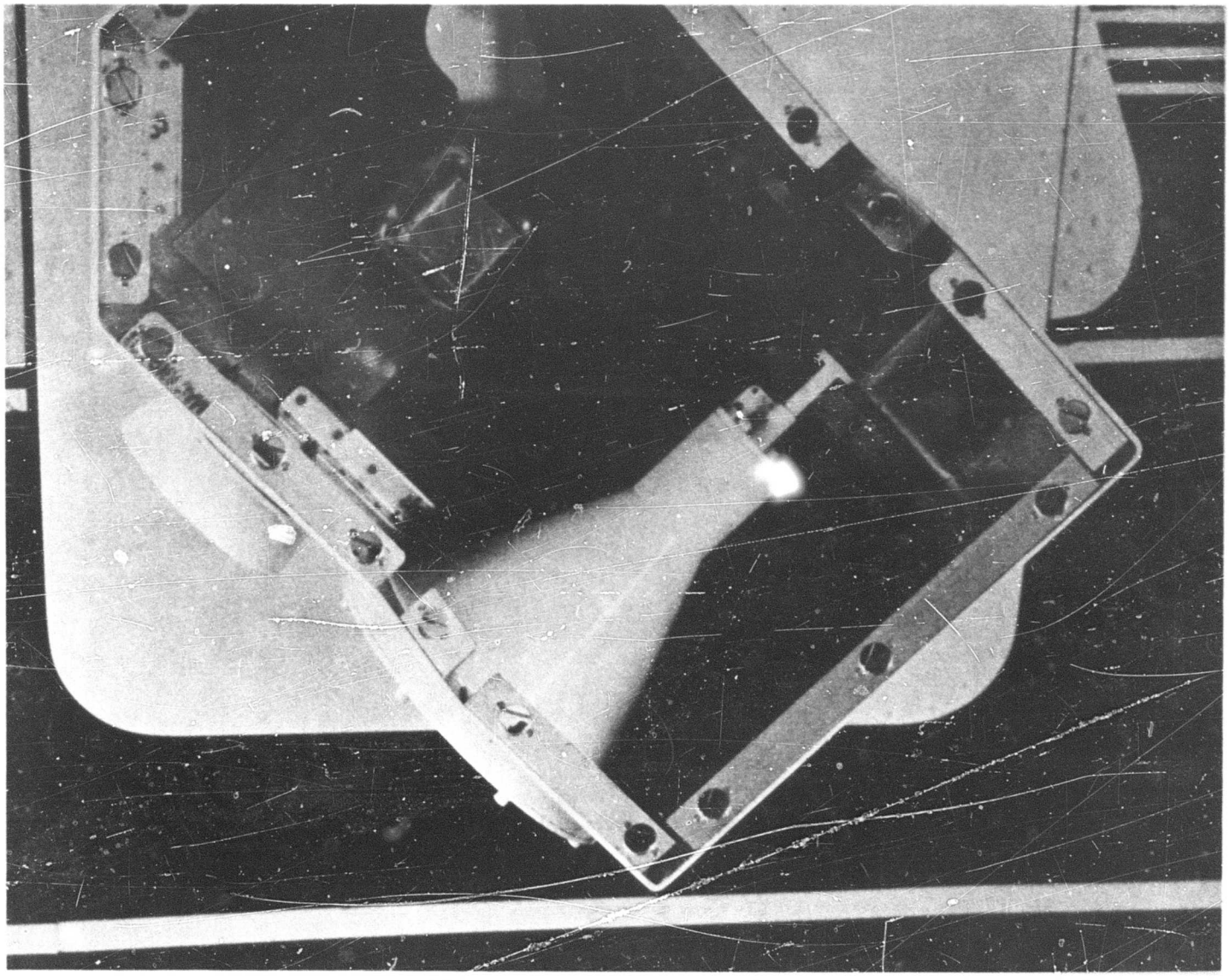

A block diagram of the radiometer system is shown on Figure 3-5. Two 12-volt, 90-amp hour batteries were used to isolate the radiometer and recording system from the aircraft power supply. A static inverter was used to convert the 12 volts DC to 115 VAC to operate the microwave system. A two-channel strip chart recorder was used to record radiometer data and camera frame number. The control panel was used to select the mode of operation. It contains a direct meter readout, switches for selection of radiometer integration time, camera frame rate, and radiometer outputs.

Radiometer sensitivities for various integration times were determined using data taken when the aircraft was parked on the asphalt runway apron. Sensitivities for three integration times are given in Table 3-1.

Table 3-1

RADIOMETER SYSTEM SENSITIVITY

Integration Time in Seconds	$\Delta T \frac{^{o}K}{\sqrt{}}$	$\frac{^{o}K}{H}$
0.1	2.4	2.5
0.5	1.5	1.1
1.0	0.64	0.45

An oil sampler was fabricated and tested for use in measuring oil film thickness. The sampler was a 2x2 foot aluminum funnel-shaped trap with a spring loaded plug. As the sampler was lifted up through the oil slick the orifice at the bottom remained open. When sufficient water had passed out the bottom the plug was released and the sample was then transferred to a graduated cylinder. Due to the high viscosity of the crude oils, large amounts of oil remained in the sampler coating the sides and

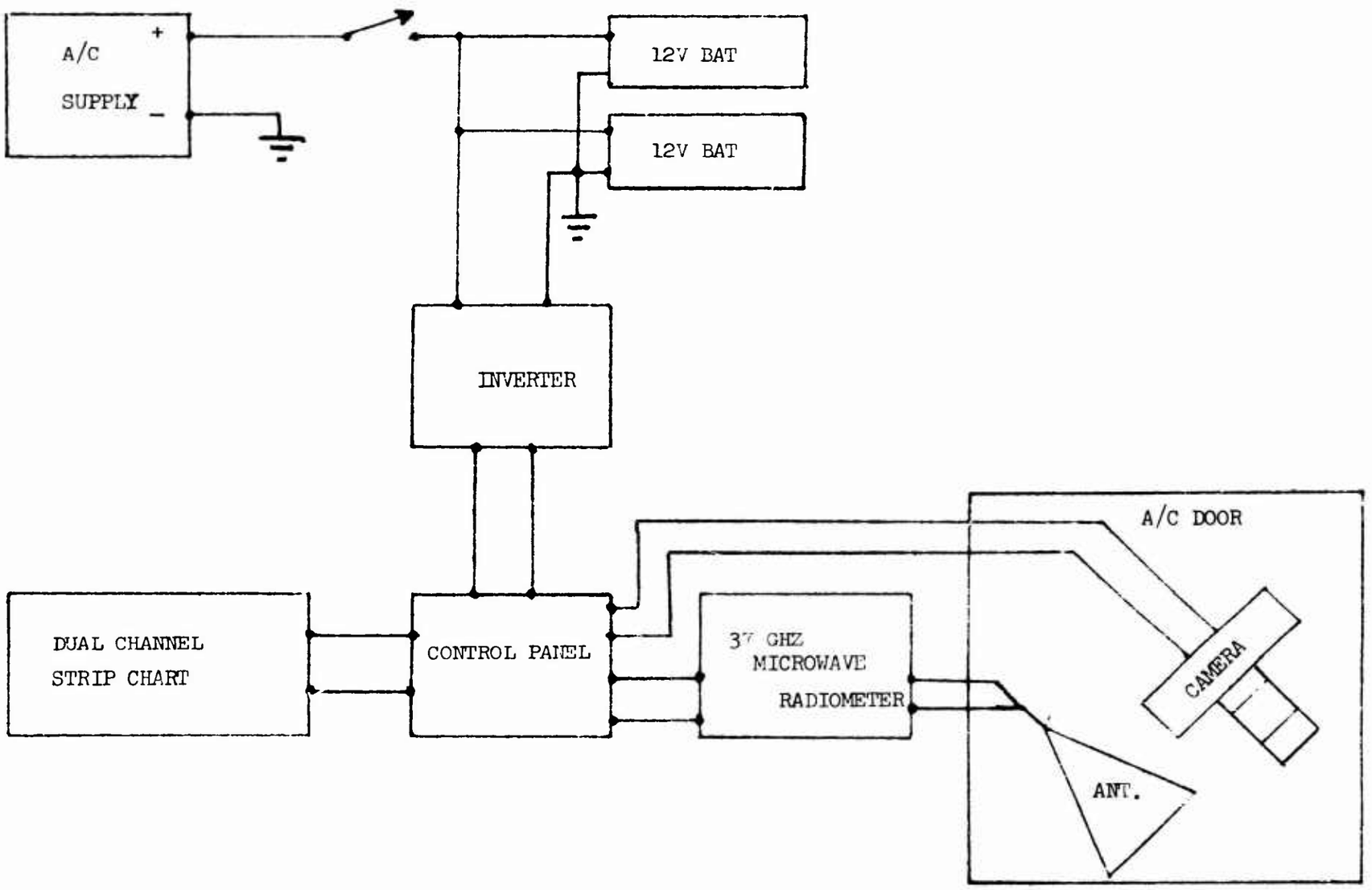

FIGURE 3-5. BLOCK DIAGRAM OF AIRCRAFT RADIOMETER SYSTEM

bottom, resulting in large uncertainties in the thickness measurement.

The thickness of oil slicks formed on the ocean surface was estimated by dividing the known volume of oil spilled by the surface area covered by the slick. The oil slick area was estimated both from the observer boat and the aircraft. The most reliable estimates were derived from the microwave data where the duration of oil slick signatures was accurately recorded and where aircraft speed was known with reasonable accuracy. This method provided an average thickness value for the entire slick. It should be noted that the slicks spread rapidly and that film thickness was not necessarily uniform throughout the slick.

From the estimated oil slick sizes the oil thickness was calculated, and graphs prepared, according to the following simple calculations. (An example graph is shown in Figure 3-6.)

$$\text{Oil Slick Thickness} = \frac{\text{Volume of Oil Dumped}}{\text{Area of Oil Slick}}$$

For 3 - 55 gallon drums of oil this becomes

$$T = \frac{22.0605 \times 3.048 \times 10^2}{A\ (\text{sq. ft.})} \quad \text{mm}$$

$$= \frac{7000}{A(\text{sq ft})} \quad \text{mm thickness}$$

In addition, correlation of the data through knowledge of the size of the main beam foot print at various altitudes and aircraft speeds was obtained by the calculations shown in Figure 3-7. From these calculations plots were made as shown in Figure 3-8 to assist in the analysis of the various oil slick brightness temperature anomalies.

3.3 MICROWAVE MEASUREMENTS

During data flights, primary emphasis was placed on measurements of beam-filling slicks of known dimension and thickness. Partial beam

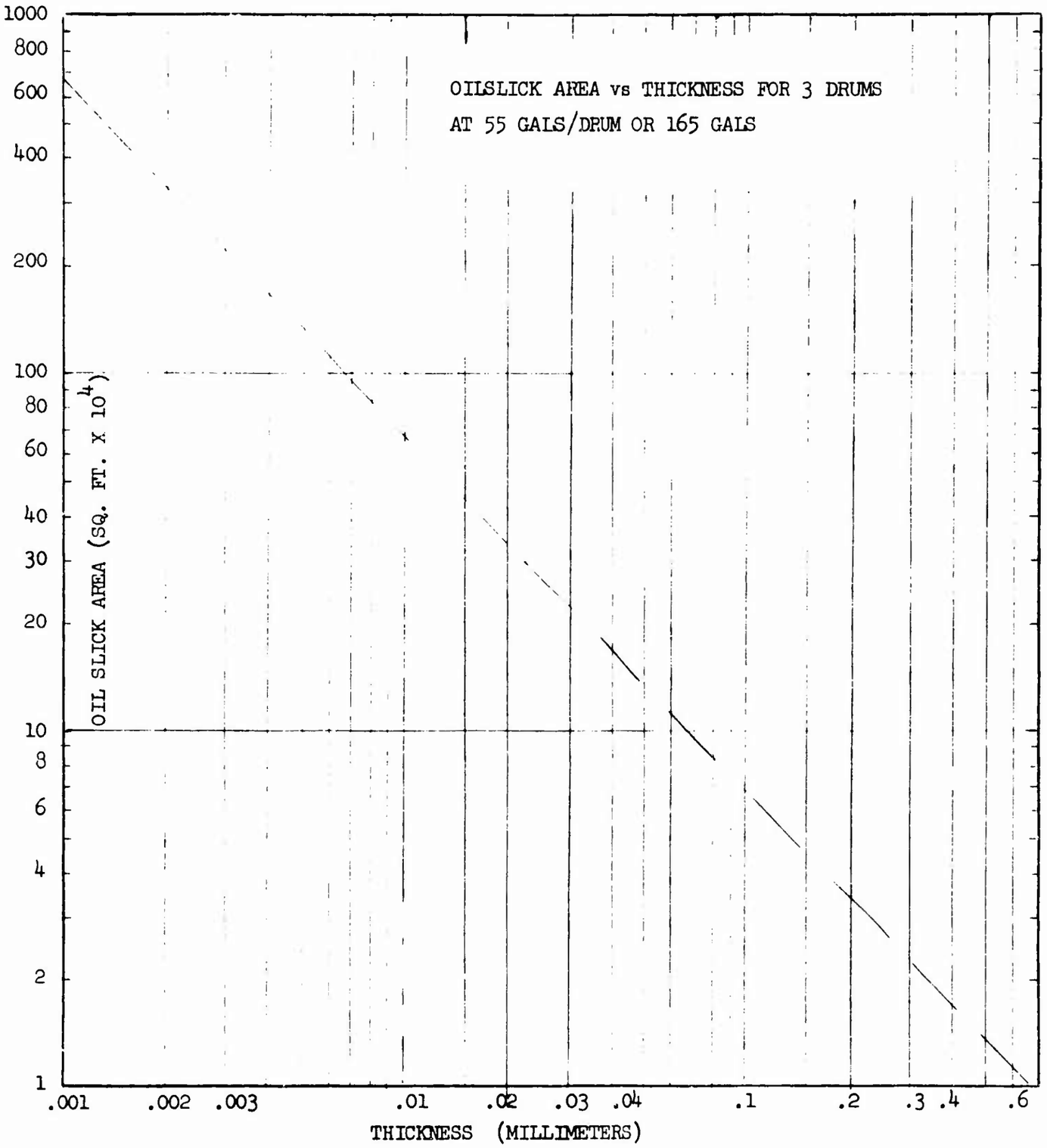

Figure 3-6. TYPICAL GRAPHS USED TO ESTIMATE THICKNESS OF OIL SLICKS

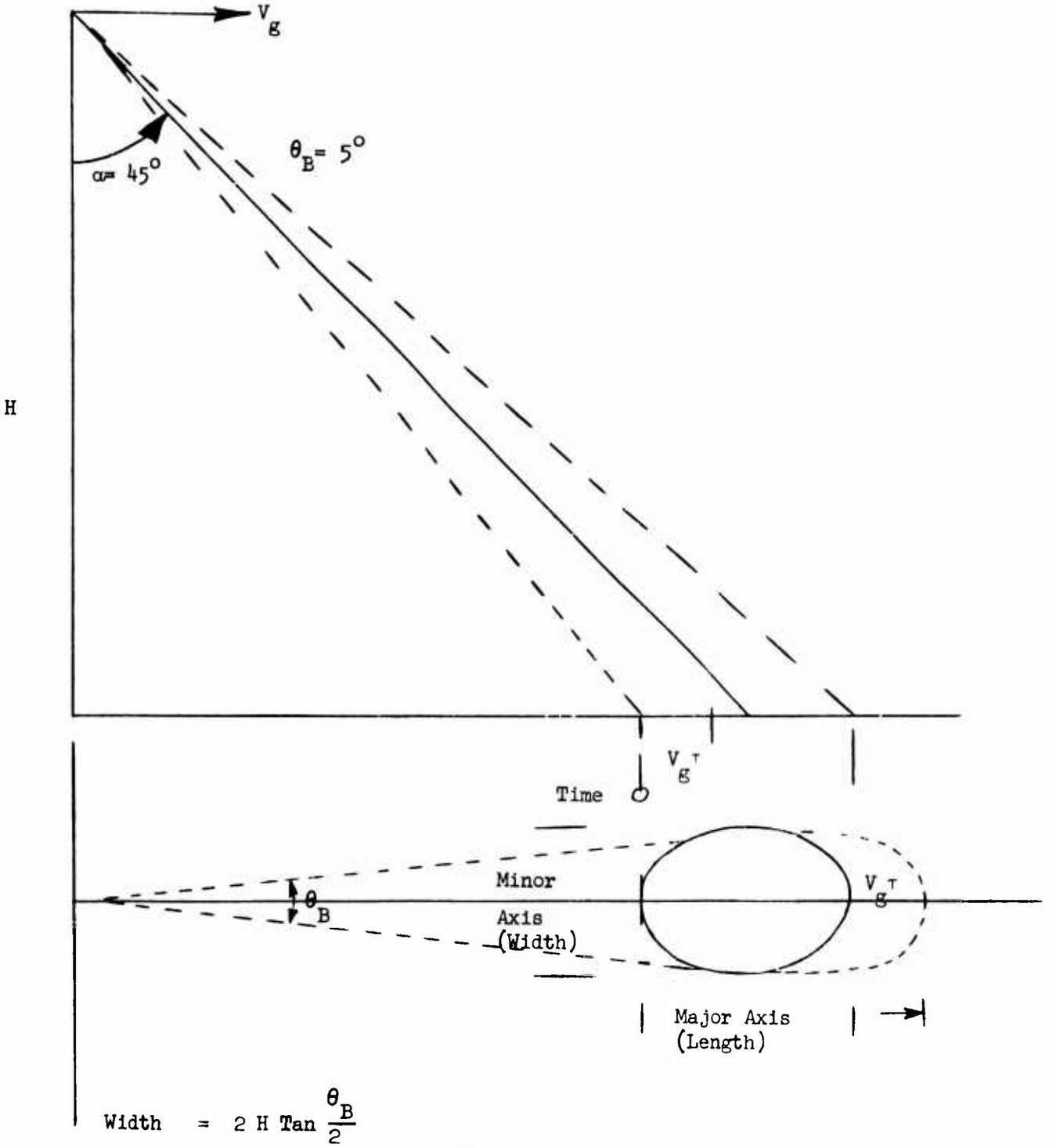

$$\text{Width} = 2\,H\,\text{Tan}\,\frac{\theta_B}{2}$$

$$\text{Length} = V_g\tau + H\left[\text{Tan}\left(\alpha + \frac{\theta_B}{2}\right) - \text{Tan}\left(\alpha - \frac{\theta_B}{2}\right)\right]$$

V_g = Aircraft Speed in Ft/Sec

α = View $\neq 45^\circ$

τ = Integration Time in Secs.

H = Altitude in Feet

θ_B = Antenna Beam Width (5°)

Figure 3-7. CALCULATIONS SCHEME FOR BEAM FOOTPRINTS

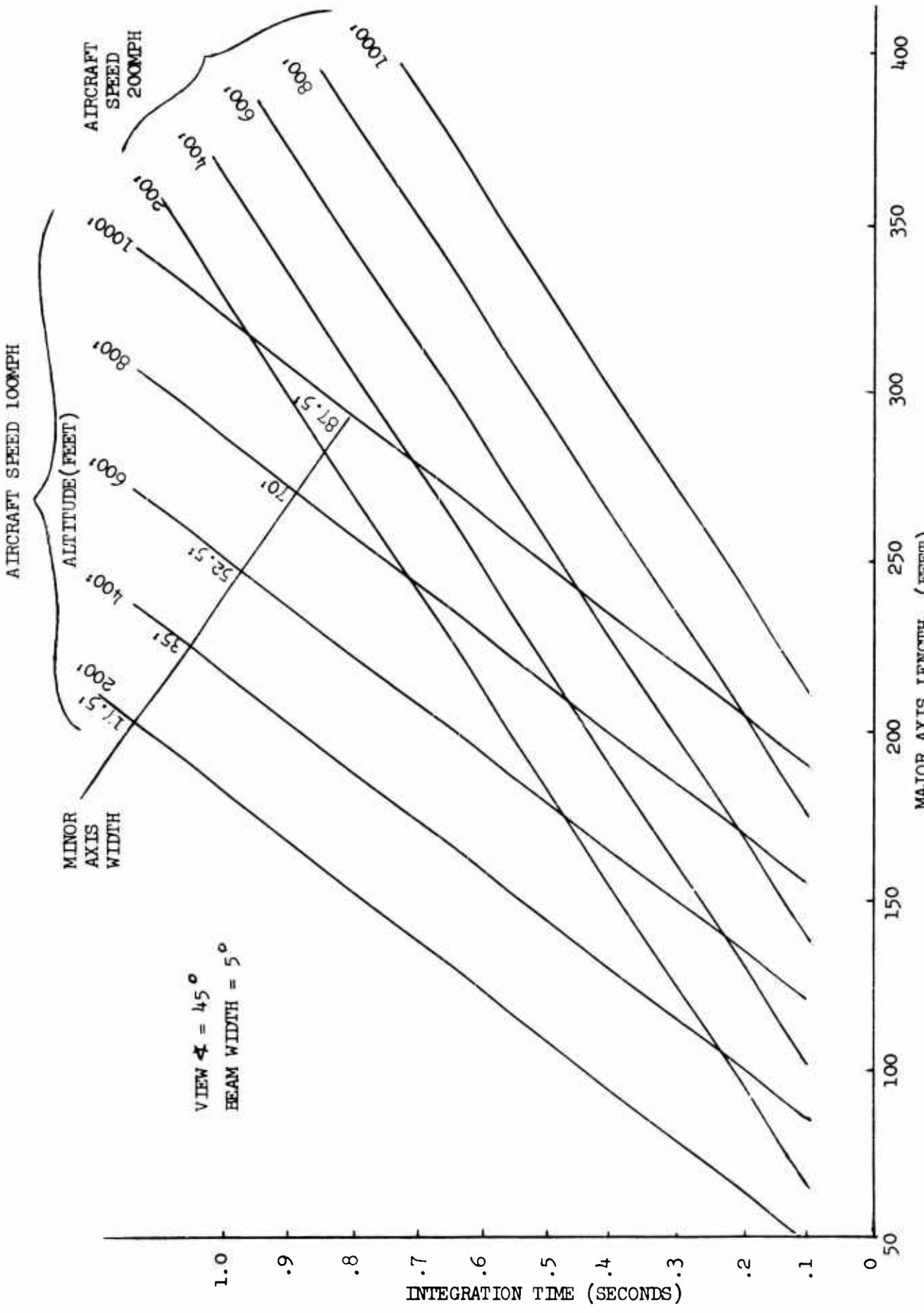

FIGURE 3-8 PLOT RELATING VARIOUS MAIN BEAM FOOTPRINT SIZE WITH AIRCRAFT SPEED AND HEIGHT AND RADIOMETER INTEGRATE TIME

fill data were considered of secondary importance. Consequently, most data flights were conducted at low altitude ranging from 200 to 500 feet. A substantial amount of unpolluted ocean data were recorded during each overflight to establish a reference level for comparing the slick signature. In the following text radiometric measurements of the slicks will be specified in terms of observed departure from the ocean background emission $\Delta T = T_B$(oil slick) - T_B (adjacent unpolluted ocean surface). Flight data are presented in chronological order. Tabie 3-2 represents a summary of the spills and missions flown.

3.3.1 SANTA BARBARA OIL SLICK

The first mission was an instrumentation checkout flight made over the Santa Barbara oil slick on 26 August. This flight was coordinated with the Aerojet (AGC) vessel which was used for obtaining correlative information. The slick was of variable thickness and appeared to be aged; it was scummy and frothy and of variable width (up to 100 feet). Overflights were made at 1400 hours and 1430 hours. Water temperature during the overflights was 19.8°C. Sea conditions were calm with large ground swells. Data obtained from these overflights were not of the highest quality. This was due, in part, to a need to experiment with different integration times to determine the suitable integration times for various flight altitudes.

3.3.2 MARINE DIESEL FUEL OIL SPILL (165 GALLONS, 28 August 1969)

On 28 August 1969 a 165 gallon diesel oil spill was made in the designated area and thirty overflights were subsequently performed at altitudes of 200 and 400 feet. Integration times of 0.1, 0.2, 0.4 and 0.5 seconds were used.

Sea conditions were calm (i.e., sea state 1) and the water temperature was 19.3°C.

Table 3-2

SUMMARY OF AT-SEA TESTS

Date	Type of Pollutant	Sea & Weather Conditions	Water Temperature	No. of Over-flights	Alti-tude (ft)	Remarks
8/26/69	Crude Gravity not known	Calm (1) With large ground swells	19.8°C	10	200	Aged crude oil in Santa Barbara Channel
8/28/69	Marine Diesel Fuel	Calm No wind	19.3°C	30	200; 400	165 gallons
9/3/69	30 API Gravity Crude	White Caps Wind 7-10 mph	19.0°C	22	200; 250; 400; 500	Slick dispersed rapidly
9/9/69	20 API Gravity Crude	Calm No wind	19.2°C	32	200; 400	
9/12/69	42 API Gravity Crude	Calm No wind	18.9°C	21	200; 250; 400	
9/12/69	Marine Diesel Fuel	Calm Slight breeze	18.9°C	8	200	350 gallons
9/12/69	Mixture at 20 API Gravity Crude Oil & Diesel Fuel	Calm Slight breeze	18.9°C	11	200	200 gallons, darkness

Radiometric temperature anomalies during the early slick formation were +12.5 and +5°K for horizontal (T_h) and vertical polarizations (T_v), respectively. As the slick spread out and became thinner, radiometric temperatures decreased to ΔT_h = +7°K and ΔT_v = +5°K when the slick was 400 feet in diameter and had an average thickness 0.04 mm. Figure 3-9 shows the decrease in brightness temperature as the thickness of the oil slick decreases. Differences in flight altitude have little effect on the radiometric response since the slicks were usually beam filling at the altitudes used for data flights. (Compare runs 17 and 19 in Appendix B where, at an altitude of 400 feet, ΔT_h = +8°K and ΔT_v = +5°K.)

The slicks formed during intentional spills were not always of uniform thickness. Figure 3-10 shows an example of a double-peaked anomaly taken when the surface of the ocean was covered with 165 gallons of diesel fuel having an average estimated thickness of 0.06 mm.

This variation in radiometric response is undoubtedly due to variations in thickness of the slick resulting from the method of spillage. This was the first spill and excessive time was lost transferring the pump from one barrel to the next so that, rather than one essentially continuous slick, there were two which gradually coalesced.

Figure 3-11 is a photograph showing diesel oil spilled on the ocean surface on August 28, 1969. Note the subsidence of the higher frequency wavelets due to the presence of the diesel oil. This has produced observable brightness temperature contrasts, expressed in terms of the frequency content of the recorded data, noted throughout the experiment.

3.3.3 30 API GRAVITY CRUDE OIL SPILL (165 GALLONS, 3 September 1969)

On the morning of 3 September 1969 the aircraft rendezvoused with the vessel at 1000 hours. Sea conditions during these overflights were choppy with winds from 7-10 mph and gusts to 15 mph. Occasional white caps and foam were present over much of the sea surface. The

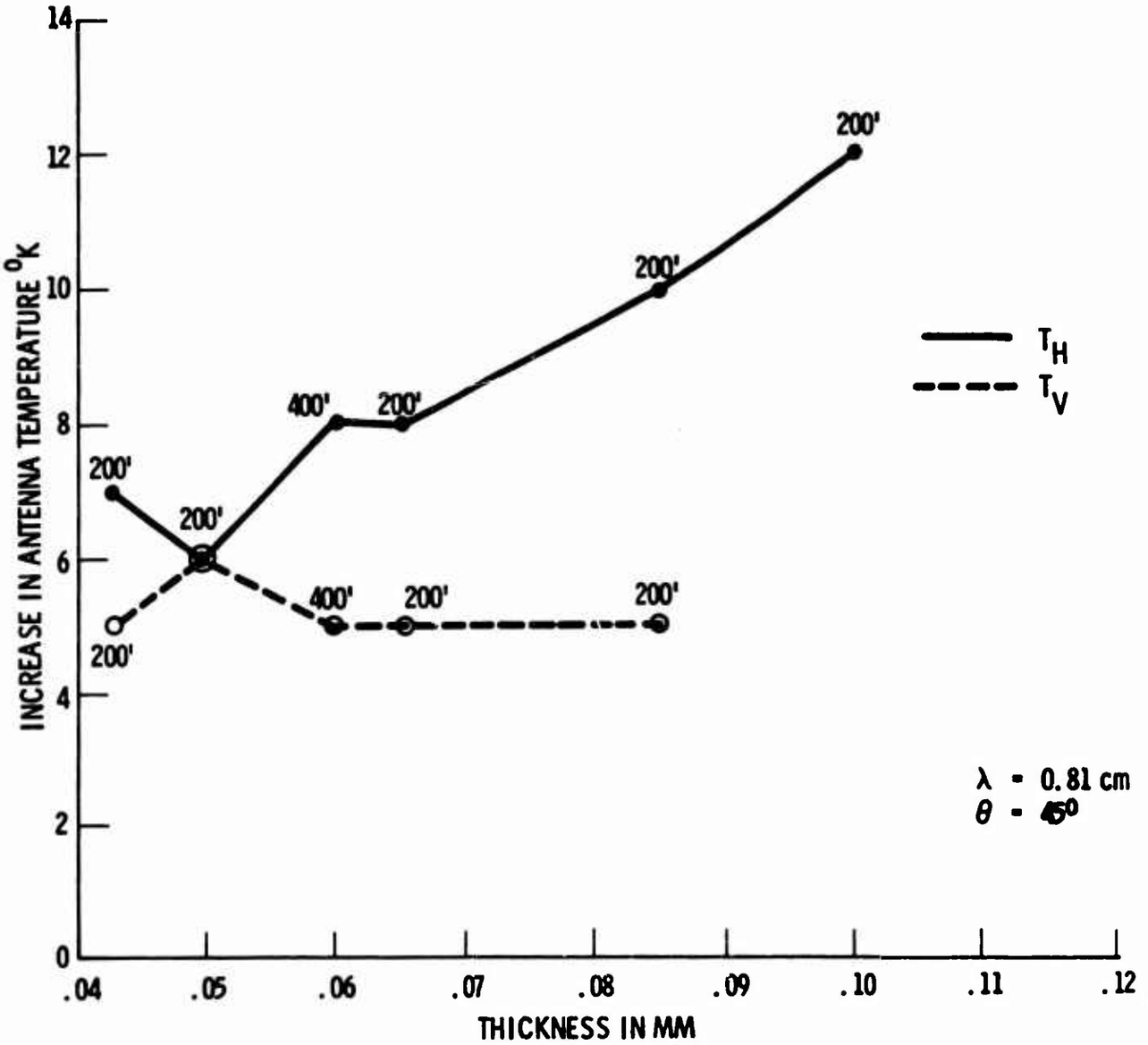

Figure 3-9. DIESEL SLICK OVERFLIGHT 8-28-69
OIL FILM THICKNESS VS ANT. TEMP. INCREASE

Date: 8/28/69 Run No. 22
Altitude = 200 Feet
Aircraft Velocity = 100 mph
Radiometric Integration Time = 0.5 Sec.
Average Thickness = 0.06 mm

Comments:

1. Note Increase In T_B Over Background Noise, Also Note the Change In Spectral Response(i.e. Increase In Low Frequency Component)
2. Note High Frequency Component Over Water Surface Without Oil.

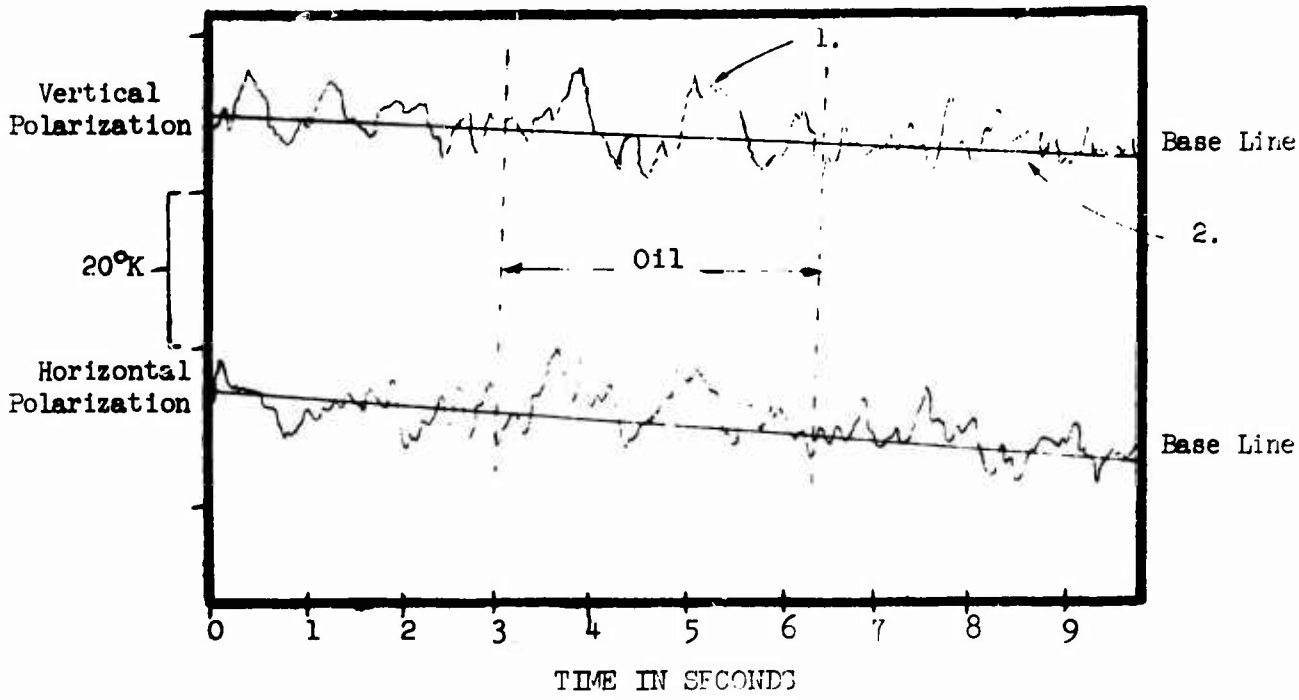

Figure 3-10. 0.81 cm RESPONSE FOR DIESEL OIL SLICK

Figure 3-11. VIEW OF DIESEL OIL SPILL 8-28-69

radiometric signature of the vessel was measured from an altitude of 400 feet at 1004. The radiometric response of the vessel appeared as an increase in antenna temperature of 30°K and 20°K for horizontal and vertical polarization, respectively. The 165 gallon oil spill was initiated at 1005 and completed at 1025 and overflights were made at altitudes of 200, 250, 400 and 500 feet using a sensor integration time of 0.5 seconds. Throughout all overflights the aircraft speed was maintained at 100 mph.

An interesting phenomenon occurred during these overflights where the vertically polarized radiometric signature was higher than the horizontal component (it should here be noted that ΔT_h was always higher under laboratory conditions where the water surface was smooth). This reversal of signatures is associated with the rough sea surface.

Ocean surface roughness is known to influence microwave emission, although the relationship between roughness and microwave emission is not fully understood. In general, the rougher the water surface, the warmer observed brightness temperature. The horizontal component, T_h, is more responsive to roughness changes. Recall that the oil slick microwave signatures are really the contrast between emission by the unpolluted ocean surface and the emission of the oil covered area. Consequently, variations in the background or unpolluted ocean surface emission influence the signature of the slick. On this particular day the choppy waves were conspicuously damped by the presence of the slick so that two opposing emission mechanisms were in operation. Emission by the oil film tends to increase observed brightness temperatures, especially the horizontally polarized component, whereas damping of the ocean surface roughness tends to lower emission from the ocean surface.

Oil slick signatures were on the order of $\Delta T_v = +7.5^{\circ}K$, and $\Delta T_h = +5^{\circ}K$ during the initial slick formation and $\Delta T_v + 6^{\circ}K$ and $\Delta T_h = -3^{\circ}K$ during the final overflights at 1105. Slick dimensions at 1105 were estimated (from the aircraft) to be 100 yds by 300 yds. These dimensions correspond to an average film thickness of 0.015 mm. It is suspected that the thickness of the slick was quite variable and that thicker portions of the slick existed. Figure 3-12 exhibits the radiometric characteristics of the 30 API gravity oil slick at 1102.

Figure 3-13 is a photograph of the 30 API oil spill on September 3, 1969. Note in this photograph the damping of the high frequency wavelets by the oil. The green color in the center area of the picture results from green marker dye placed in the water.

3.3.4 20 API GRAVITY CRUDE OIL (165 gallons, 9 September 1969)

Weather conditions during the morning and early afternoon of 9 September prevented the aircraft from making visual contact with the ground truth vessel. The low overcast and fog partially lifted and contact was made at 1530 hours. The 20 gravity spill was initiated at 1540. To assist the aircraft in flight line orientation, small quantities of urine dye were placed in the water at the point of initial spillage and at the end of the spill. The oil dump was completed at 1600.

Figure 3-14 shows the condition of the sea surface and the damping effect of oil on the waves. Note the oil slick is directly below and slightly to the right of the aircraft in the photo. Overflights were made at altitudes of 200 and 400 feet using small scale radiometer integration times of 0.5 and 1.0 second.

Due to drifting of the vessel during spillage the slick was elongated in a northeast-southwest direction. Overflights were made both along the long axis and perpendicular to it. Data do not indicate any appreciable difference in the radiometric response, a function of flight direction.

The radiometric signature of the 20 gravity crude ranged from a maximum of $+8^{\circ}K$ for the horizontal polarization and $+7^{\circ}K$ for the vertical polarization. An example record taken approximately two minutes after

Date: 9-3-69 RUN 21
Altitude = 400 Feet
Aircraft Velocity = 100 mph
Radiometer Integration Time = 0.5 sec.
Average Slick Thickness ≈ 0.01 mm

Comments:

1. Horizontal Polarization Signature is negative.

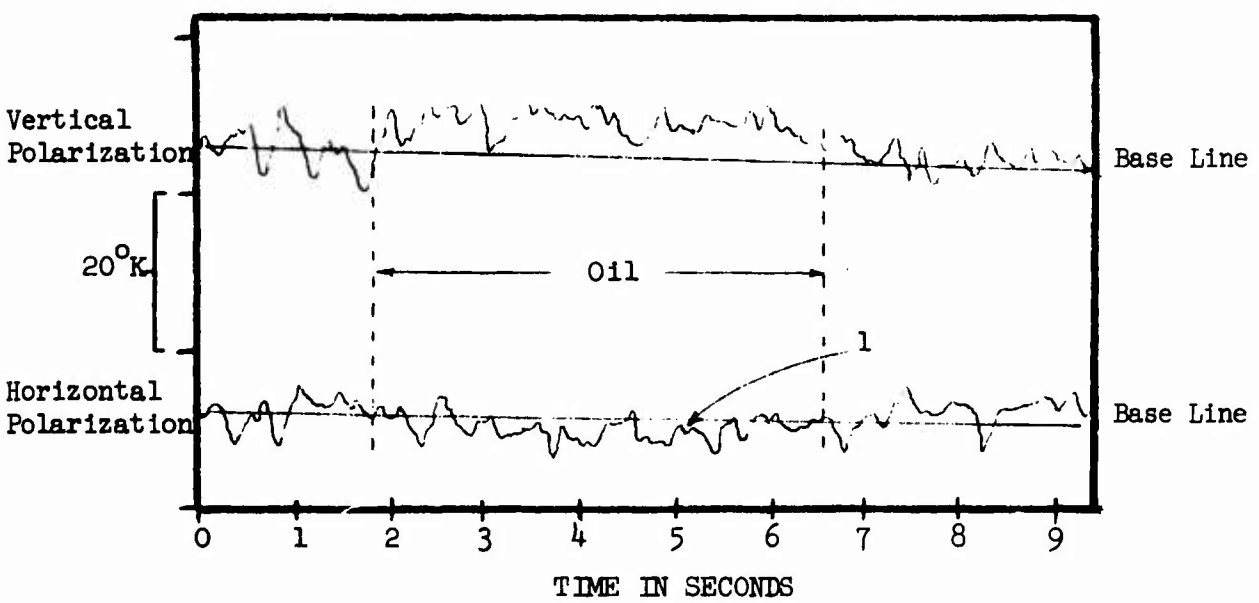

Figure 3-12. 0.81 cm RESPONSE FOR 30 API GRAVITY CRUDE OIL SLICK

Figure 3-13. PHOTO OF 30 API GRAVITY CRUDE OIL SPILL 9-3-69

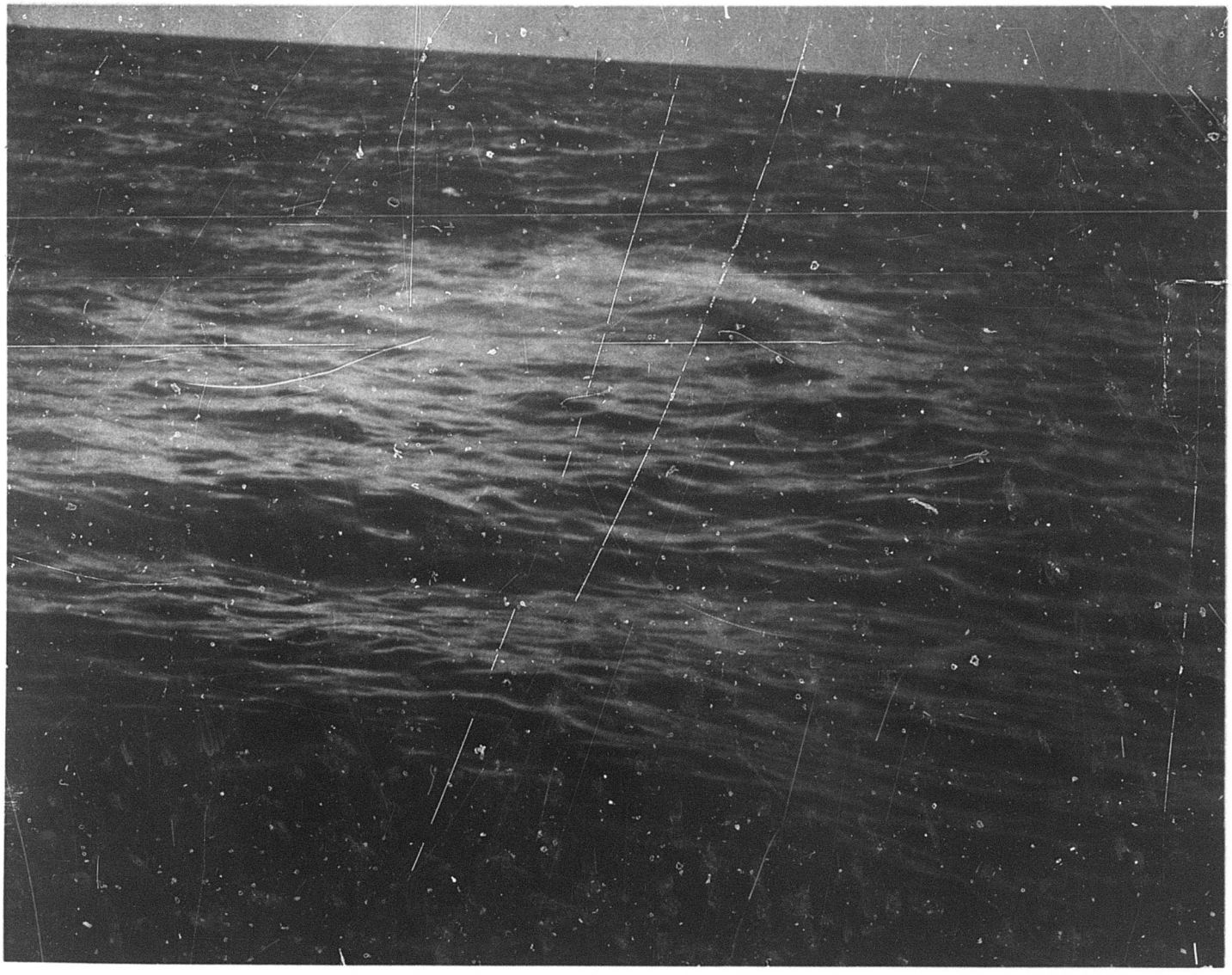

Figure 3-14. PHOTO OF 20 API GRAVITY CRUDE OIL SPILL 9-9-69

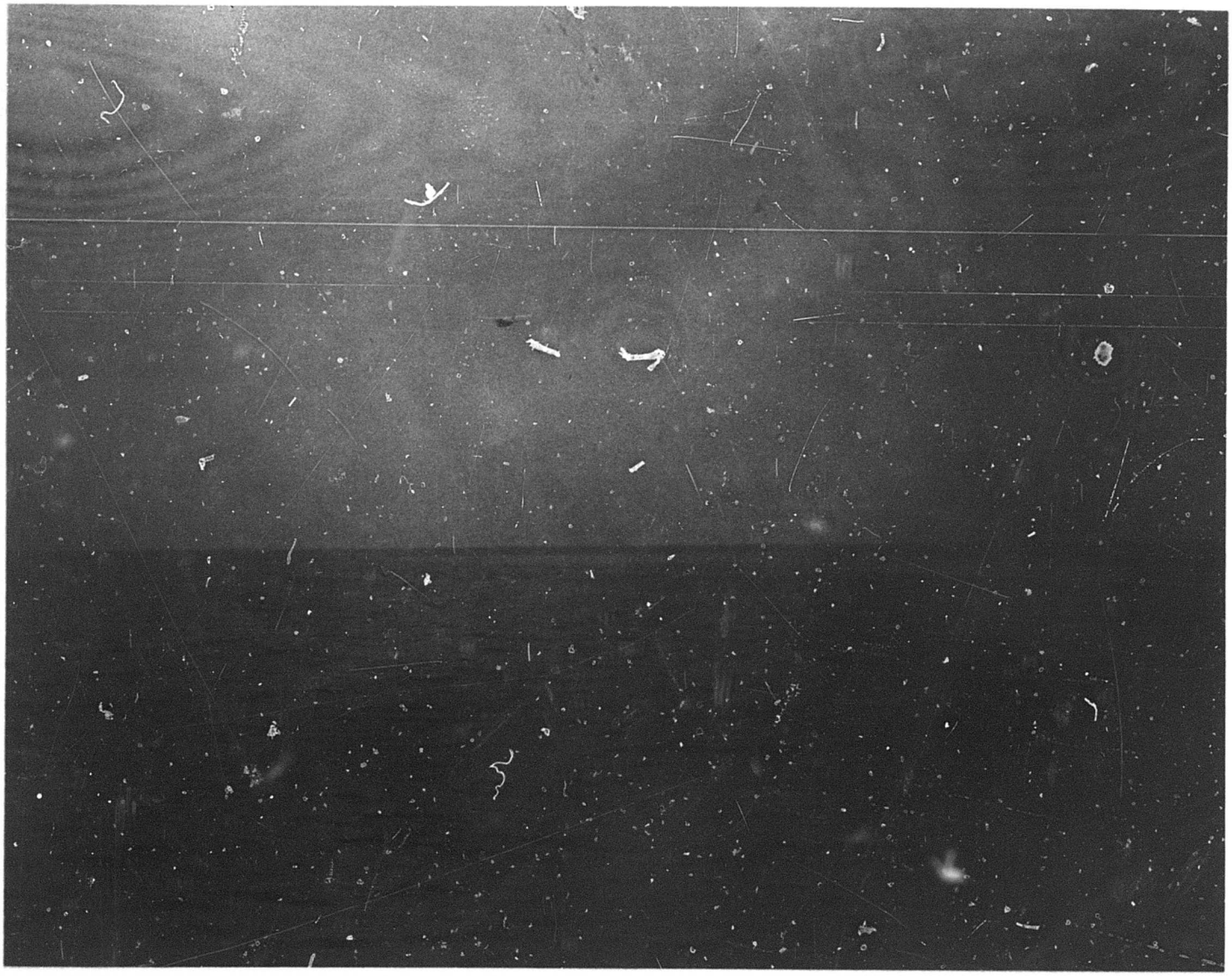

completion of the spill (oil relatively thick) is shown in Figure 3-15. Note the predominant single anomalous peak in this run. Another example of the radiometric response is from data flight 13, twenty minutes after completion of the spill. Average film thickness calculated for the slick during this pass was 0.05 mm; however, the surface craft observers noted that the oil was not uniformly distributed but consisted of irregular thicker and thinner areas. The anomaly from this overflight is shown in Figure 3-16. This figure shows the variant effects due to the irregular oil distribution. It should be noted that the horizontal polarization signature is indicative of the discrete patches of thicker oil. The dimensions of the slick at the time of the overflight was estimated to be 250' x 400'.

Thirty-one data flights were made over the oil slick. Data tabulated in Appendix B shows ΔT_h decreasing from the initiation of the spill to the end of the overflights. The minor variations in the somewhat linear decrease are probably the result of flights of portions of the slick with various thicknesses of oil. Also, some of the overflights were along the edge of the slick. The decreasing ΔT_h becomes a negative anomaly when estimated thicknesses of the oil slick are below 0.02 mm. This phenomena is shown in Figure 3-17. At this point emission by the oil is overshadowed by the dampening effect of oil on the sea surface roughness. This suggests that thin oil films which are too thin to be detected due to emission by the oil, can produce a detectably calmer sea condition. This phenomenon of negative horizontal polarization signatures was noted for the more viscous crude oils. It is assumed that the more viscous oils have a greater tendency to subdue the sea state condition than the less viscous, higher gravity crudes and refined petroleum products.

The vertical polarization temperature does not seem to be as greatly influenced by variations in the oil film thickness as does the horizontal polarization. This is attributed to the greater sensitivity of the horizontal polarization to roughness phenomena at the 45° viewing angle.

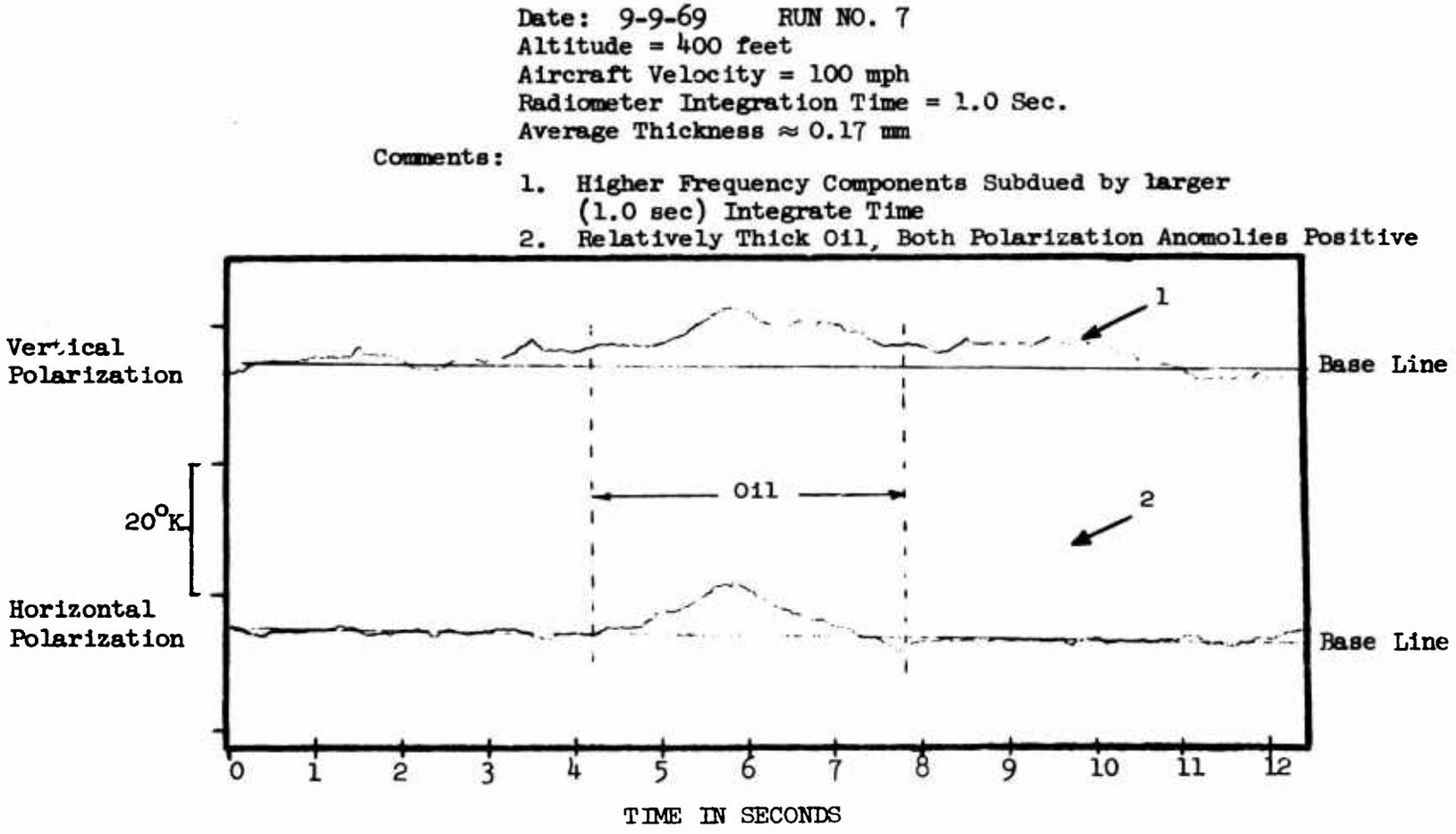

Figure 3-15. 0.81 cm RESPONSE FOR 20 API GRAVITY CRUDE OIL

Date: 9-9-69 RUN 13
Altitude ≈ 250 Feet
Aircraft Velocity = 100 mph
Radiometer Integration Time = 1.0 seconds
Average Thickness ≈ 0.05 mm

Comments:

1. Multiple Peaks over Oil Slick

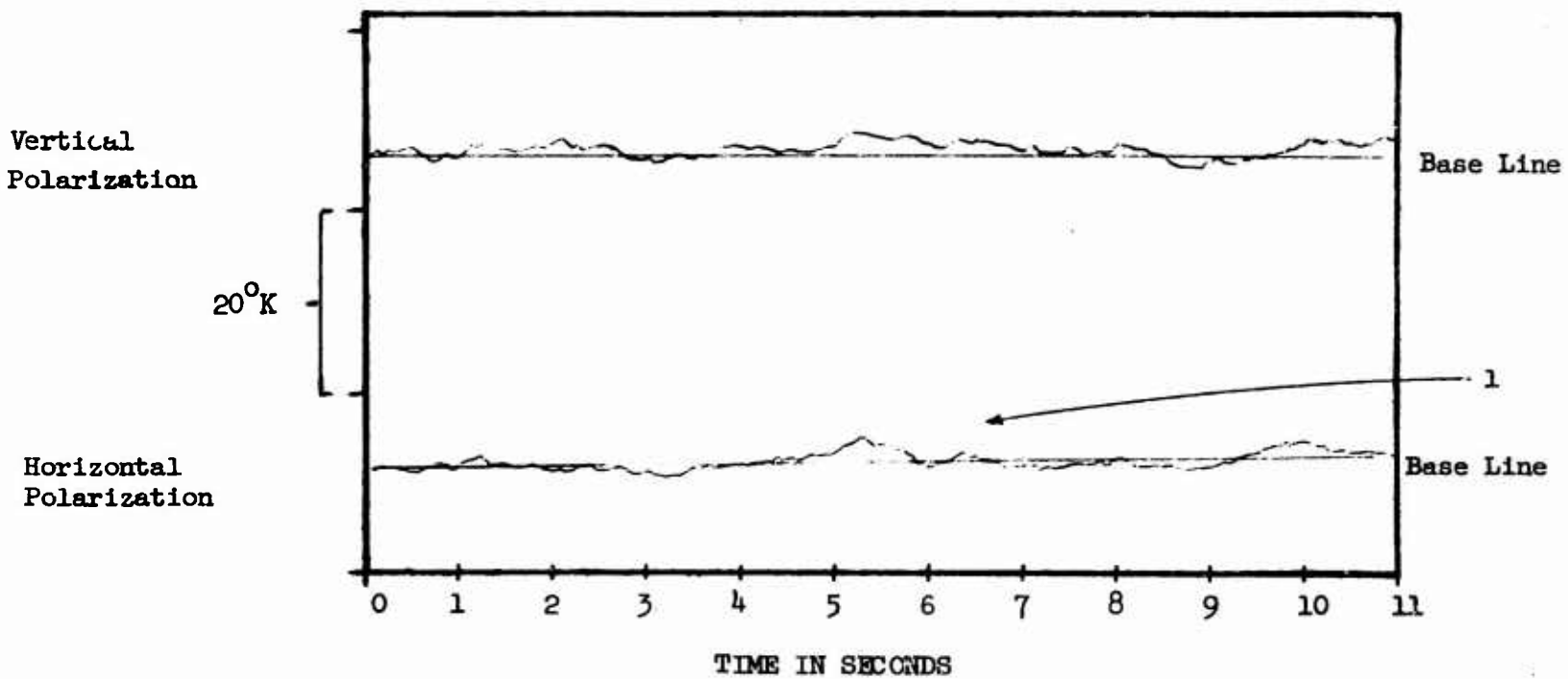

Figure 3-16. 0.81 cm RESPONSE FOR 20 API GRAVITY CRUDE OIL SLICK

Date: 9/9/69 (RUN No. 23)
Altitude = 200 Ft
Aircraft Velocity = 100 mph
Radiometer Integration Time = 1.0 sec
Average Thickness ≈ < 0.01 mm

Comments:

1. Note Negative Horizontal Polarization Signature

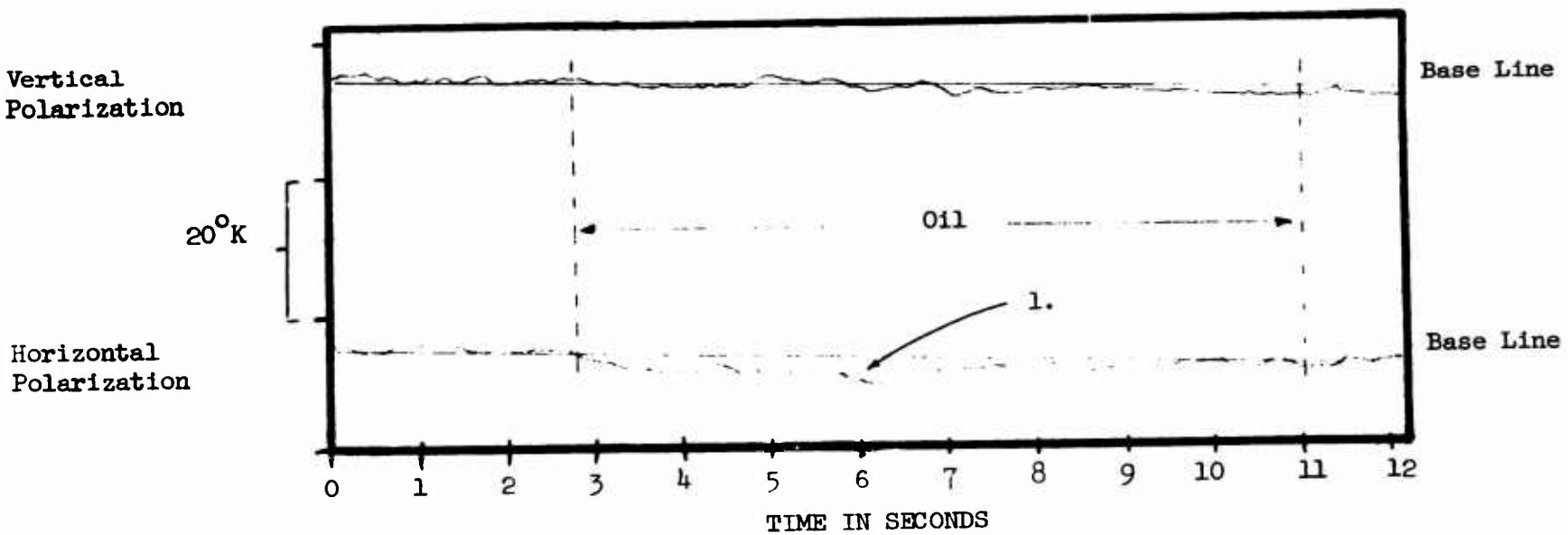

Figure 3-17. 0.81 cm RESPONSE FOR 20 API GRAVITY CRUDE OIL SLICK (60 MINUTES AFTER INITIATION OF SPILL)

3.3.5 MULTIPLE SPILLS (42 API Gravity, Marine Diesel and Mixed (50-50) 20 API and Marine Diesel Fuel)

On 12 September 1969 a 65-foot off-shore drilling rig tender was rented from General Marine Transport, Inc. of Santa Barbara, California. A larger vessel capable of carrying a larger cargo was used to compare various pollutants under similar conditions. Sea surface conditions during these spills was calm and the weather was clear. The first oil slick was produced by spilling 165 gallons of 42 API gravity crude oil. The second slick consisted of 350 gallons of marine diesel pumped from the vessel's fuel tanks. A third slick was produced by dumping 200 gallons of mixed 20 gravity crude and diesel fuel. Data flights began at 1818 and continued past sunset.

The 42 gravity crude oil was dumped over the stern of the vessel and the total quantity of three drums was dispersed in less than five minutes. Initially, the slick was quite small because of the rapid rate of oil spillage. Within 10 minutes, however, the slick had dispersed and reached dimensions of 250' x 100'. Twenty-one data flights of this slick were made between 1818 and 1925 at altitudes of 200, 250 and 400 feet.

Maximum radiometric anomalies recorded were $\Delta T_v = +8.0^{\circ}K$ and $\Delta T_h = +10^{\circ}K$. The recorded anomalies were somewhat variable but the slick was detectable after 50 minutes. Figure 3-18 shows the radiometric response 12 minutes after the spill (approximate thickness 0.2 mm) and Figure 3-19 shows the response after 50 minutes. It is interesting to note the magnitude of the anomaly after 50 minutes. The investigators can offer no explanation for the higher vertical polarization temperatures recorded toward the end of this experiment.

At 1850 the vessel left the 42 gravity crude oil slick and proceeded to spill 350 gallons of Marine Diesel fuel. Figure 3-20 is a photo of the diesel oil spill. The diesel oil shows as the lighter coloration in the upper section of the photographed sea surface. Ten overflights were made of the diesel slick from an altitude of 200 feet between 1900 and 1925. The

Date: 9/12/60 Run No. 5
Altitude = 200 Ft.
Aircraft Velocity = 110 mph
Radiometer Integration Time = 1.0 Sec.
Average Thickness ≈0.2 mm

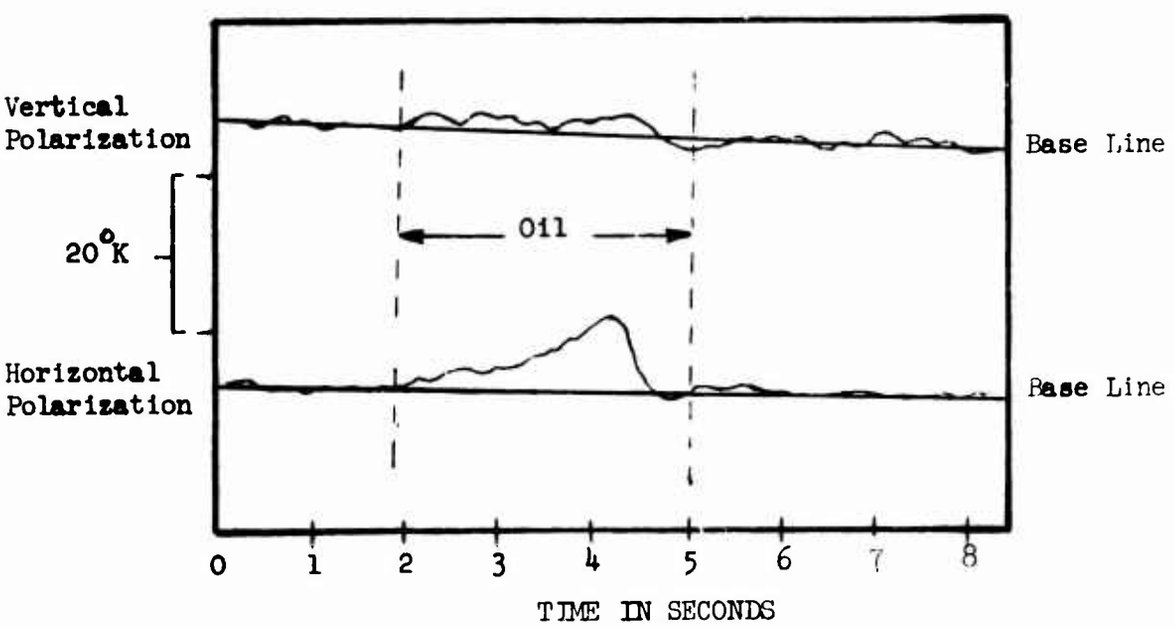

Figure 3-18. 0.81 cm RESPONSE FOR 42 API GRAVITY CRUDE OIL

Date: 9-12-69 RUN No. 15
Altitude = 200 Feet
Aircraft Velocity = 110 mph
Radiometer Integration Time = 1.0 sec
Average Thickness ≈ 0.04 mm

Comments:

1. Note increase in T_B from that measured Run 5 (Figure 3-18)

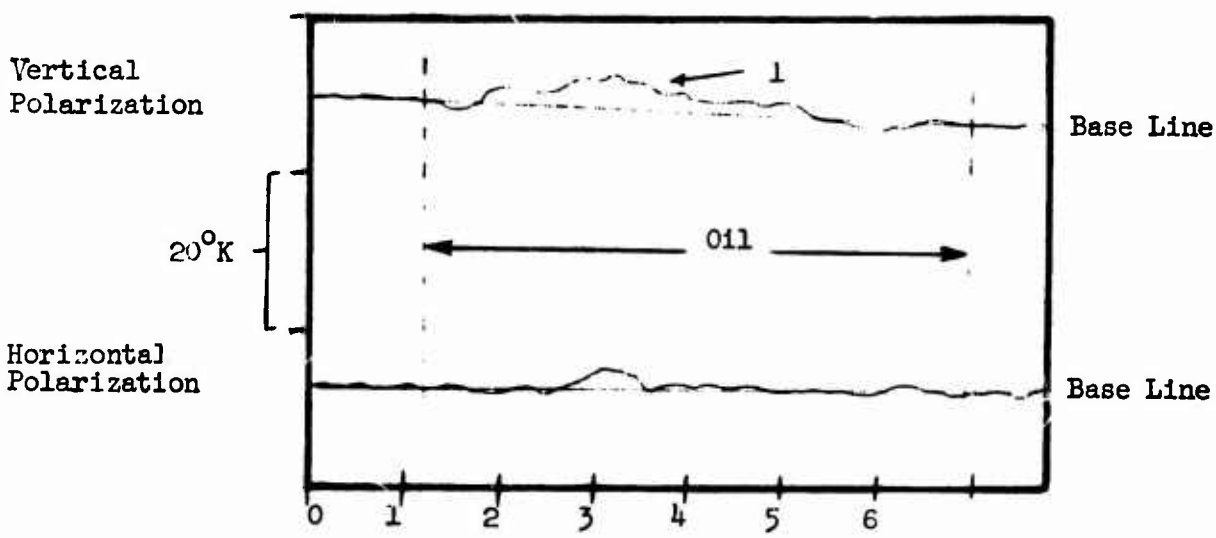

Figure 3-19. 0.81 cm RESPONSE FOR 42 API GRAVITY CRUDE OIL SLICK (50 MINUTES AFTER INITIATION)

Figure 3-20. PHOTO OF DIESEL OIL SPILL 9-12-69

radiometric signatures for this slick were considerably lower than those recorded for the 42 gravity crude oil slick. The maximum radiometric signatures were 5°K for both polarizations, as shown in Figure 3-21. As the slick dispersed and thinned the polarization temperature difference decreased. In fact, the last two overflights recorded vertical polarization anomalies that were larger than the horizontal polarization anomalies. This is shown in Figure 3-22.

At 1925, 200 gallons of a mixture of 20 API gravity crude oil and diesel fuel were spilled. Eight overflights of the slick were made at an altitude of 200 feet. Representative samples are shown in Figures 3-23 and 3-24. The radiometric anomalies recorded were of small magnitude. The smaller anomalies are possibly due to misses rather than less radiometric response. These flights occurred at sunset and alignment over the slick was questionable. The maximum signature was +4.5°K for vertical polarization and +3.5°K for the horizontal polarization.

Date: 9/12/69
Altitude = 200 Ft.
Aircraft Velocity = 110 mph
Radiometer Integration Time = 1.0 sec
Average Thickness ≈ 0.20 mm

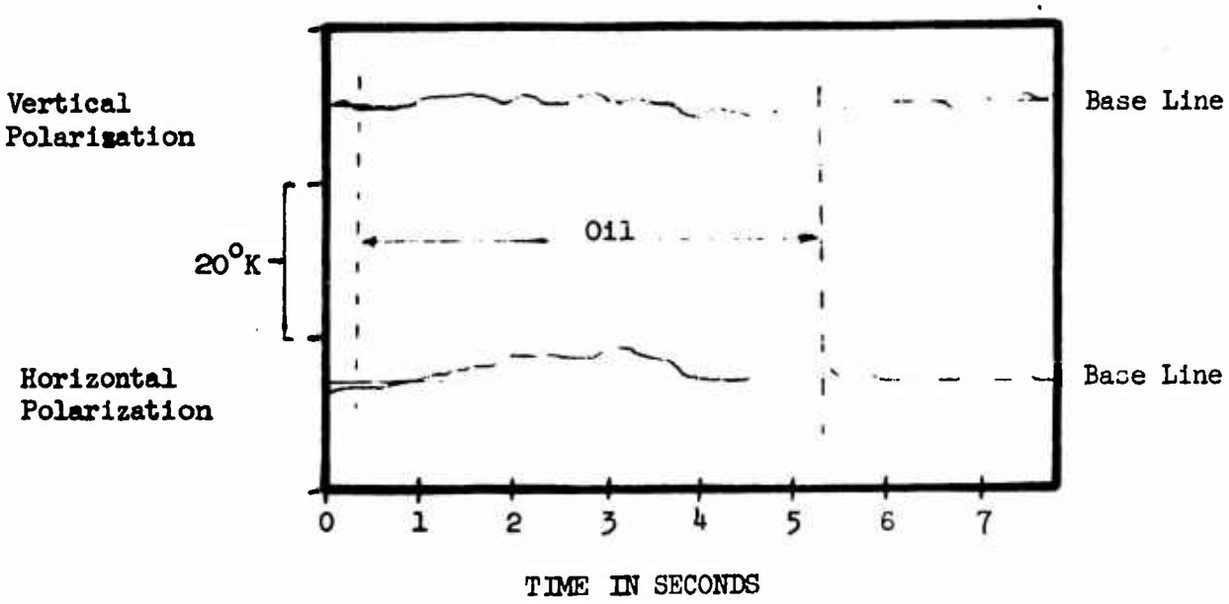

Figure 3-21. 0.81 cm RESPONSE FOR DIESEL OIL SPILL

Date: 9/12/69 Run No. 29
Altitude: 200 feet
Aircraft Velocity = 110 mph
Radiometer Integration Time = 1.0 sec
Average Thickness 0.02 mm

Comments:

1. Note Increase In Brightness Temperature From That of Fig. 4-12
2. Note Brightness Temperature Inversion

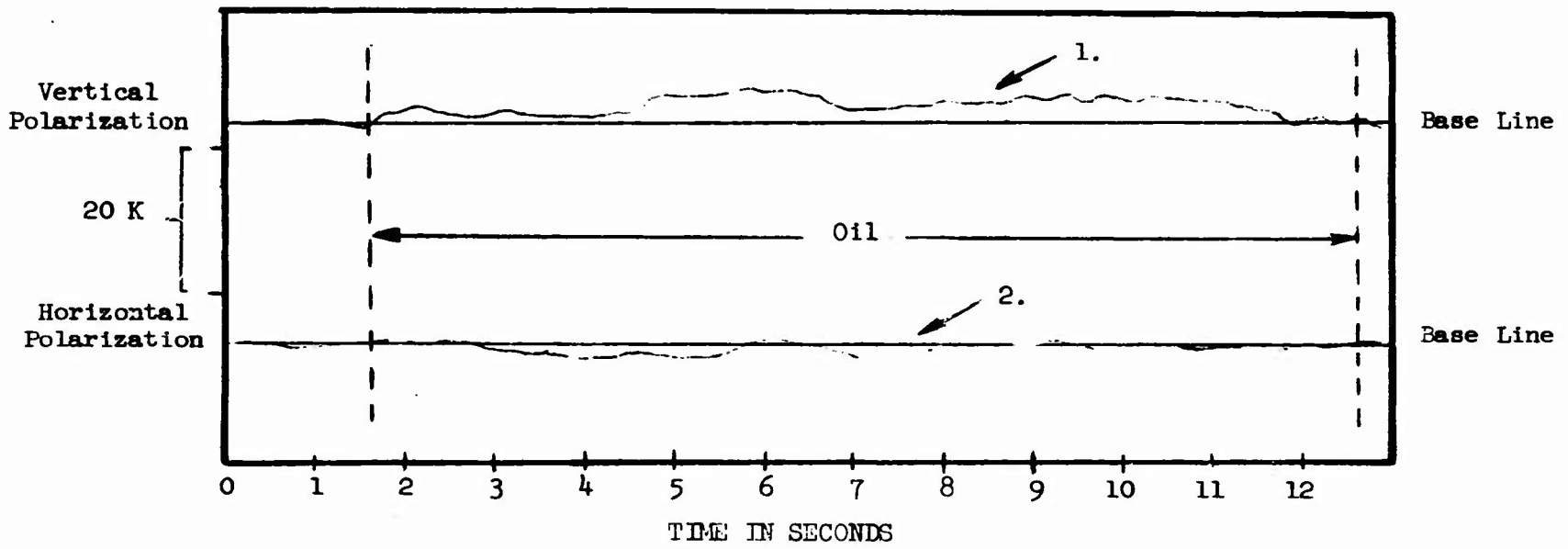

Figure 3-22. 0.81 cm RESPONSE FOR DIESEL OIL

Date: 9/12/69 Run No. 34
Altitude = 200 Ft.
Aircraft Velocity = 110 mph
Radiometer Integration Time = 1.0 Sec.
Average Thickness ≈ 0.05 mm

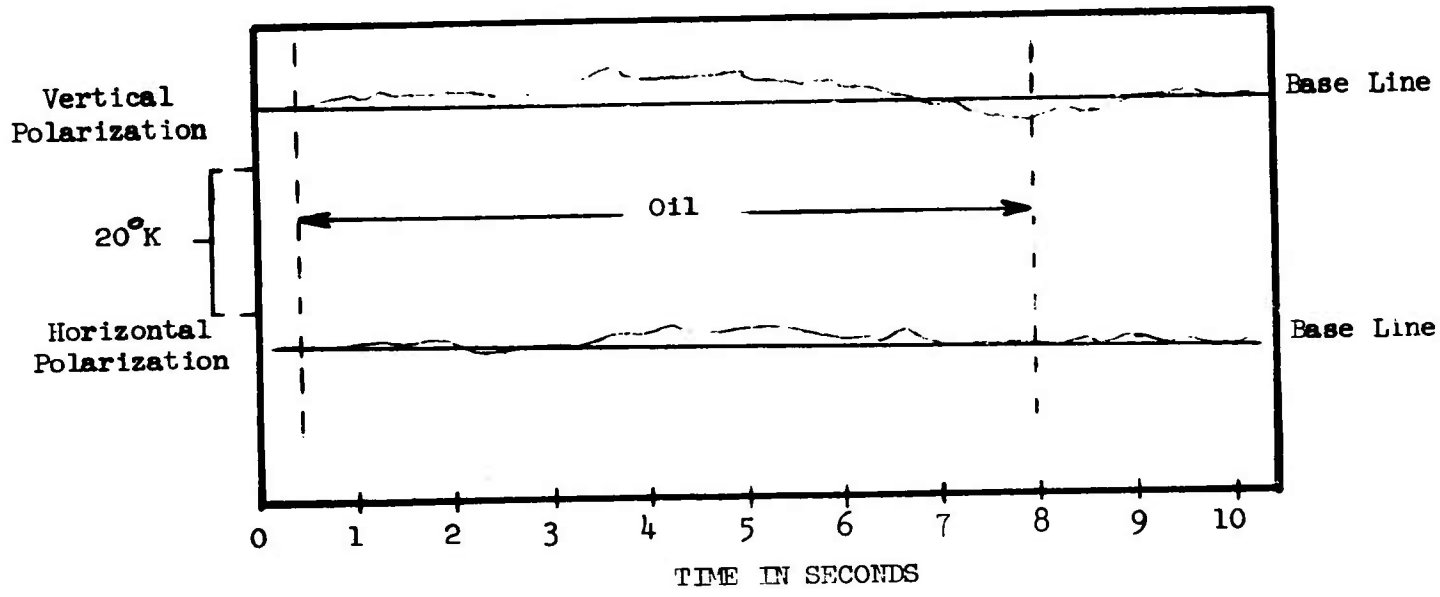

Figure 3-23. 0.81 cm RESPONSE FOR 20 API GRAVITY OIL

Date: 9/12/69 Run No. 46
Altitude = 200 ft.
Aircraft Velocity = 110 mph
Radiometer Integration Time = 1.0 Sec
Average Thickness ≈ 0.01 mm

Comments:

1. Note Brightness Temperature Inversion

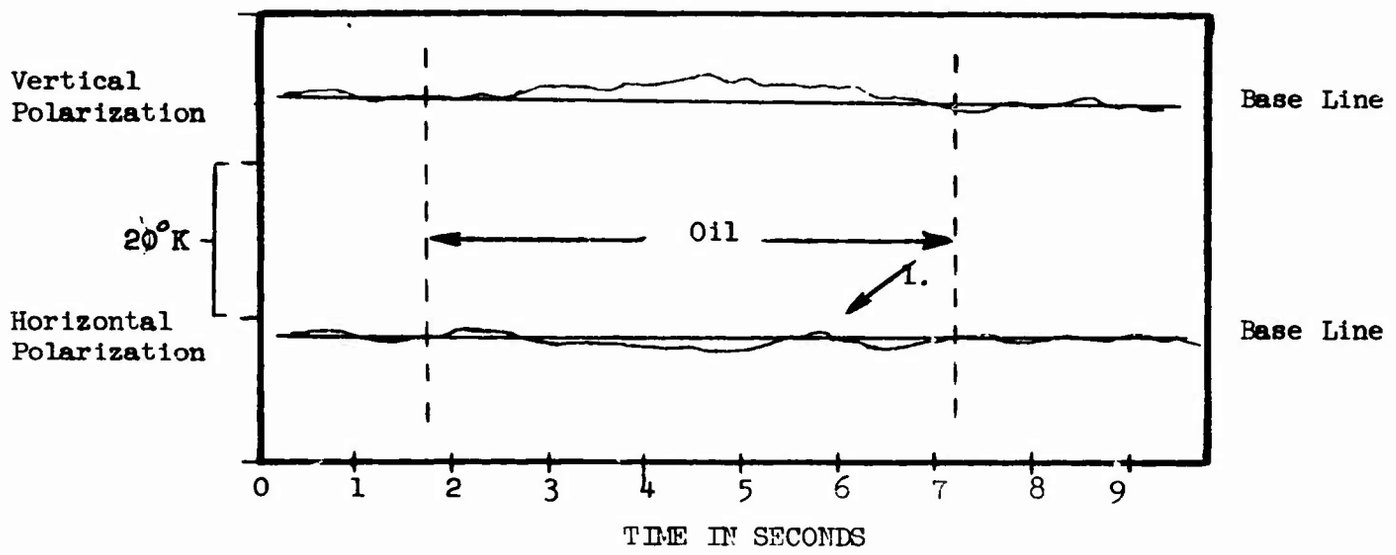

Figure 3- . 0.81 cm RESPONSE FOR 20 API GRAVITY OIL

BLANK PAGE

Section 4

CONCLUSIONS AND RECOMMENDATIONS

4.1 GENERAL

A laboratory and airborne measurements program was conducted to determine the feasibility of using microwave radiometry for detection and surveillance of oil pollution. During the course of the study oil slicks on the open ocean wereidentified unambiguously for film thicknesses as small as a few tens of microns using an 8.1 mm radiometer. An examination of the operational requirements of an oil pollution surveillance system and sensor specifications inferred from the measurement program show that a suitable microwave imager with in-flight display can be designed to achieve the aforementioned detection capability. Specific results of laboratory and airborne studies are provided below.

4.2 LABORATORY RESULTS

Laboratory measurements of crude and refined petroleum films on sea water were performed using dual-polarized 8.1 mm and 2.2 cm radiometers. The dielectric properties of these petroleum products were also determined for a sensor wavelength of 8.1 mm. These observations indicate the following:

(1) The microwave signature of an oil film is inversely proportional to sensor wavelength (e.g. the signature increases with decreasing wavelength).

(2) Minimum detectable oil film thicknesses (on calm water surface) using the 8.1 mm sensor were of the order of 0.1 to 0.3 mm (100 to 300 microns).

(3) All oil film signatures were positive (radiometrically warmer than unobscured water) for flat water surfaces.

(4) The horizontally polarized signatures were more responsive to oil films than the vertically polarized component.

(5) Antenna viewing angles of 30 to 45^{o} above nadir afford best all-around sensor performance.

(6) The real part of the dielectric constant of oil is inversely proportional to API gravity at microwave frequencies.

(7) The API gravity of an oil film decreases with age.

(8) Microwave signatures observed in the laboratory increase with increasing film thickness.

4.3 OIL SLICK OVERFLIGHTS

Airborne measurements of various oil slicks were performed using a dual-polarized 8.1 mm radiometer mounted in a Cessna 210 aircraft. Data were collected for a range of oil types, film thicknesses and sea surface conditions. The following conclusions were drawn from these observations:

(1) Minimum detectable oil film thicknesses were of the order of 10 to 20 microns (diesel fuel, 20° and 30° crude).

(2) Ocean surface roughness affects the microwave signature of an oil slick since the brightness temperature of the ocean increases with increasing sea state and the unobscured ocean surface represents the background against which oil slick signatures must be detected. At present, this relationship is not well defined and a number of agencies are performing research on the emission characteristics of varying sea states.

(3) Oil slicks modify sea state by reducing surface roughness, particularly the higher frequency components such as wavelets, small scale waves, breaking waves, etc.

(4) The two just mentioned phenomena interact in a complex manner giveing rise to the following observations. For comparatively thick slicks of about 50 microns average thickness or more, ΔT_h was consistently larger than ΔT_v for the sea states encountered. For comparatively thin slicks of 10 to 20 microns average thickness, ΔT_h was consistently negative whereas ΔT_v was in all cases positive. This suggests that the additional emission from an oil slick overshadows the decrease in ocean emission associated with reduction of surface roughness when film thicknesses are about 50 mm or more (for conditions encountered in the airborne tests). When film thicknesses of 10 to 20 microns were observed, the additional emission from the oil was apparently more than offset by a reduction in ocean emission due to reduced surface roughness. It is apparently the latter effect which permitted detection of the thin slicks. (It will be recalled that laboratory observations indicated that slicks thinner than 100 microns were unmeasurable on a flat water surface.) These data indicate that a "crossover" point

exists where the two opposing contributions offset one another. Vertical polarization signatures (ΔT_v) were generally small and no consistent correlation was made with film thickness. It should be noted that the negative ΔT_h signatures can be uniquely associated with oil slicks since there is no other mechanism known to cause such a signature. Small positive signatures, on the other hand, could possibly arise from drifting debris, etc. Pattern recognition techniques will, of course, aid in identification.

(5) Airborne observations combined with laboratory experiments indicate that sensor wavelengths of 8 mm or less should be considered for detection systems. Sensors with appreciably larger wavelengths are not as responsive, and therefore should not be considered. There are practical limitations associated with selecting a shorter sensor wavelength. Severe atmospheric attenuation occurs for wavelengths less than about 8 mm. The nearest usable atmospheric window occurs for wavelengths of approximately 3 mm (94 GHz).

(6) Possible configurations of an oil pollution surveillance system are summarized in Appendix C. It should be pointed out that the system configuration described in Appendix C is included to acquaint the reader with parameters affecting system design and is not intended to be the ultimate system configuration. This work, predicated on measurement results and operational requirements specified by the U. S. Coast Guard, shows that a suitable microwave imager can be designed and fabricated to achieve, under operational conditions, the detection capabilities obtained during the flight program. It is highly desirable, however, that additional experimental data be gathered for better definition of detection probability over a range of sea surface conditions. The following section contains several specific recommendations.

4.5 RECOMMENDATIONS

Additional oil slick signature data are needed for better definition of the capabilities and/or limitations of oil pollution surveillance using microwave radiometry. Additional data covering a range of oil types and sea conditions are needed:

(1) For better definition of oil slick detection probability over a range of sea conditions

(2) To develop techniques for estimation of film thicknesses from measured signatures

(3) For definition of oil pollution surveillance system sensor specifications

The following recommendations encompass additional laboratory and sea measurements using sensor wavelengths of 3 mm (94 GHz) and 8.1 mm (37 GHz) simultaneously. The 3 mm radiometer will be available in May 1970. Also recommended are more sophisticated techniques for data analysis.

1. Laboratory Investigations - Measure 3 mm and 8.1 mm emission of two (2) low viscosity oil films on sea water (40° and higher crudes wherein films remain continuous and thicknesses can be estimated) as a function of film thickness, antenna viewing angle and age of pollutant. Cross-correlate 3 mm and 8.1 mm results and compare with work reported herein to verify the $\Delta T \alpha 1/\lambda$ relationship observed in earlier laboratory studies.

2. Sea Investigations - Conduct additional airborne measurements of controlled spills using sensor wavelengths of 3 mm and 8.1 mm simultaneously. Flights must be conducted over an adequate period of time to assure data acquisition over a range of sea conditions including higher sea states than were encountered in the first flight program. A twin engine aircraft should be used for this work. (Cost is about $10.00 per hour more than the single engine aircraft used in the first flights.) It will be instrumented with the two radiometers, an aerial camera, a digital data acquisition system and stripchart recorder. A large vessel (40 feet or more) will be used to permit multiple spills during a given sea trial. This permits comparison of signatures from several types of oil slicks under the same sea conditions. Three or four spills appear to be a manageable number for overflights. These slicks will be measured for a large period of time, preferably several days or until they dissipate. The investigators were unable to accomplish this during the first flight program because of the rate at which slicks drifted and heavy fog during the experiment. Slick movement is affected by prevailing winds and the ocean current. Hence, water dyes, buoys, etc. don't stay with the slicks and the only sure means of tracking them for an extended period of time is to maintain visual contact using the observer boat. Also, slicks formed while the boat is underway will be examined.

3. Analysis of Measurements - All airborne sensor data will be processed to provide brightness temperature profiles of flight data and the dual wavelength signatures will be compared with oil type, film thickness, aging and

sea surface conditions. Also, the dual wavelength data will be cross-correlated and compared with film thickness. Recall that sensor response is a function of film thickness and observational wavelength, so that cross-correlation of the two signatures may permit determination of film thickness.

In addition to analytical methods used for the first flight data where amplitudes of ΔT_h and ΔT_v were compared with slick signatures, we will examine the frequency distribution of the measured microwave noise. This will be accomplished by recording radiometer outputs on a computer compatible format using AGC's high speed data acquisition system. This permits the analyst to use various spectral techniques (e.g., power spectral density, etc.) to examine measured microwave noise spectra. From this analysis we may be able to distinguish between the noise spectra of the slick and adjacent sea, since the corresponding ocean wave spectra are different. This line of investigation can be followed for modest cost and should be considered, especially where very thin slicks are encountered.

4. Results - Results of the additional measurements and associated analyses will be summarized in a comprehensive report. This document will include an evaluation of capabilities and/or limitations associated with the use of microwave radiometry for oil pollution surveillance including detection, mapping (area) and volume determination (thickness x area) aspects of the problem. Also, specific recommendations will be provided concerning optimum configuration of a surveillance system.

BLANK PAGE

APPENDIX A

DIELECTRIC CONSTANT AND ABSORPTIVITY DATA FOR BUNKER "C" FUEL OIL, GASOLINE, AND 20, 30, and 40 API GRAVITY CRUDE OILS

The horizontal and vertical absorptivities of different grades of crude oils at varying thicknesses over ocean water are presented for a wavelength of 0.81 cm as a function of angle of observation from 0 to 70 degrees from nadir. The errors in repeatability are believed to be less than 0.003.

GASOLINE - HORIZONTAL

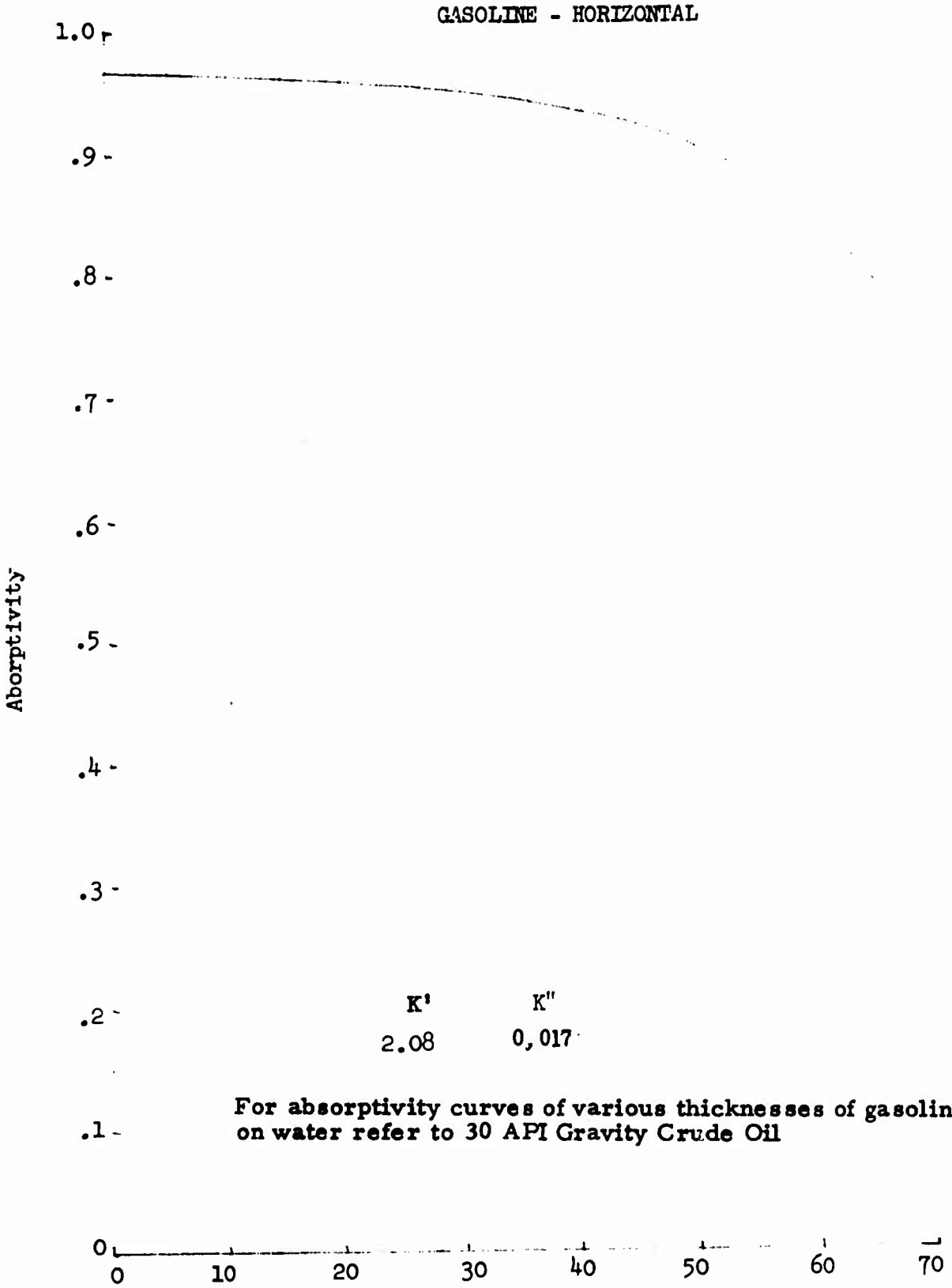

For absorptivity curves of various thicknesses of gasoline on water refer to 30 API Gravity Crude Oil

GASOLINE - VERTICAL

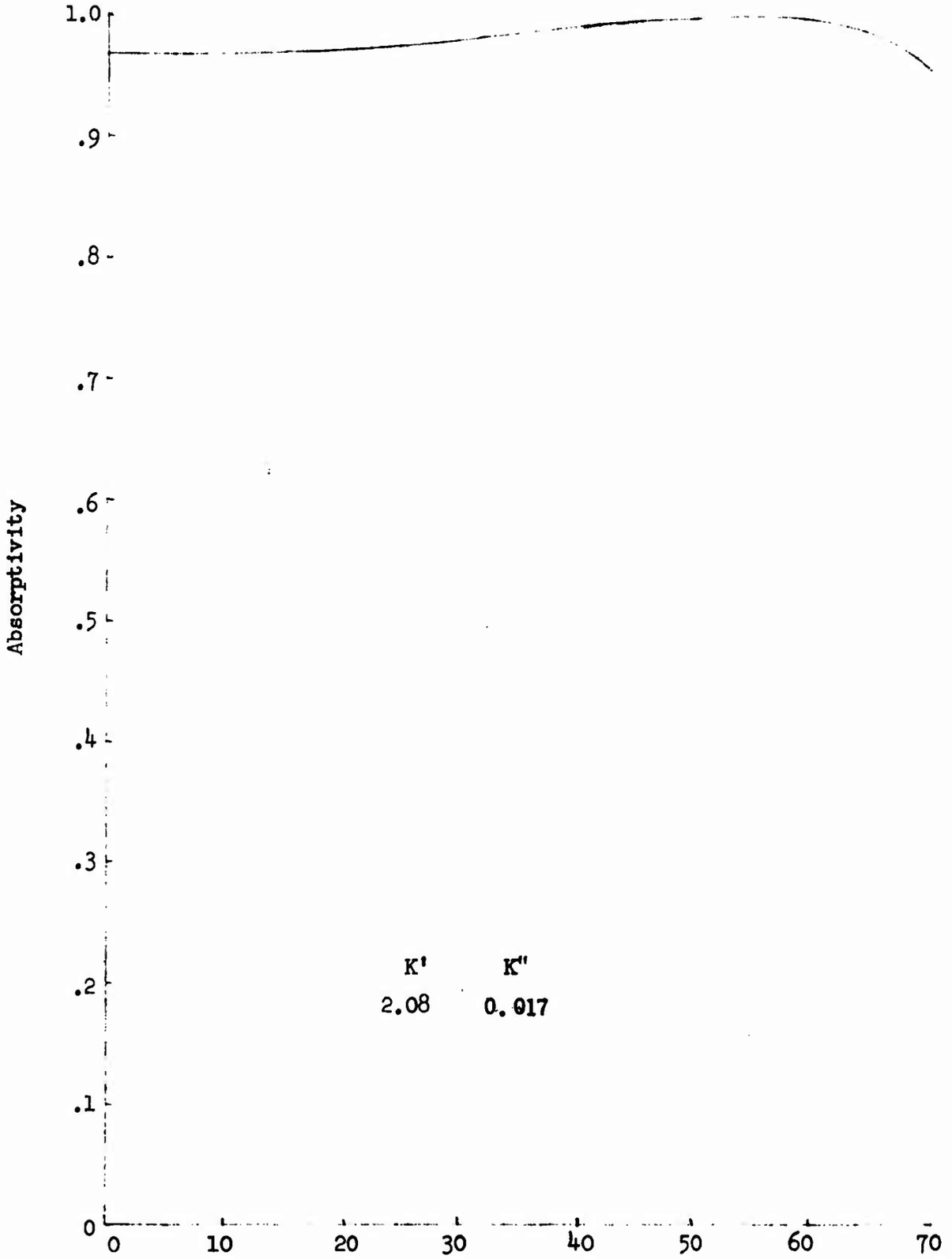

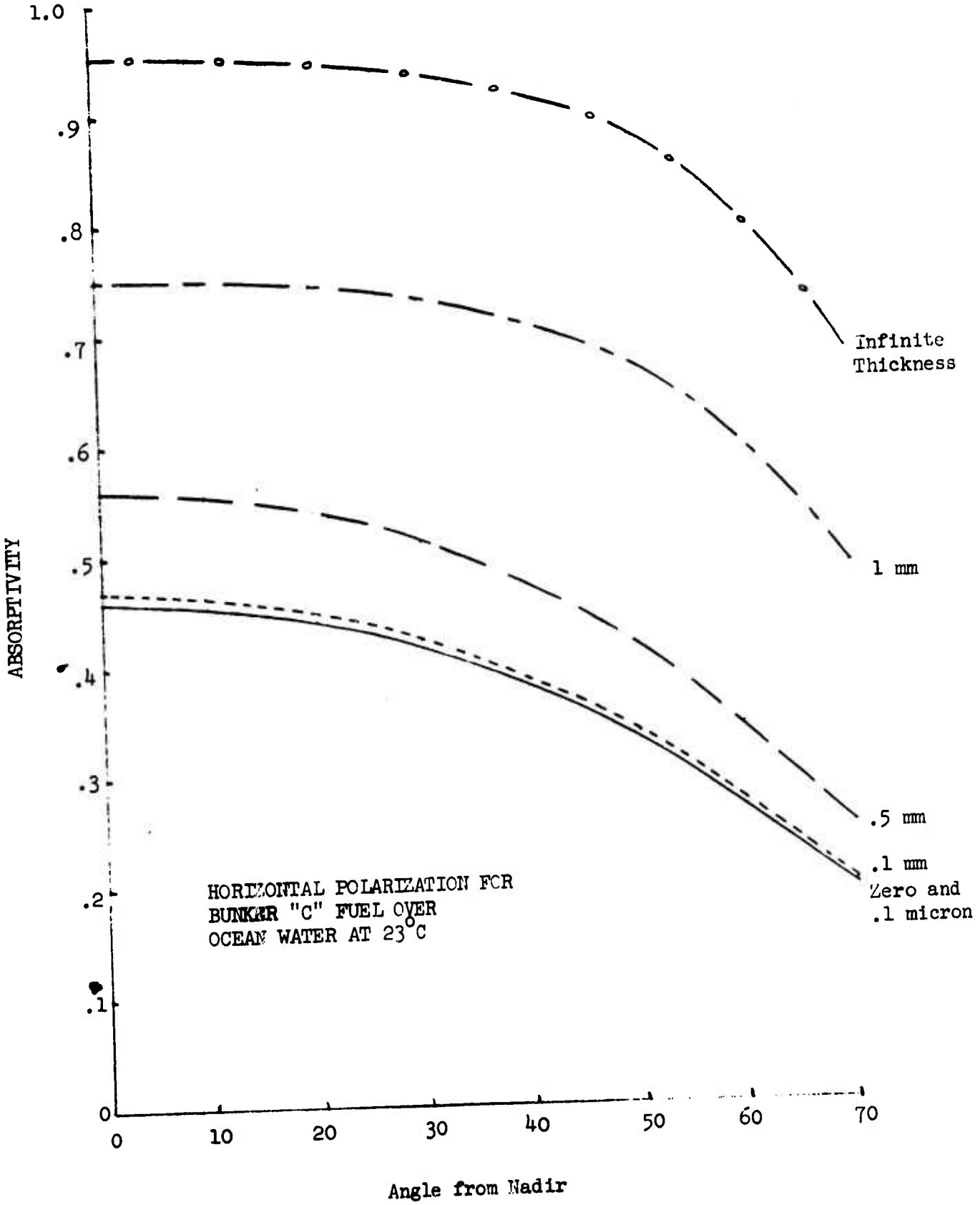
1.0
.9
.8
.7
.6
.5
.4
.3
.2
.1
0
ABSORPTIVITY
Infinite Thickness
1 mm
.5 mm
.1 mm
Zero and .1 micron
HORIZONTAL POLARIZATION FOR
BUNKER "C" FUEL OVER
OCEAN WATER AT 23°C
0
10
20
30
40
50
60
70
Angle from Nadir

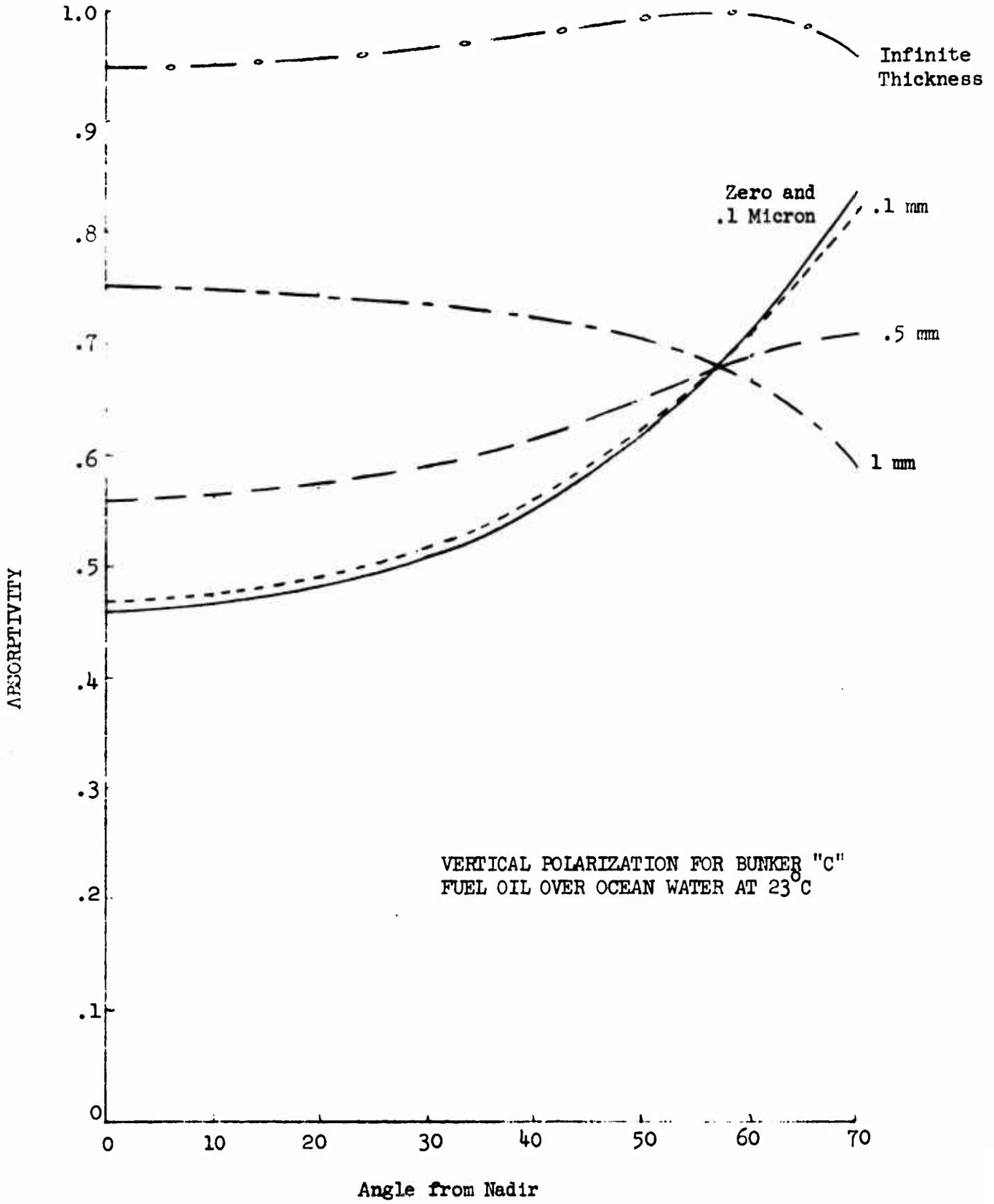
1.0
.9
.8
.7
.6
.5
.4
.3
.2
.1
0
ABSORPTIVITY
Infinite Thickness
Zero and .1 Micron
.1 mm
.5 mm
1 mm
VERTICAL POLARIZATION FOR BUNKER "C" FUEL OIL OVER OCEAN WATER AT 23°C
0
10
20
30
40
50
60
70
Angle from Nadir

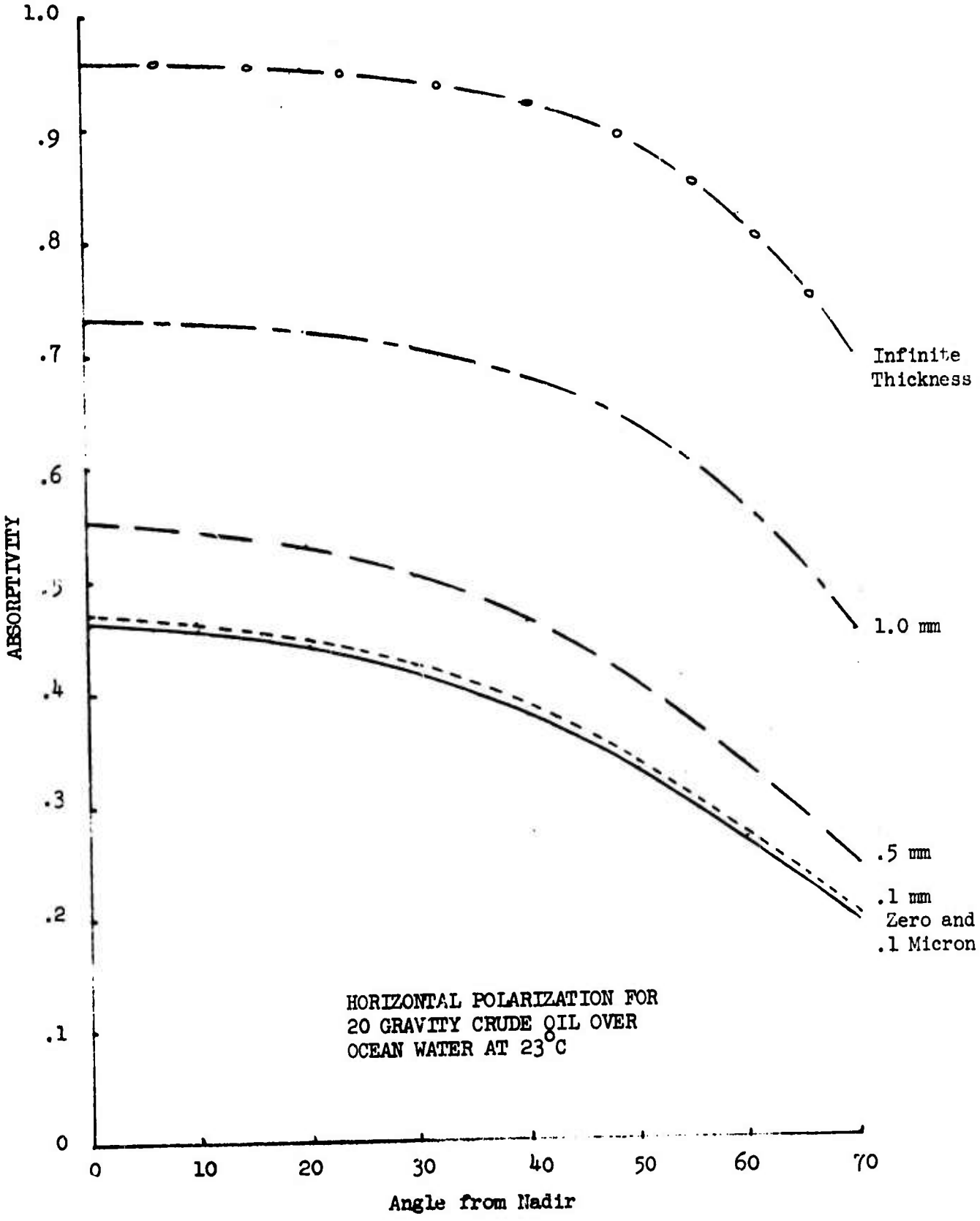
1.0
.9
.8
.7
.6
.5
.4
.3
.2
.1
0
ABSORPTIVITY
Infinite Thickness
1.0 mm
.5 mm
.1 mm
Zero and .1 Micron
HORIZONTAL POLARIZATION FOR 20 GRAVITY CRUDE OIL OVER OCEAN WATER AT 23°C
0
10
20
30
40
50
60
70
Angle from Nadir

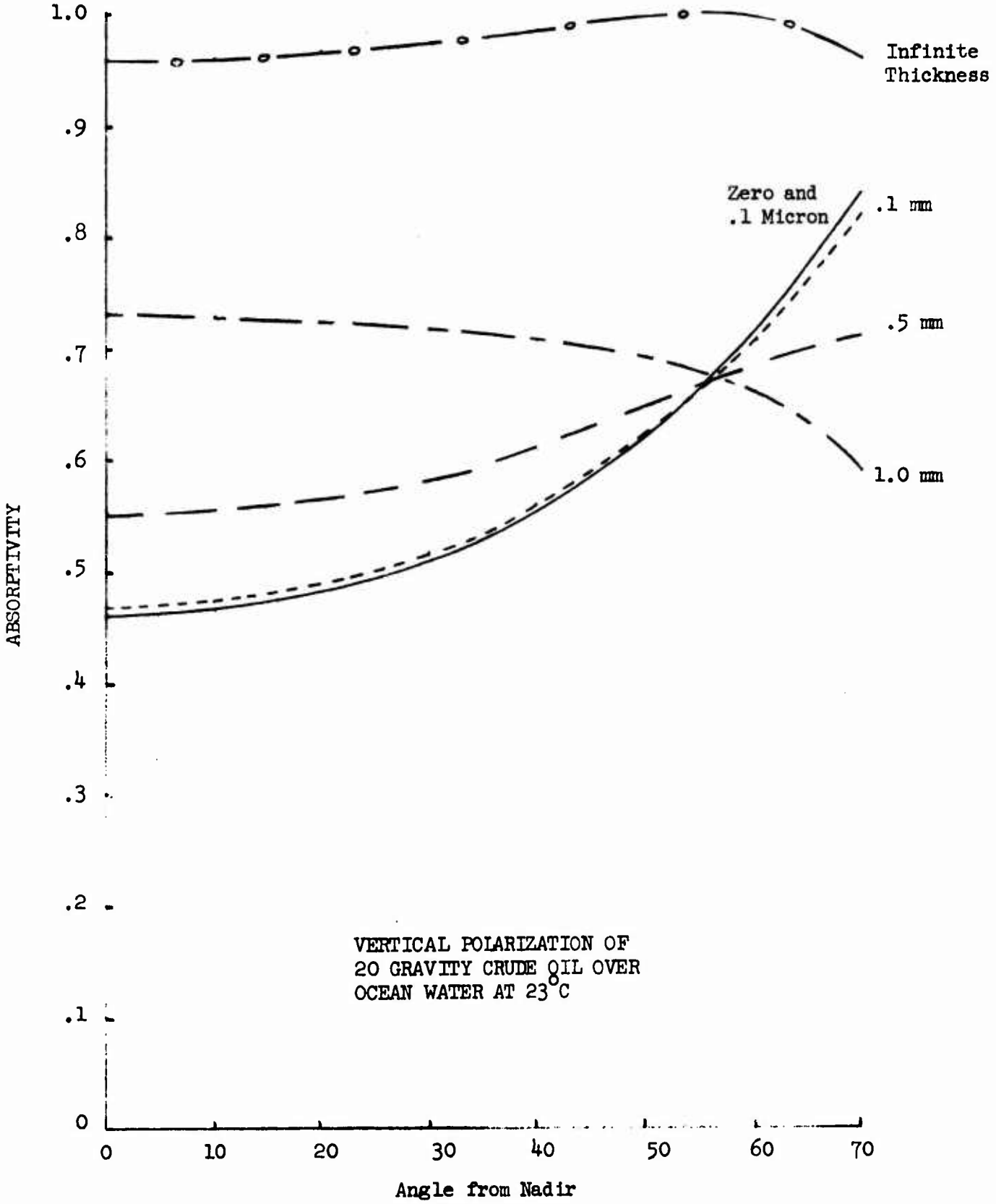

VERTICAL POLARIZATION OF
20 GRAVITY CRUDE OIL OVER
OCEAN WATER AT 23°C

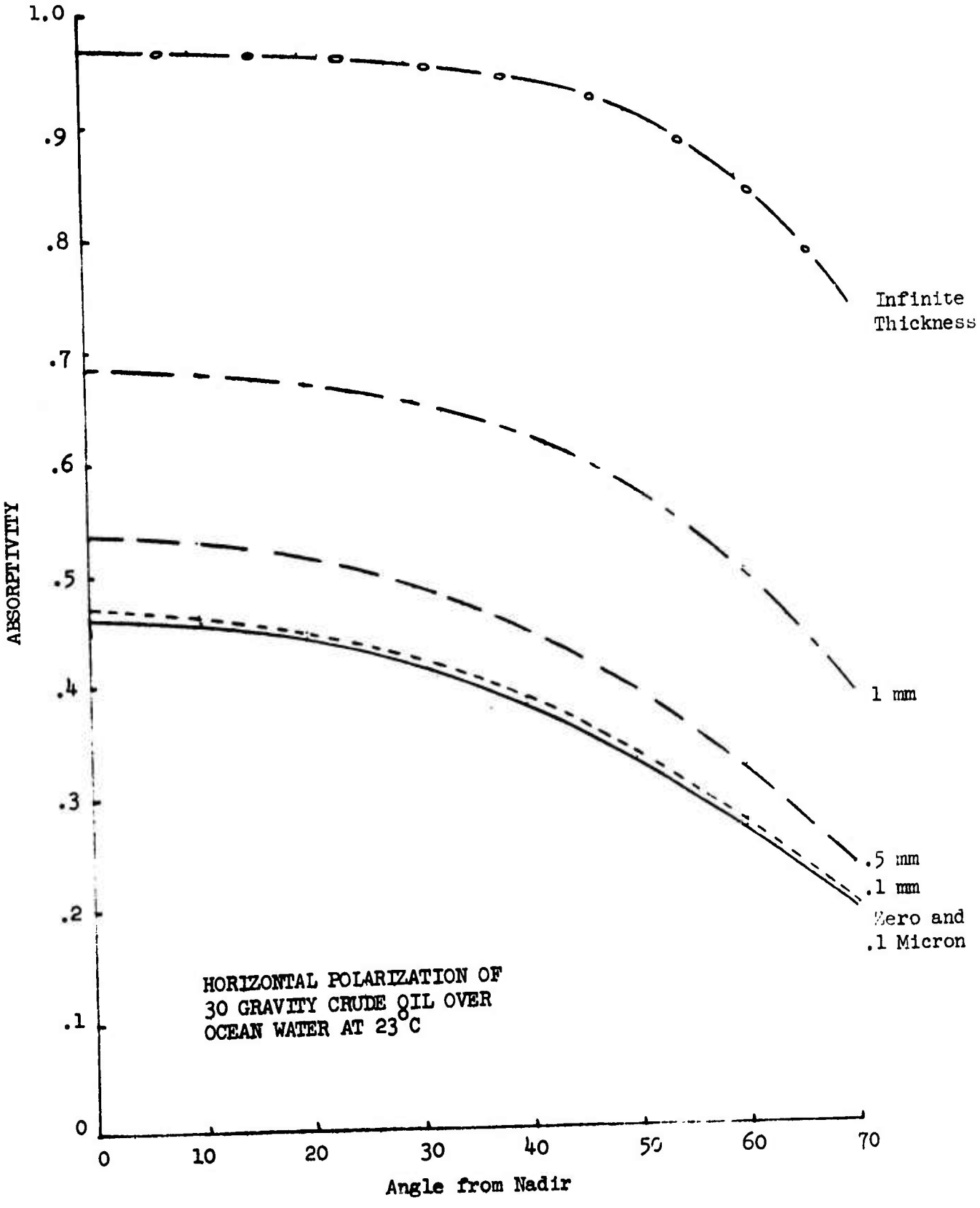
1.0
.9
.8
.7
.6
.5
.4
.3
.2
.1
0
ABSORPTIVITY
0
10
20
30
40
50
60
70
Angle from Nadir
Infinite Thickness
1 mm
.5 mm
.1 mm
Zero and .1 Micron
HORIZONTAL POLARIZATION OF
30 GRAVITY CRUDE OIL OVER
OCEAN WATER AT 23°C

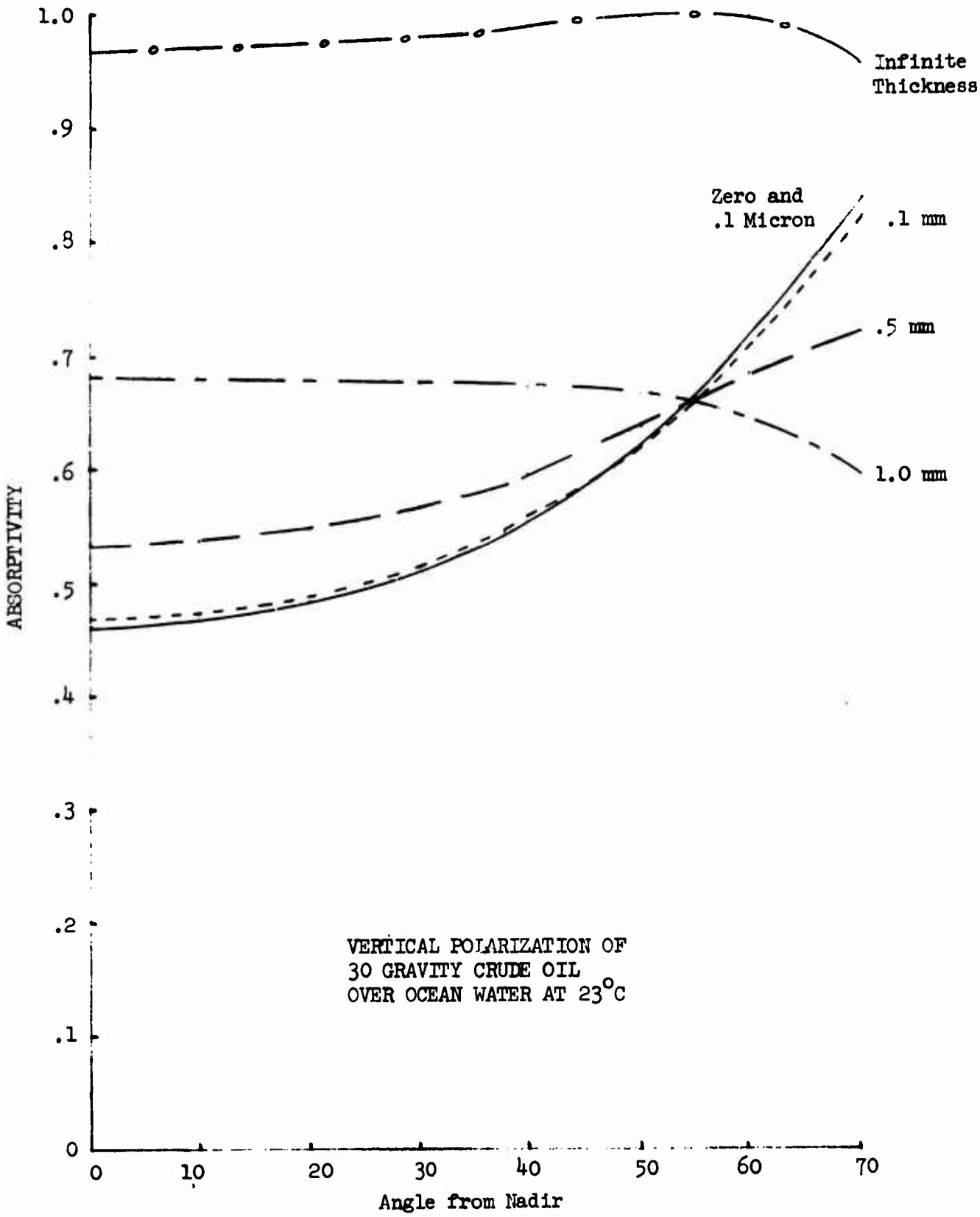
1.0
.9
.8
.7
.6
.5
.4
.3
.2
.1
0
ABSORPTIVITY
Infinite Thickness
Zero and .1 Micron
.1 mm
.5 mm
1.0 mm
VERTICAL POLARIZATION OF
30 GRAVITY CRUDE OIL
OVER OCEAN WATER AT 23°C
0
10
20
30
40
50
60
70
Angle from Nadir

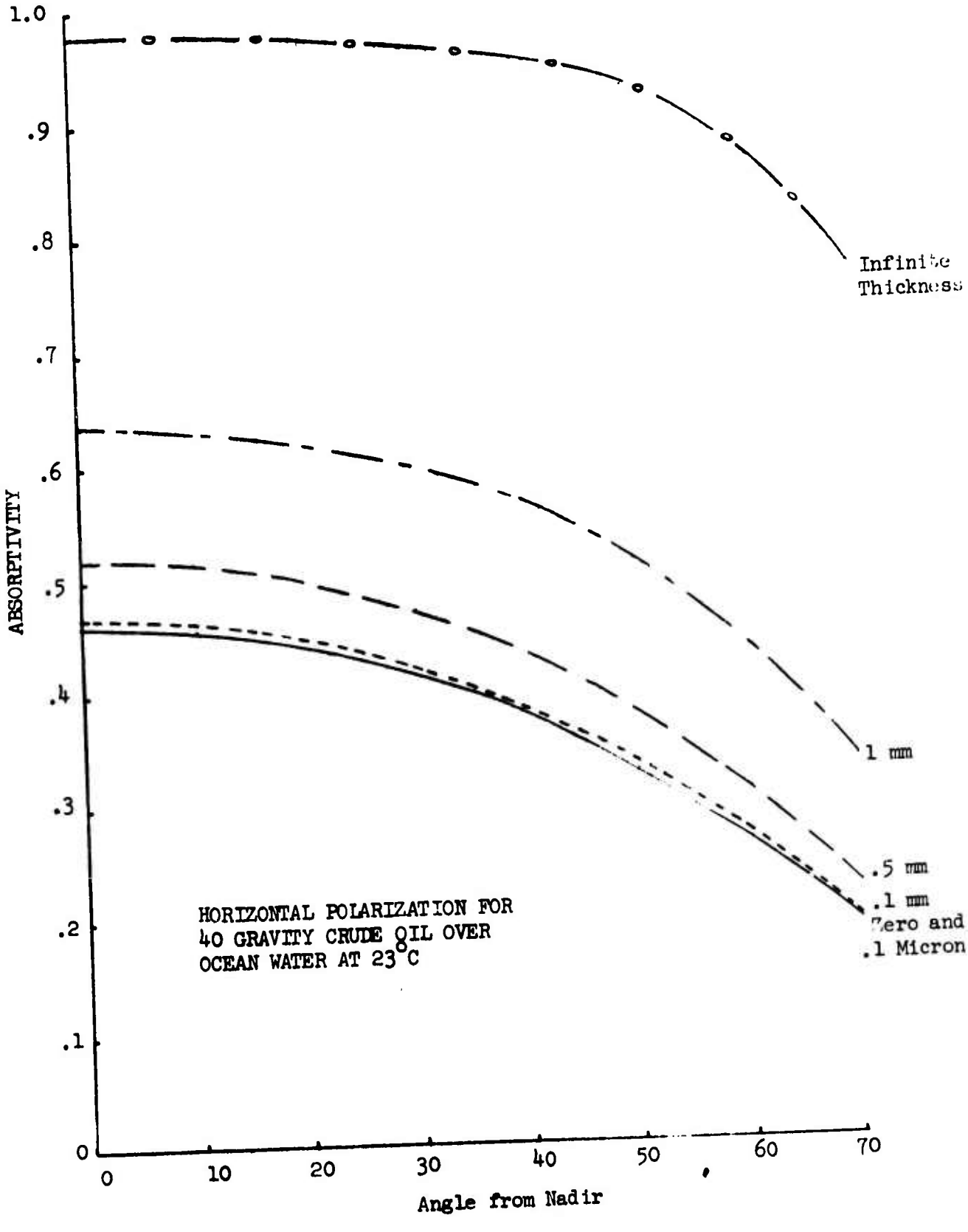
1.0
.9
.8
.7
.6
.5
.4
.3
.2
.1
0
ABSORPTIVITY
0
10
20
30
40
50
60
70
Angle from Nadir
Infinite Thickness
1 mm
.5 mm
.1 mm
Zero and .1 Micron
HORIZONTAL POLARIZATION FOR
40 GRAVITY CRUDE OIL OVER
OCEAN WATER AT 23°C

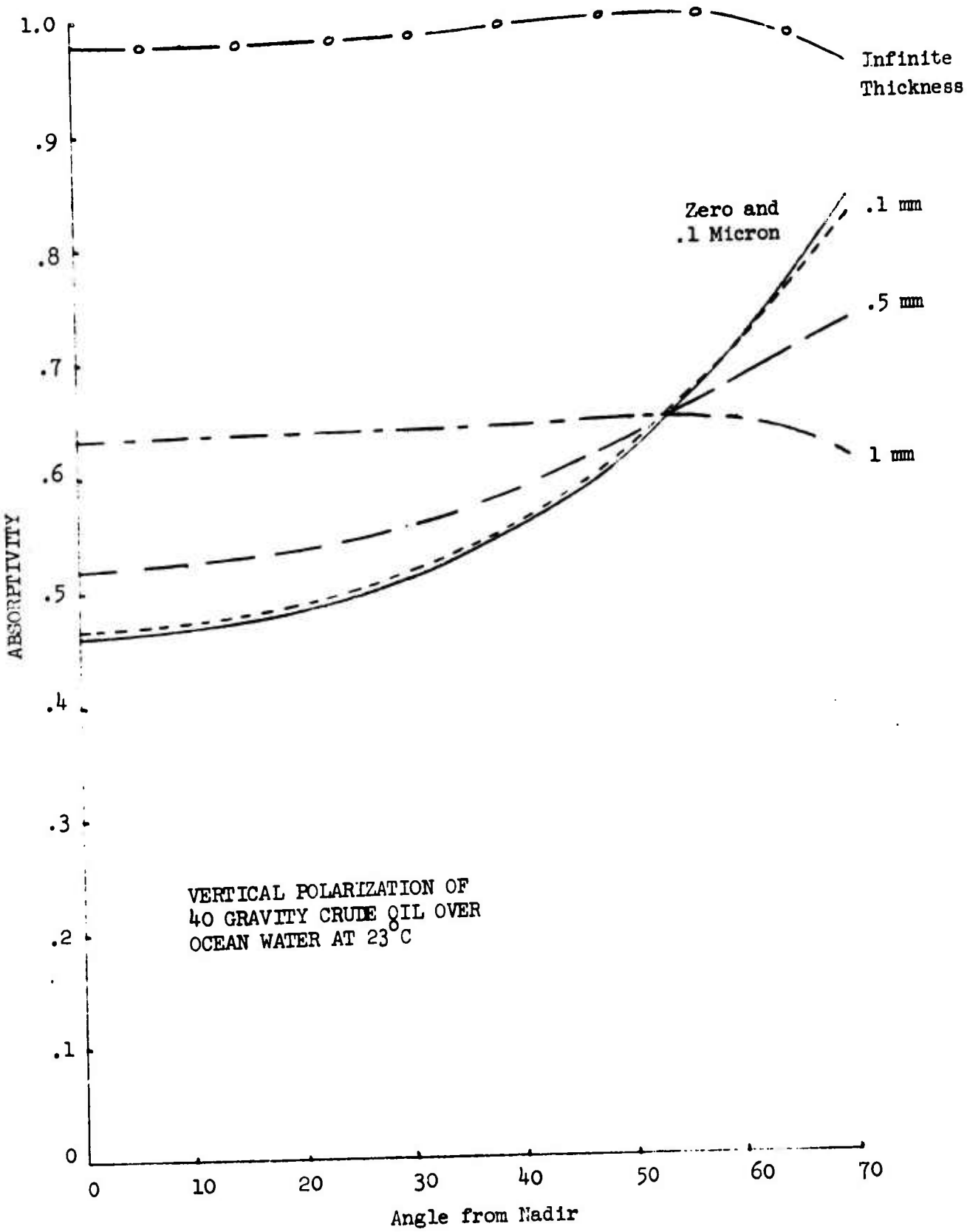
1.0
.9
.8
.7
.6
.5
.4
.3
.2
.1
0
ABSORPTIVITY
Infinite Thickness
Zero and .1 Micron
.1 mm
.5 mm
1 mm
VERTICAL POLARIZATION OF
40 GRAVITY CRUDE OIL OVER
OCEAN WATER AT 23°C
0
10
20
30
40
50
60
70
Angle from Nadir

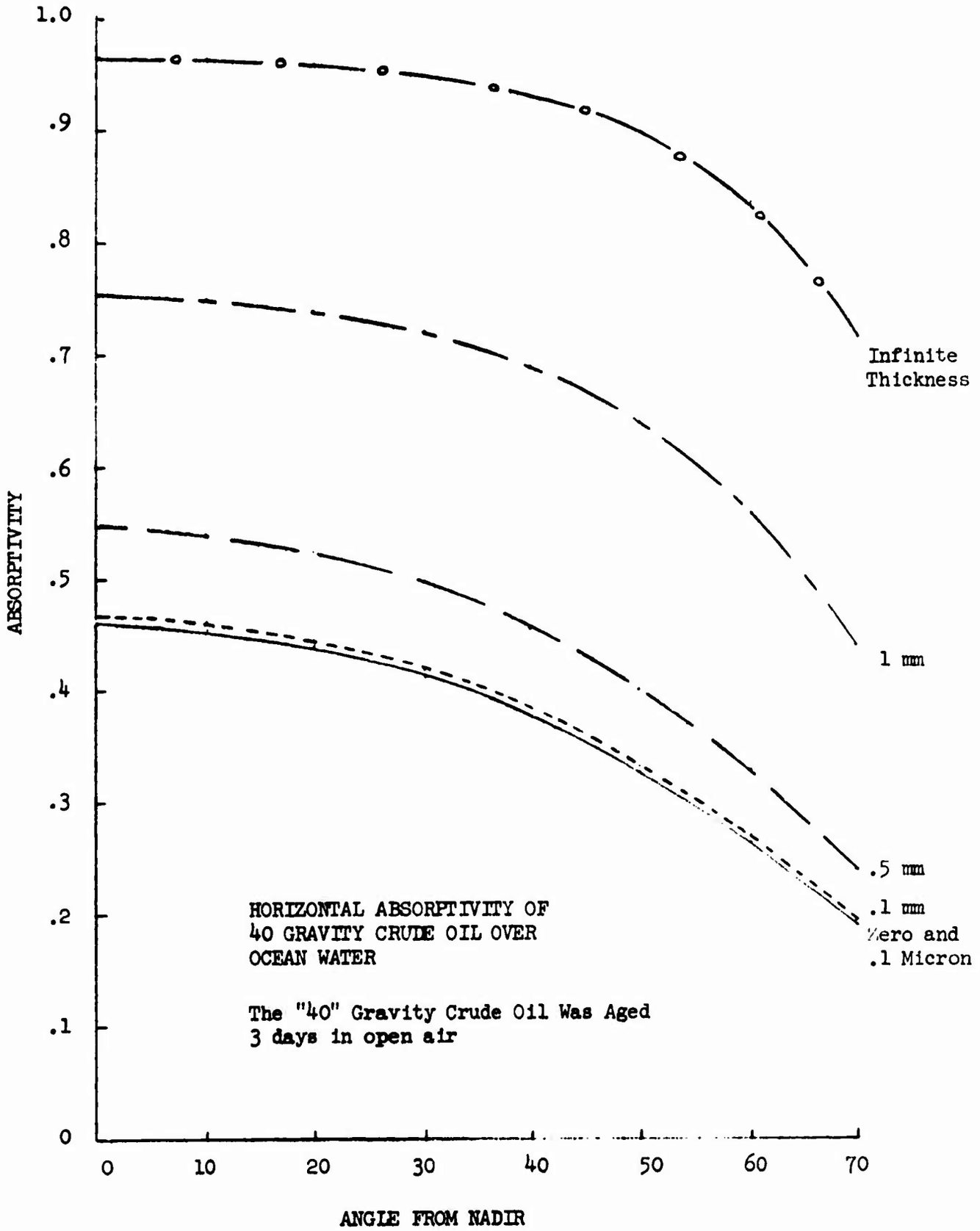
1.0
.9
.8
.7
.6
.5
.4
.3
.2
.1
0
ABSORPTIVITY
0
10
20
30
40
50
60
70
ANGLE FROM NADIR
Infinite Thickness
1 mm
.5 mm
.1 mm
Zero and .1 Micron
HORIZONTAL ABSORPTIVITY OF 40 GRAVITY CRUDE OIL OVER OCEAN WATER
The "40" Gravity Crude Oil Was Aged 3 days in open air

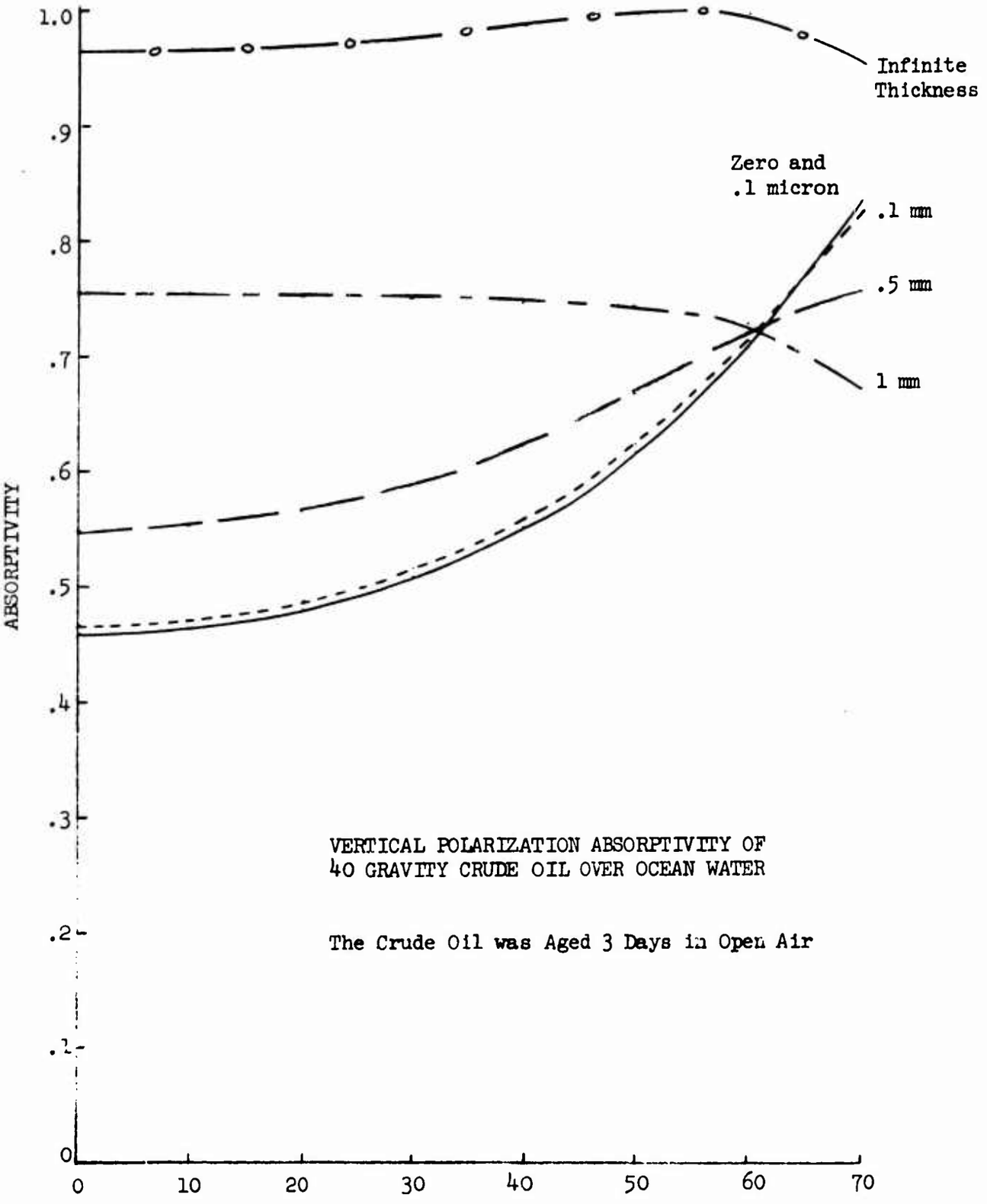

VERTICAL POLARIZATION ABSORPTIVITY OF
40 GRAVITY CRUDE OIL OVER OCEAN WATER

The Crude Oil was Aged 3 Days in Open Air

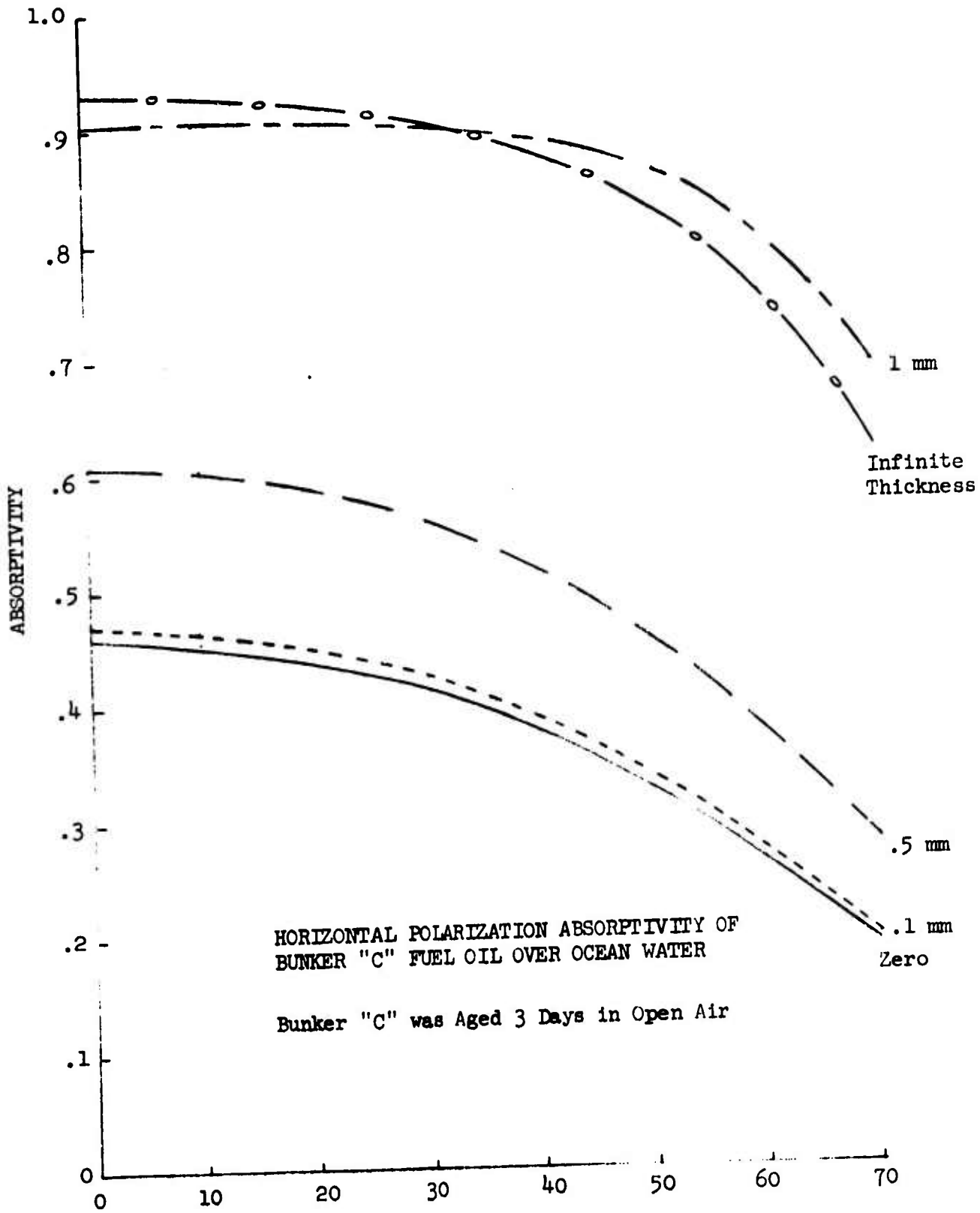
1.0
.9
.8
.7
.6
.5
.4
.3
.2
.1
0
ABSORPTIVITY
1 mm
Infinite Thickness
.5 mm
.1 mm
Zero
HORIZONTAL POLARIZATION ABSORPTIVITY OF BUNKER "C" FUEL OIL OVER OCEAN WATER
Bunker "C" was Aged 3 Days in Open Air
0
10
20
30
40
50
60
70
ANGLE FROM NADIR

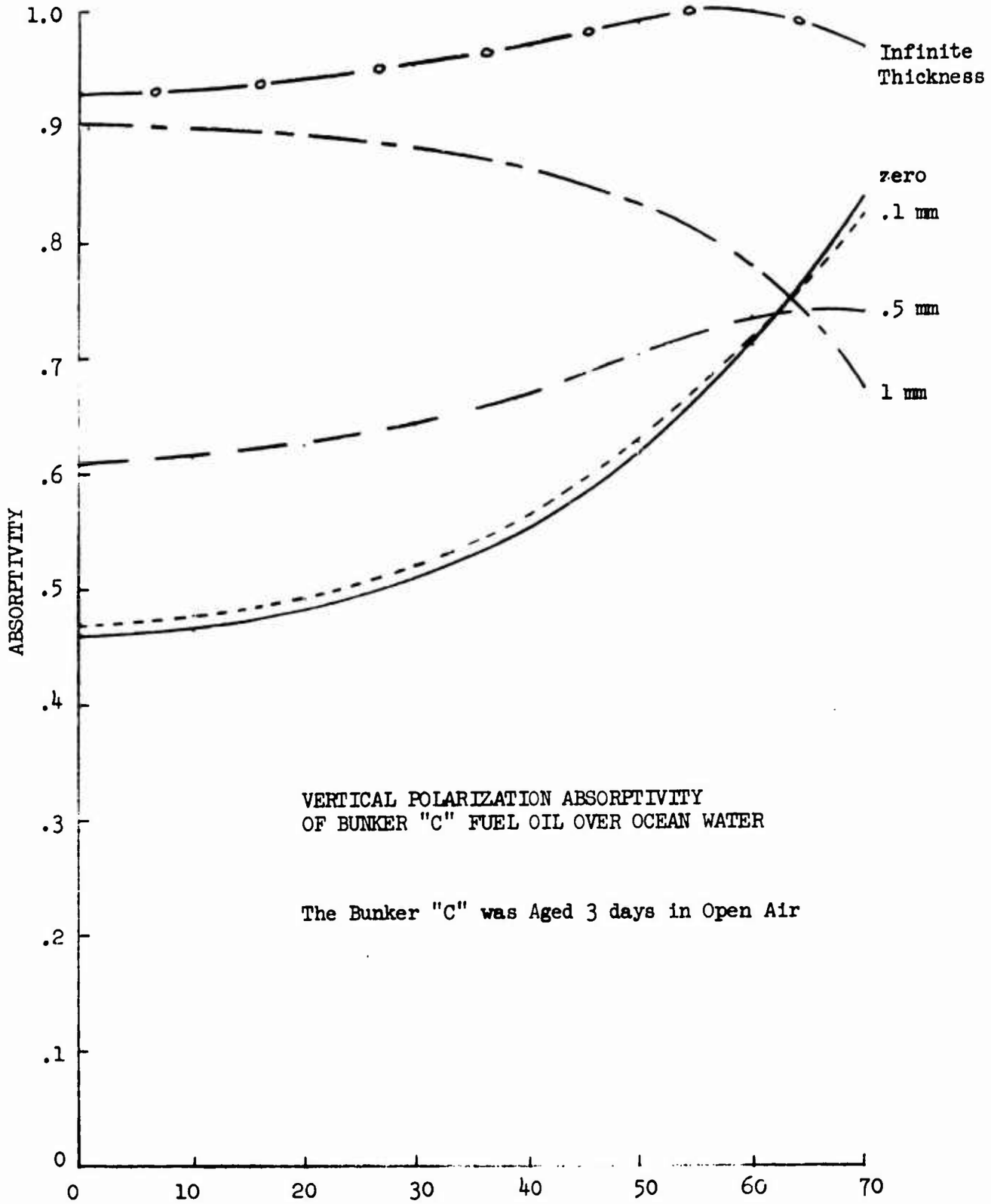

VERTICAL POLARIZATION ABSORPTIVITY
OF BUNKER "C" FUEL OIL OVER OCEAN WATER

The Bunker "C" was Aged 3 days in Open Air

BLANK PAGE

APPENDIX B

TABULATED DATA FROM THE AT-SEA TESTS

ABBREVIATIONS AND SYMBOLS USED IN APPENDIX B

GHZ	Gigahertz - cycles per second x 10^9
t_i	Integrate Time of Radiometer
30^o	30 (API) gravity oil
ΔT_V	Change in Brightness Temperature (Vertical Polarization) over Oil Slick
ΔT_H	Change in Brightness Temperature (Horizontal Polarization) over Oil Slick

Spill No: 1 Date: 8-28-69
Type of Oil: Diesel

Location: South of Anacapa

Aircraft Speed: 100 Mph
Aircraft Altitude: *200 ft.

Radiometer: 37 GHz, 0.81 cm
Integrate Time: *0.5 sec.

Run No.	Time	Remarks	Qual.	ΔT_V (^oK)	ΔT_H (^oK)	Spill Area x 10^4 (sq.ft.)	Thickness (mm)	Estimated Time Over Spill: Distance	Time
1		Boat only	F	13	19	-	-	-	-
2		Boat only	F	6	0	2		140 ft	.9 sec.
3		Oil	F	5	12	3		170	1.1
4		Miss	F	-	-	3	0.11(est)	170	1.1
5			F	0	9	4	0.11	200	1.3
6			F	5	15	4	0.11	200	1.3
7			F	8	22.5	5	0.11	220	1.5
8		Boat and Oil	F/F	15/10	23/10	5	0.11	220	1.5
9			F	9	35	6	0.11	245	1.6
10		Miss (spill complete)	-	-	-	6	0.11	245	1.6
11			F	0	12	7	0.10	265	1.8
12		Miss	-	-	-	7	0.10	265	1.8
13			F	0	5	8	0.09	280	1.9
14			F	5	10	8	0.09	280	1.9
15		t_i = 0.2 sec	F	6	12	9	0.08	300	2.0
16		Miss? t_i = 0.2 sec	-	-	-	9	0.08	300	2.0
17			F	5	8	10	0.07	310	2.1
18		Miss? Alt = 400 ft	-	-	-	10	0.07	310	2.1
19		Alt = 400 ft.	F	5	8	11	0.06	330	2.2
20		Miss? Alt = 400 ft, t_i = 0.4 sec	-	-	-	11	0.06	330	2.2
21		Miss Alt = 400 ft, t_i = 0.1 sec	-	-	-	12	0.06	345	2.3
22		Alt = 400 ft, t_i = 0.1 sec	F	7	8	12	0.06	345	2.3
23		Miss	-	-	-	13	0.05	360	2.4
24			F	6	6	13	0.05	360	2.4
25		Miss	-	-	-	14	0.05	370	2.5
26			P	?	3	14	0.05	370	2.5
27			P	?	10	15	0.04	390	2.6
28			P	-	-	15	0.04	390	2.6
29			P	5	7	16	0.04	400	2.7
30		Est. size of oil slick: 400 ft Dia.	P	?	5	16	0.04	400	2.7

Not Recorded

*Unless otherwise noted

Spill No: 2 Date: 9-3-69
Type of Oil: 30° Crude
Aircraft Speed: 100 Mph
Aircraft Altitude: *200 ft.

Location: South of Anacapa

Radiometer: 37 GHz, 0.81 cm
Integrate Time: *0.5 sec.

Run No.	Time	Remarks	Qual.	ΔT_V (°K)	ΔT_H (°K)	Spill Area x 10^4 (sq.ft.)	Thickness (mm)	Est. Time Over Spill Distance	Time
1	10:04	Boat only, Alt.= 400 ft	F	20	30	2			
2	10:08	Miss	P	-	-	4			
3	10:12	Miss	P	-	-	6		75 ft	1 sec
4	10:15	75 gals spilled	F	5	4	8	0.09	150	1
5	10:18	105 gals spilled	F	7.5	5	10	0.07	225	2
6	10:21	Oil & Boat, 135 gals spilled	P	-	-	12		300	2
7	10:24	Oil & Boat, 165 gals spilled	P	-	-	14	0.05	375	3
8	10:27		F	6	5	16	0.04	450	3
9	10:30	Miss?	P			18	0.04	525	4
10	10:31		F	3	?	21	0.03	600	4
11	10:35	Miss?	P	-	-	23	0.03	675	5
12	10:37	Alt = 400 ft	P	4	4	25	0.03	750	5
13	10:40	Miss? Alt = 400 ft	P			27	0.03	825	6
14	10:44	Alt = 400 ft	F	7	5	29	0.02	900	6
15	10:45		F	5	?	31	0.02	975	7
16	10:48		P	-	-	33	0.02	1050	7
17	10:52		P	?	5	35	0.02	1125	8
18	10:55		P	-	-	37	0.02	1200	8
19	10:57	Miss	P	-	-	39	0.02	1275	9
20	10:59	Alt = 500 ft	F	6	5	41	0.02	1350	9
21	11:02	Alt = 400 ft	F	6	3	43	0.02	1425	10
22	11:05	Miss (est size of slick 300 ft x 1500 ft)	P	-	-	45		1500	10

*Unless otherwise noted

Spill No: 3 Date: 9-9-69
Type of Oil: 20° Crude
Aircraft Speed: 100 Mph
Aircraft Altitude: *200 ft

Location: South of Anacapa

Radiometer: 37 GHz, 0.81 cm
Integrate Time: *1.0 sec.

Run No.	Time	Remarks	Qual.	ΔT_V (°K)	ΔT_H (°K)	Spill Area x 10^4 (sq.ft.)	Thickness (mm)	Est. Time Over Spill Distance	Est. Time Over Spill Time
1	15:42	Boat only	G	3	16				
2	15:45	1 Barrel + Boat	G	5	7	0.2		50 ft	.2 sec
3	15:51	1 Barrel + Boat	G	2.5	5	0.3		50	.4
4	15:52	2 Barrels	G	5	7	0.4		50	.6
5	15:56			0	5	0.6		50	.7
6	15:58	Dump complete	P	0	2	1.5	0.44	50	.9
7	16:00	Alt = 400 ft	G	6	7.5	2	0.34	100	1.0
8	16:04	Alt = 400 ft	G	6	5.0	3	0.24	150	1.3
9	16:07	Across slick Alt = 400 ft	P	0	2.5	4	0.17	200	1.4
10	16:10	Alt = 400 ft, t_i = 0.5 sec	P	5	3.0	6	0.11	250	1.6
11	16:14	Miss? t_i = 0.5 sec	P	5	8.0	8	0.08	300	1.7
12	16:17		F	2.5	0	10	0.07	350	1.9
13	16:20		F	2.5	5	12	0.07	400	2.1
14	16:24		P	2.5	2.5	15	0.05	450	2.2
15	16:27		F	7	3	13	0.04	500	2.4
16	16:30		P	7	0	21	0.03	550	2.6
17	16:33		P	5	2.5	25	0.03	600	2.7
18	16:37		F	5	2.5	28	0.02	650	2.9
19	16:47		P	5	-2.5	34	0.02	725	3.1
20	16:50	500 ft x 800 ft	F	7	-2.5	40	0.02	800	3.3
21	16:54	Special Traverse ?	G	5	-3.0	48	0.01	900	3.5
22	16:57	500 ft x 800 ft	G	3	2.5	56	0.01	1000	3.8
23	17:00	6-800 ft x 1200 ft	P	2	-5.0	66	0.01	1100	4.0
24	17:04		F	3		72	0.01	1150	4.2
25	17:08	Pass lengthwise - no photos	F	2.5	-2.0	78	0.01	1200	4.4
26	17:11	Crosswise pass	F	5	-2.0	85	0.01	1250	4.5
27	17:12	Boat Pass Miss?		-		91	0.01	1300	4.7
28	17:18	Boat & Oil		3	-3.0	98	0.01	1350	4.9
29	17:21		F	-2.5	-2.5	103	0.01	1400	5.0
30	17:24		F	3	-5	106	0.01	1450	5.2
31	17:28					120	0.01	1500	5.4
32	17:30		F	2.5	-2.5	128	0.01	1550	5.5

*Unless otherwise noted

Spill No: 4 Date: 9-12-69 Location: South of Anacapa

Type of Oil: 42°

Aircraft Speed: 110 MPH Radiometer: 37 GHz, 0.81 cm

Aircraft Altitude: *200 ft Integrate Time: 1.0 sec.

Run No.	Time	Remarks	Qual.	ΔT_V (°K)	ΔT_H (°K)	Spill Area x 10^4 (sq.ft.)	Thickness (mm)	Est. Time Over Spill Distance	Time
1	18:18	165 gal. spilled	G	16	30				
2	18:22		P	0	- 3			98 ft	.65 sec
3	18:24		F	3	1	0.08		126	.84
4	18:28		P	<2.5	- 2			182	1.2
5	18:30	Boat?	G	3	10	3	0.23	210	1.4
6	18:33	Alt. = 400 ft	G	2.5	7.5			252	1.68
7	18:38	Miss? Alt. = 400 ft	P	2.5?	0	6	0.11	342	2.28
8	18:40	Miss? Alt. = 400 ft	P	4.0?	1?			370	2.47
9	18:41	Alt. = 400 ft	P	0	2.0?			384	2.56
10	18:44	Alt. = 250 ft	P	2.5?	-2.0?			426	2.83
11	18:46	Alt. = 250 ft	P	2.5	-2.0	12	0.06	454	3.03
12	18:51		F	0	2.5			524	3.50
13	18:52		G	2.5	5.0			538	3.58
14	18:55	Miss?	G	-3?	0			580	3.87
15	18:58		G	7	3			612	4.09
19	19:08		G	8.0	8.6			752	5.00
20	19:14		P	2.5?	3.0?			836	5.50
23	19:15		P	0	0			850	5.67
24	19:19		F	3.0	2.5			906	6.02
27	19:22		F	5.0	-1.0			948	6.30
32	19:25		F	3.5	4.0			990	6.60

*Unless otherwise noted

Spill No: 5
Type of Oil: Diesel
Aircraft Speed: 110 MPH
Aircraft Altitude: 200 ft

Date: 9-12-69

Location: South of Anacapa

Radiometer: 37 GHz, 0.81 cm
Integrate Time: 1.0 sec

Run No.	Time	Remarks	Qual.	ΔT_V (^oK)	ΔT_H (^oK)	Spill Area x 10^4 (sq.ft.)	Thickness (mm)	Est. Time Over Spill Distance	Time
16	19:00	350 gal spilled	F	0	3.0				
17	19:03		G	0	6.0				
18	19:05	Oil spilled (all)	P	2.5	3.0	7	1.9	700	4.7 sec
21	19:12		G	5.0	5.0	33	0.04	1400	9.4
22	19:13		G	2.5	2.5			1500	10
25	19:15?		P	7	3	54	0.02	1700	11.4
29	19:19		F	3.0	5.0			2100	14.0
31	19:25	Boat?	F	4.0	4.5			2700	18.0
33			G	4.0	2.5				
38			G	4.0	3.0				

Spill No. 6
Type of Oil: Mixture, Diesel & 20°

Location: South of Anacapa

Aircraft Speed: 110 MPH
Aircraft Altitude: 200 ft

Radiometer: 37 GHz, 0.81 cm
Integrate Time: 1.0 sec

Run No.	Time	Remarks	Qual.	ΔT_V (°K)	ΔT_H (°K)	Spill Area x 10^4 (sq.ft.)	Thickness (mm)	Est. Time over Spill Distance	Time
16	19:25	200 gal. spilled	F						
34	19:31		G	4.0	2.5				
35		Dark	G	3.5	3.5	14	.05	250 ft	1.7 sec
36		"	F	4.0	2.0			370	2.47
41	19:47		F	4.0	3.0			700	4.66
42	19:50	Miss	F	3.0	2.5	50	.01	880	5.8
43	19:52							1080	7.2
44	19:55		F	4.5	2.5			1260	8.4
45	19:57	Miss						1380	9.2
46	20:00		F	4.0	2.0	90	.01	1560	10.4
47	20:04			3.0	3.0			1800	12.0

APPENDIX C

AIRBORNE OIL POLLUTION DETECTION SYSTEM CONSIDERATIONS

BLANK PAGE

LIST OF ABBREVIATIONS AND SYMBOLS

APPENDIX C

agc	Automatic Gain Control
D_a	Antenna Aperature
db	Decibel
GHz	Gigahertz 10^9 cycles per second
IF	Intermediate Frequency
Kd	Constant for water droplets
KHz	Kilohertz 10^3 cycles per second
K_o	Constant for Atmospheric Oxygen
K_v	Constant for Water Vapor
h	Aircraft Altitude
L. O.	Local Ocillator
MC	Mega Cycles
M_d	Water Droplet Mass in gm/m^3
M_v	Water Vapor Mass in gm/m^3
r. f.	Radio Frequency
rms	Root Mean Square
R_s	Slant Range
S	Beam Pattern (Cross Track Direction)
S'	Beam Pattern (Down Track Direction)
S/N	Signal to Noise Ratio
T_d	Beam Dwell Time
T_s	Time for completion of one scan

LIST OF ABBREVIATIONS AND SYMBOLS (Continued)

T_x	Microwave Attenuation
v/h	$\frac{\text{Aircraft Velocity}}{\text{Altitude of Aircraft}}$
V	Aircraft Velocity
θ	View Angle
θ_a	Antenna Beamwidth
$\dot{\theta}$	Beam Scan Rate

REQUIREMENTS FOR AN OIL SLICK DETECTION SYSTEM

The proliferation of oil spillage from off-shore drilling operations and sea-going vessels has become a major consideration in the preservation of natural resources and the prevention of undue pollution of coastal waters. Various techniques have been attempted to enable patrolling aircraft to detect such spillages, and hopefully identify the source and extent of the spill. Most of these attempts have met with only marginal success, to the extent that an improved oil slick detection system is still an open requirement.

Operationally, the system will be used from an airborne vehicle, such as the HC-130B aircraft or the HH-52A helicopter. Patrol altitudes may range from 500 feet to 2000 feet, and hopefully, may be conducted day or night in clear and overcast weather. The airborne surveillance system should possess as wide a field of view as practicable and be capable of resolving small oil slicks. Sensor data should be presented on an operator's display to facilitate real time identification of the oil spillage and the vessel responsible for the spillage.

It is the purpose of this section to discuss the system configuration geometry imposed by the typical aircraft operational scenarios and physical restraints. A candidate microwave radiometric system is described which will satisfy the operational and phenomenological requirements with a hardware design which is within the current technology.

The oil slick investigations conducted during performance of this program, along with certain operational requirements, form the basis for configuring a detection system. The airborne measurements data indicate that oil film thicknesses of substantially less than 0.1 mm are detectable. Signatures during initial slick formation were typically on the order of 20°K horizontal polarization and 10°K vertical polarization. The smallest signatures which could be positively and consistently identified were of the order of

3.5°K. In many instances smaller signatures were identifiable, however, for the purpose of this discussion we will consider the minimum detection requirement as 3.5°K. A representative rms noise figure of the ocean background was calculated to be 1.65°K, representing the roughest seas encountered during the at-sea tests. For a confidence level of 90% the oil slick signature must be twice this value. The following system discussion will use a minimum anomaly of 3.5°K.

The measurement work indicates that a constant antenna viewing angle of 30° to 45° produces the most favorable oil slick signature. Hence, a scanning beam radiometer must maintain a constant incidence angle with respect to the surface. The scanning beam will then generate a conical section as it scans the field of view.

Figure C-1 depicts the geometry involved in a scanning system with an incidence angle of 40°. As may be seen from the figure, the requirement of a constant 40° incidence angle limits the width of the area scanned to + and -45°. Also, it is seen that the total width scanned increases very little when the vertical scan axis is rotated much over a ±45° sector. This then sets a practical limit to the total path scanned beneath the aircraft of ~60° wide.

The beamwidth of the scanning antenna is next determined by considering the minimum resolution detection capability required by the airborne system. An examination of the dispersion pattern of a slick behind a ship indicates that a 100 ft wide slick width may be representative of the minimum expected. Hence, at the maximum operational altitude of the patrol aircraft the antenna beam pattern projected on the plane of the ocean surface should be 100 feet across.

An altitude of 2000 feet and a view angle from nadir of 40° gives a slant range R_s of:

$$R_s = \frac{h}{\cos\theta} = \frac{2000}{\cos 40^\circ} = 2,610 \text{ ft}$$

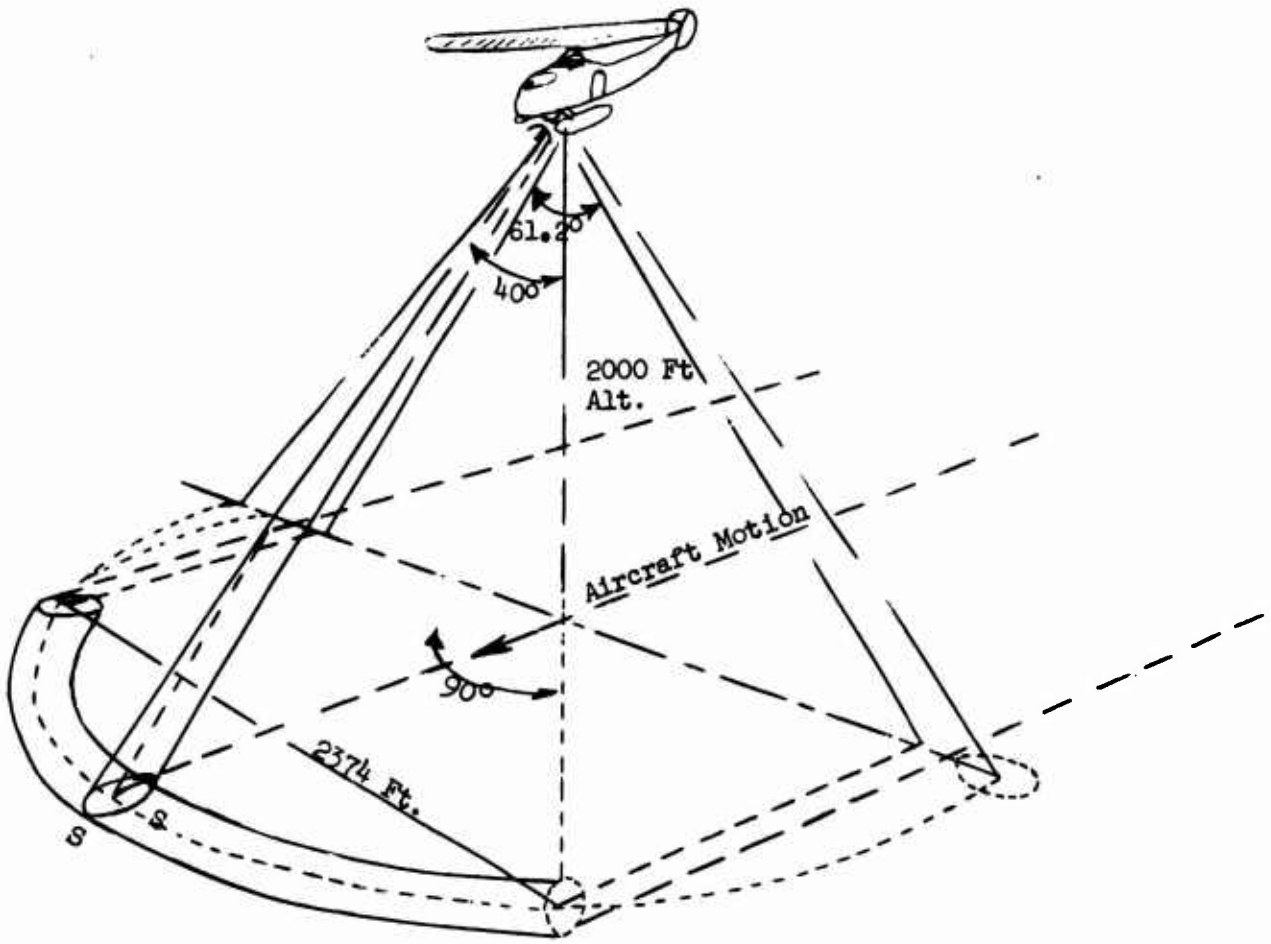

Figure C-1. Geometry of Scanning System with an Incidence Angle of 40°

The antenna beamwidth θ_a, required to produce a 100 ft wide beam pattern (S) in the cross track direction is given by:

$$\theta_a = \frac{(57.3)S}{R_s} = \frac{(57.3)100}{2610} = 2.2 \text{ degrees.}$$

In the down-track direction, the beam projection (S) is lengthened by the 40° view angle to give

$$S' = \frac{R_s \theta_a}{57.3 \cos 40^\circ} = \frac{2610(2.2)}{57.3 \cos 40^\circ}, \text{ where } \theta_a \text{ is in degrees.}$$

$$S' = 131 \text{ feet}$$

The time permitted for the beam to scan across the 90° sector is a function of the aircraft's forward cruise velocity. This is a necessary factor in order to enable the scanning beam to give a 100% area coverage in the direction of aircraft motion. To meet the 100% coverage criteria, the beam is required to completely traverse the 90° scan sector in the time of the aircraft's position will advance one beamwidth along the ocean surface. This is a very important consideration, as both the radiometric receiver integration time, and the antenna scanning rate are thus constrained.

In order to utilize the maximum receiver integration time and the minimum antenna scan rate required, the slowest vehicle velocities will be considered, which will provide the overall system performance and minimize hardware complexity.

The HH-52A helicopter uses a typical cruise speed of 90 knots. This is equivalent to 152 ft/sec ground velocity. The time permitted for one scan is then:

$$T_s = \frac{S'}{V} = \frac{131}{152} = .862 \text{ seconds}$$

The maximum receiver integration time should not exceed time for the beam to traverse its own width, or else the beam resolution limit will

not be realized.

The beam scan rate, $\dot{\theta}_a$, is then

$$\dot{\theta}_a = \frac{s}{T_s} = \frac{90^o}{.862 \text{ sec}} = 104 \text{ degrees/sec}$$

The beam dwell time, T_d, is consequently

$$T_d = \frac{\theta_a}{\dot{\theta}_a} = \frac{2.2}{104} = .0206 \text{ seconds}$$

The optimum receiver integration time for the best signal-to-noise ratio and probability of detection is around one-half the beam dwell time, or .[illegible]onds.

At this point, consideration must be given to the receiver performance requirement to detect the oil slick. From the at-sea airborne measurements, two parameters are of greatest interest: (1) The minimum oil slick signature expected, and (2) the radiometric rms value of the ocean background noise. These values were 3.5^o Kelvin signature for around a 0.05 mm oil film, and a 1.6^oK rms ocean background noise. The ocean noise contribution was observed during a sea state of about 2; for calmer seas, a lower background noise would be obtained. The significance of this is the ratio between background noise and oil slick signature. In this case it is found to be:

$$S/N = \frac{3.5}{1.6} \simeq 2.2$$

This corresponds to a 2 sigma, or 95% probability of detection of the minimum signal. For good, clear image quality on the display, a S/N ratio of 10 db is recommended. This would correspond to a 16.0^o Kelvin signature on a sea state of 2. The question of sea background noise is an uncertainty of this point, as these data were obtained at a relatively low altitude of around 500 feet. At a two thousand foot altitude a 100 ft diameter

beam footprint would average the sea noise contribution considerably. The precise extent is not known at this time, however. The results of three over-sea flights have been plotted in Figure C-2 and, indicating the relative reduction in rms ocean noise as a function of beam spot size. For this reason, the system aspects of radiometer receiver noise should be kept as low as possible to preclude system noise limitations in the more favorable background noise conditions.

One other effect may also contribute to the enhancement of oil slick areas. This involves the smoothing effect oil imparts to a rough sea surface. This is to say, that a reduction of sea background noise in oil slick areas could produce a recognizable effect on the display image, in that the observor would be able to see "smooth" areas by virtue of having a lower average noise content. This effect would be cummulative to the basic change in radiometric temperature produced by the oil slick, in that more visual information would be present in the display image.

Actual measurements in this area are needed to understand more fully the magnitude of background noise smoothing to be expected by an oil slick on a surly sea.

RECEIVER DESIGN CONSIDERATIONS

The receiver sensitivity requirement should be about 3 sigma less than the 1.6°K background noise, which is on the order of 0.5°K rms at the previously established integration time of .01 seconds. Relating this to a one second ΔT is done by the inverse square root of the integration time; i.e.,

$$\Delta T_{1\ sec} = \frac{\Delta T_{.01}}{\sqrt{.01}} = \frac{.5}{\sqrt{.01}} = .05^{\circ}\ \text{Kelvin rms}$$

This order of receiver performance cannot be met by conventional mixer-IF receiver techniques, but requires a parametric r.f. amplifier

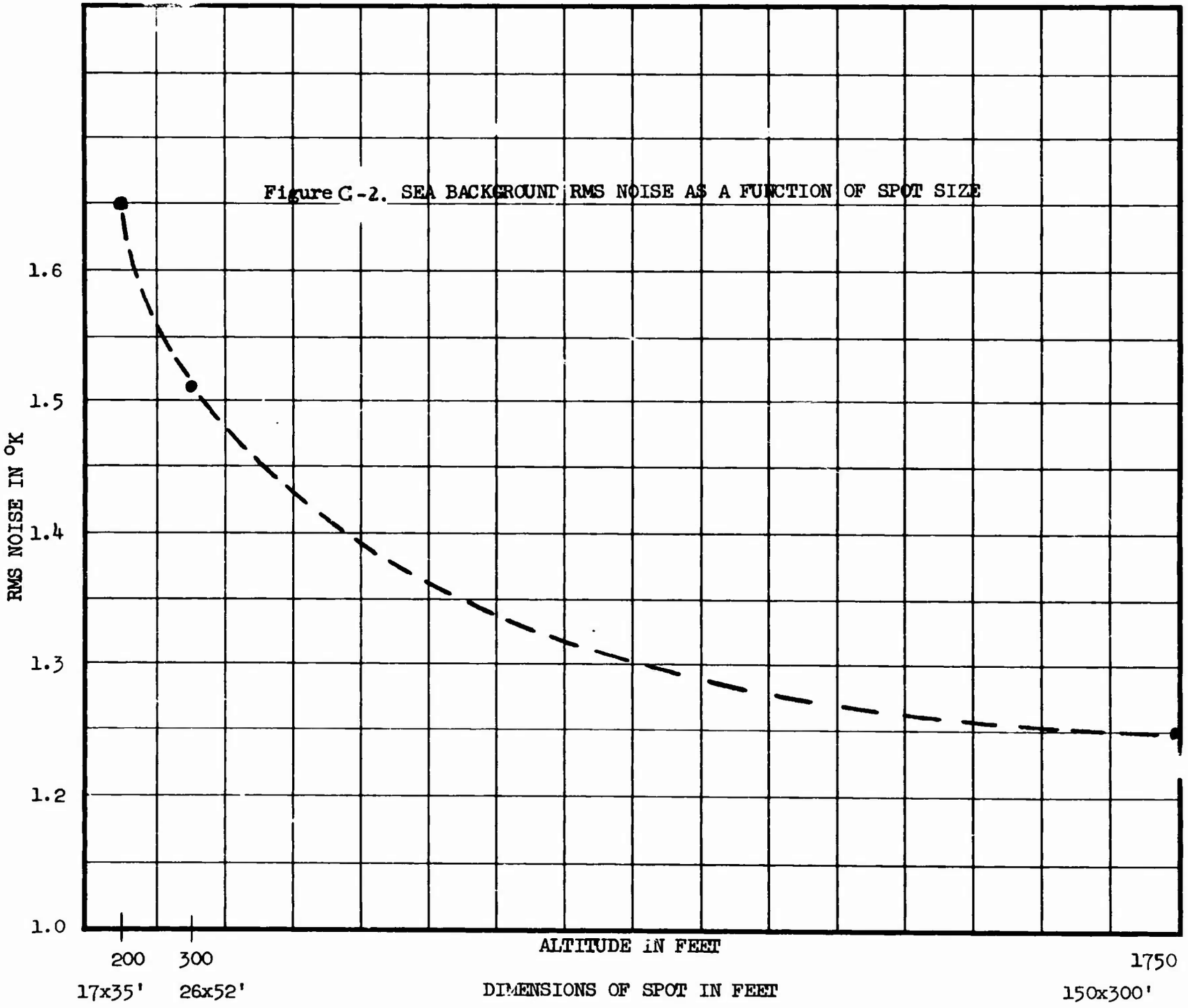

Figure C-2. SEA BACKGROUND RMS NOISE AS A FUNCTION OF SPOT SIZE

stage. Parametric amplifiers at 35 GHz have been built and are operating satisfactorily. These units have a noise figure on the order of 3-1/2 db and bandwidths of 600 MC, which produce the required receiver sensitivities of .05°K for 1 second integration times.

The requirement of a contrast imaging system radiometer does not demand absolute temperature measurements, as only point-to-point variations in the scene contrasts are required to produce an image. Making use of this fact permits the use of a total power radiometer receiver design, rather than the conventional Dicke approach. This produces a factor of two improvement in the receiver sensitivity, while at the same time reducing the system cost and complexity. This would give a .025°K ΔT paramp receiver sensitivity. Figure C-3 is a block diagram of such a receiver design, which is currently under investigation at AGC for other system applications.

A unique feature of this design permits automatic gain stabilization (agc) without resorting to the aforementioned Dicke technique of continuously switching the receiver input between the antenna and a known reference load. This concept utilizes a modulated noise injection technique, which is coupled continuously into the r.f. input waveguide. A constant amplitude of the added noise signal is analogous to a fixed temperature, and a 10 KHz modulation frequency permits subsequent separation from the relatively low frequency fluctuations of the antenna signal produced by the beam traversing across ocean scene anomalies. This extracted 10 KHz constant "temperature" signal, then provides a gain reference for agc action. An additional feature of this design concept uses the pump klystron simultaneously as a local oscillator. The 70 GHz pump frequency is obtaind via a frequency doubler stage. This approach permits the pump frequency to be synchronously locked with the L.O. frequency which is reported to provide an additional factor of two in receiver composite gain.

ANTENNA REQUIREMENTS

The antenna beamwidth requirement of 2.2 degrees was established by the system resolution demands of 100 ft at a 2610 ft slant range. At 37 GHz, the antenna aperture required is obtained by[1]:

---

1. Silver, S. (ed): "Microwave Theory & Design," MIT Rad Lab Series, Vol. 12, McGraw-Hill, N.Y., 1949.

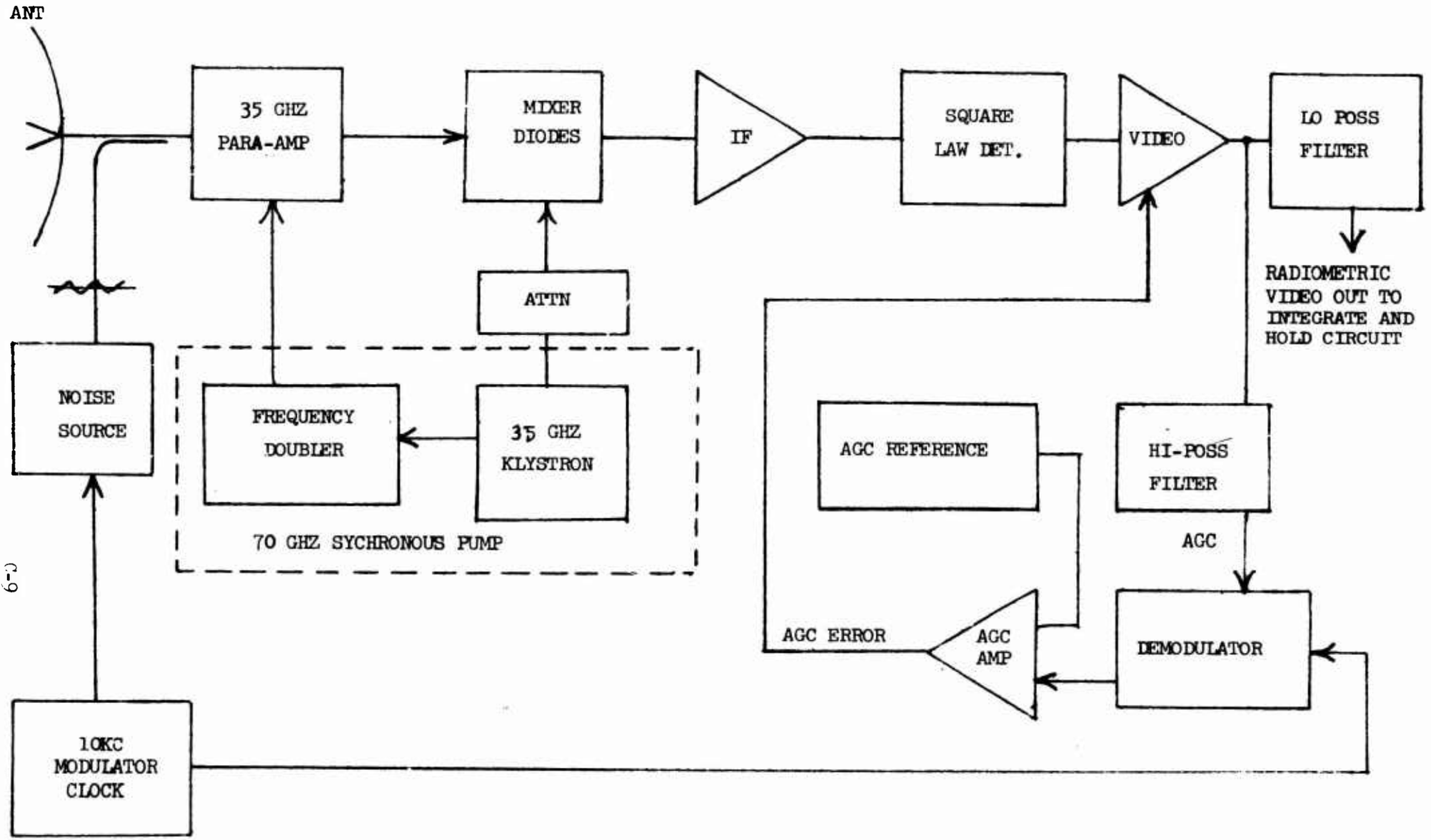

FIGURE C-3. RADIOMETRIC RECEIVER BLOCK DIAGRAM

$$D_a = \frac{69\lambda_{cm}}{\theta^o} = \frac{69(.81)}{2.2} = 25.4 \text{ cm}$$

$D_a \cong$ 10 inches diameter,

where the constant 69 is taken for a cosine distribution across the aperture, as shown by Silver.

The basic type of antenna employed in the design is difficult to trade off at this time; however, the candidates are either a mechanically-scanned system, such as a parabolic dish, or a dielectric-lens; or an electronically scanned phased array. A considerable advantage in simplicity and cost is offered by the dish or lens, but the requirement for rapid mechanical scanning can be restrictive. The scan rate calculated in Section C.1 of 104 degrees/second, however, is not too severe for a mechanically-scanned antenna, although a stabilized mechanical scanning drive will significantly increase the mechanical complexity. If a higher aircraft velocity is desired, and/or a lower altitude, the increase in scan speed required will necessitate a phased array antenna. Additionally, the phased array typically has a higher beam efficiency of around 90%, as compared to about 80% for a dish or lens.

From a system standpoint, the phased array provides both the antenna function and the scanning mount operation, thus simplifying the aircraft mounting and radome problems.

From a standpoint of cost and installation simplicity, the phased array appears to offer the best initial solution. The parabolic dish would require both the complex scanning mount and a larger radome demanded by a mechanically-scanned system.

Although the antenna loss in the phased array is expected to be on the order of 2 db, this is virtually offset by the effective losses of a dish having a lower beam efficiency, higher radome loss, and an inefficient scan flyback.

It should be noted here that the results of the recent oil slick measurements are actually a bit low, as corrections for the antenna and

waveguide losses are not included. These losses have been measured as 1.24 db for the vertical polarization and 1.32 db for the horizontal.

A similar system at 35 GHz was developed for the Air Force, although a complex, three-channel receiver arrangement was utilized. This system was primarily an airborne passive radiometric target tracker, but had been modified to permit a mechanically-scanned mapping mode with a constant incidence scan angle. This system was flown in a helicopter and produced radiometric mapping data from which images were subsequently formed.

A photograph of this hardware system installation is seen in Figure C-4. An image recorded of an irregular lake is seen in Figure C-5. The antenna diameter of 12 inches produced a 1.8 degree beam.

DATA PROCESSING AND DISPLAY

As the subject oil slick detection system requires a real time display, provisions are needed for the storage and rapid retrieval of the radiometric data obtained by about 30 or 40 sequential beam scans. Similar systems have been built by Aerojet and flown, or are to be flown in airborne radiometric scanning systems.

The block diagram in Figure C-6 represents the functional aspects of an operational system. The radiometric signal output from the receiver is averaged in an integrate and hold circuit where it is sampled and digitized by a solid state digital converter. The digitized signal then passes through an image data processer where the data are arranged in the proper format and stored in the memory in a rectified image format. At the end of a given scan the antenna beam reverses and begins a new data scan every 0.88 seconds. This new line of data is digitized and written in the memory in the position occupied by the line before. The first line having been transferred to a lower position in the memory. The memory has sufficient capacity to store the required number of bits corresponding to, say, 40 scan lines. As each line is scanned, the total number of data lines in the memory is shifted down to the next lower memory position. As the 41st line is scanned it "pushes" the first line out of the memory register.

Figure C-4. TYPICAL HARDWARE INSTALLATION ON HELICOPTER

Figure C-5. RADIOMETRIC IMAGE OF SMALL LAKE SHOWING CONTRAST OF WATER AND LAND

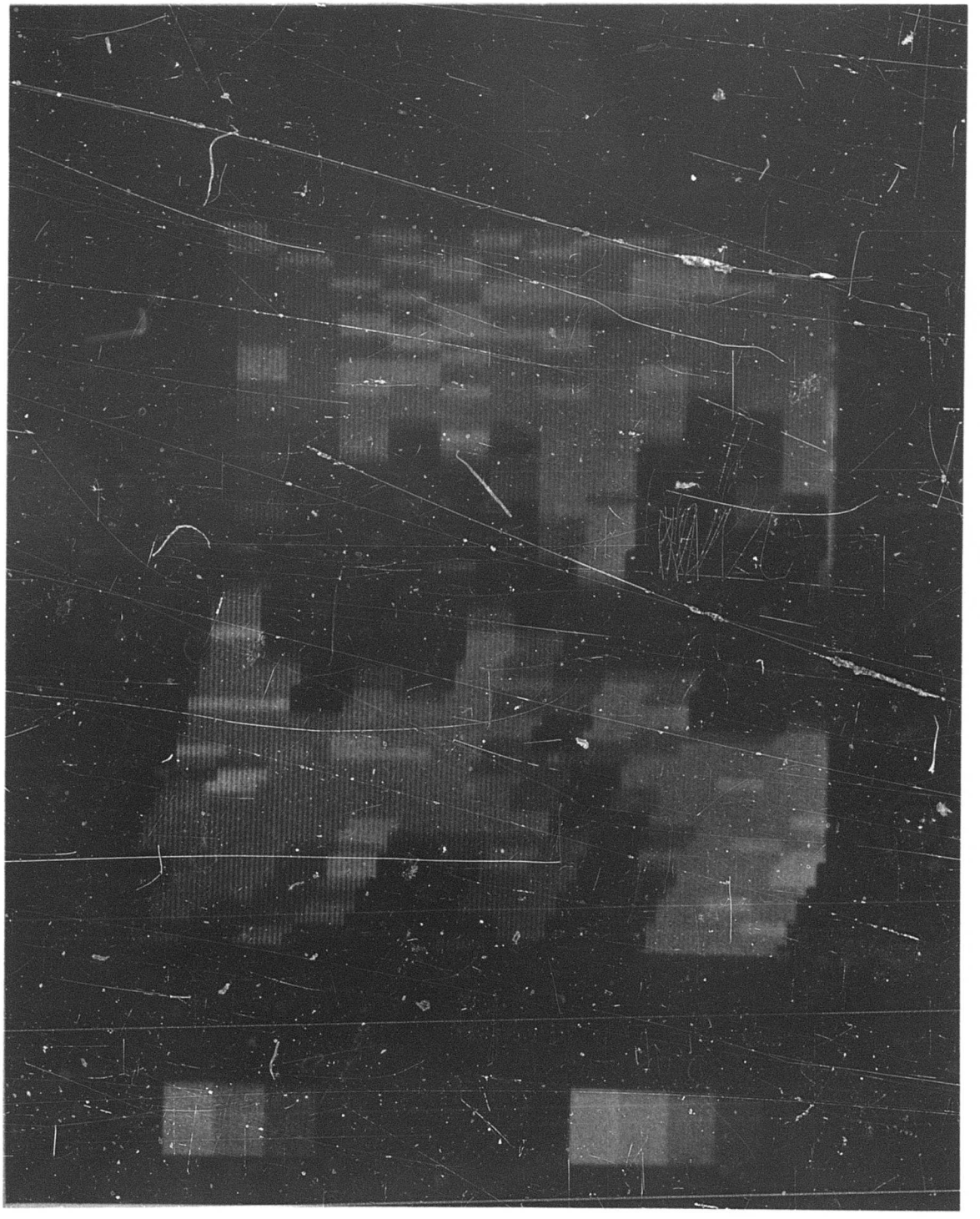

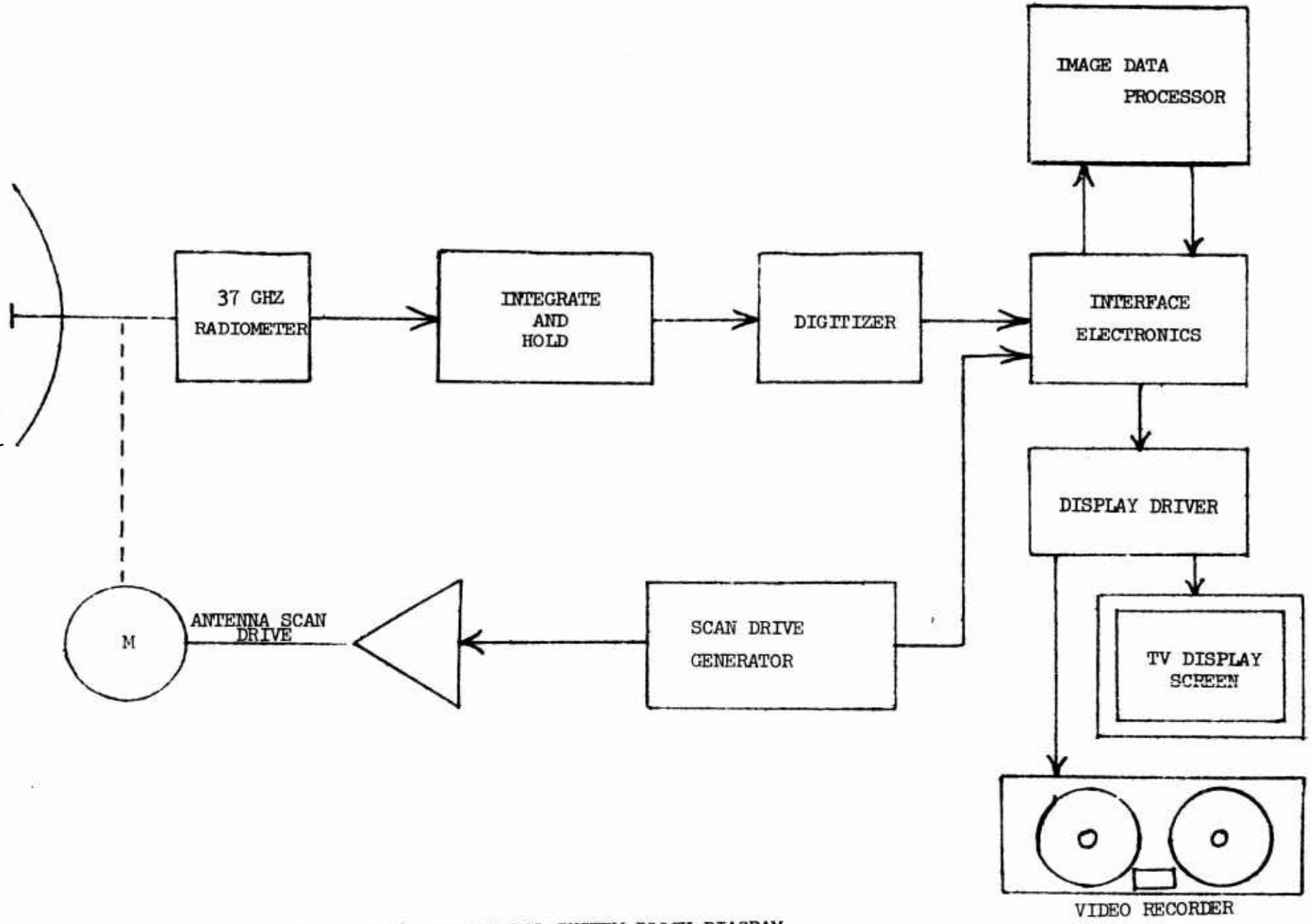

FIGURE C-6. CONCEPTUAL SYSTEM BLOCK DIAGRAM

The image data thus stored in the computer memory is continuously scanned or read at a T.V. synchronous rate. This stored scene data is subsequently displayed by the display driver on the T.V. screen to produce a visual image of the radiometric data stored in the memory.

As the aircraft flies forward, the displayed image on the screen is made to drift downward at a rate corresponding to the v/h ratio of the aircraft. A reproduction of such an image formed by the aforementioned 35 GHz Air Force system, is seen in Figure C-5. The dark, irregular area is Legg Lake.

WEATHER ATTENUATION EFFECTS

The operational requirements of the oil pollution detection system necessitate that surveillance be conducted in day or night and under conditions of cloud cover. As there are little diurnal effects on microwave radiometric signatures, the prime meteorological effect will be operation under conditions of cloud cover. Typical water droplet densities encountered during the winter along the Eastern Coast are around 0.2 gm/m^3 (2).

The microwave attenuation due to path loss at these cloud densities may be calculated in the absence of scattering from:

$$T_x = T_o \exp - (K_o + K_v M_v + K_d M_d)x$$

where T_o is the signature contrast without path loss (i.e., clear weather), and T_x is the new contrast due to attenuation. Also, K_o is a constant due to atmospheric oxygen, K_v is the constant for water vapor, M_v the water vapor mass in gm/m^3, K_d the constant for water droplets, and M_d the water droplet mass in gm/m^3. At 35 GHz, the constant for atmospheric oxygen (K_o) is 5.48×10^{-3}, the constant for water vapor (K_v) is 3.68×10^{-3} and the constant for water droplets is 162×10^{-3}.

(2) Meterological Handbook

For relatively constant air temperature over the range of interest 2000 ft above sea level the water droplet attenuation constant K_d can be considered constant. The oxygen and water vapor constants, K_o and K_v, respectively, are constant since little pressure variations occur over the range of 2000 ft.

Thus, assuming the atmospheric model below

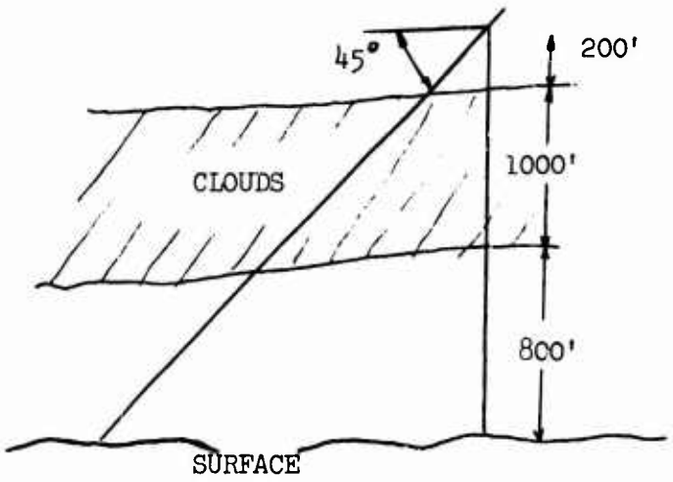

we can calculate T_x. We obtain

$$T_x = 0.950\ T_o \text{ and if we consider } T_o = 3.5^o$$

$$= (.950)(3.5) = 3.32^o \text{Kelvin.}$$

The ratio of T_x to T_o is seen to be,

$$\frac{T_x}{T_o} = \frac{3.32}{3.5} = .95, \text{ i.e. } 95\%$$

Consequently, only a 5% signal loss is incurred due to path loss under average winter operating conditions. It should be noted that the above calculation does not consider the basic signature reduction in T_o due to overcast skys. This effect however is on the same order of magnitude as the path loss attenuation factor.

It should be noted that atmospheric attenuation is apt to be excessive during rainfall and under these conditions, the detection system would be ineffective.

UNCLASSIFIED

Security Classification

DOCUMENT CONTROL DATA - R & D

(Security classification of title, body of abstract and indexing annotation must be entered when the overall report is classified)

1. ORIGINATING ACTIVITY (Corporate author) Aerojet-General Corporation	2a. REPORT SECURITY CLASSIFICATION Unclassified 2b. GROUP N/A

3. REPORT TITLE

RADIOMETRIC DETECTION OF OIL SLICKS

4. DESCRIPTIVE NOTES (Type of report and inclusive dates)

Final Report - 14 March thru 26 October 1969

5. AUTHOR(S) (First name, middle initial, last name)

A.T. Edgerton and D.T.Trexler

6. REPORT DATE	7a. TOTAL NO. OF PAGES	7b. NO. OF REFS
January 1970	130 (viii + 122)	6

8a. CONTRACT OR GRANT NO.	9a. ORIGINATOR'S REPORT NUMBER(S)
DOT - CG - 93228 - A b. PROJECT NO.	SD 1335 - 1
c.	9b. OTHER REPORT NO(S) (Any other numbers that may be assigned this report)
d.	

10. DISTRIBUTION STATEMENT

11. SUPPLEMENTARY NOTES	12. SPONSORING MILITARY ACTIVITY
	U.S. Coast Guard Office of Research and Development Applied Technology Division, Wash. DC

13. ABSTRACT

A study has been performed to assess the feasibility of using microwave radiometry for detection of oil pollution. The investigation stems from the U.S. Coast Guard's requirement for an airborne surveillance system which can detect oil pollution during inclement weather and during the hours of darkness. Laboratory and airborne measurements were made of a variety of oil base pollutants. Laboratory investigations included microwave response as a function of oil film thickness, physical temperature of the oil-water system, pollutant type, sensor wavelength, antenna polarization, and observation angle. These studies consisted of dual-polarization radiometric measurements (observational wavelengths of 0.8cm and 2.2cm) of Bunker C fuel oil, gasoline, and 20, 30, and 40 API gravity crude oil. The dielectric properties of these pollutants were also measured by means of a 0.81 cm ellipsometer. The results of the laboratory measurements were used to select the most suitable microwave radiometer for the airborne measurements. The airborne measurements were of small oil slicks on the open ocean off the Southern California Coast. Measurements were made from a ~~Cessna~~ 210 aircraft instrumented with a dual-polarized 0.81 cm radiometer oriented with a forward antenna viewing angle of 45° from nadir. Pollutants examined during the tests include marine diesel fuel; 20, 30, and 40 API gravity crude oils; and a mixture of diesel fuel and 20-gravity oil. Measurements were made under various atmospheric and low sea state conditions, including several at night.

DD FORM 1 NOV 65 1473

UNCLASSIFIED

Security Classification